Dimenzioniranje čeličnog priključka stup - temelj

Omazić, Filip

UNIVERSITY OF SPLIT
FACULTY OF CIVIL ENGINEERING, ARCHITECTURE AND GEODESY

MASTER'S THESIS

FILIP OMAZIĆ

Split, 2020.

UNIVERSITY OF SPLIT
FACULTY OF CIVIL ENGINEERING, ARCHITECTURE AND GEODESY

Filip Omazić

Design of column bases in buildings

Master's thesis

Split, 2020.

SVEUČILIŠTE U SPLITU
FAKULTET GRAĐEVINARSTVA ARHITEKTURE I GEODEZIJE

Filip Omazić

Dimenzioniranje čeličnog priključka stup-temelj

Diplomski rad

Split, 2020.

Dimenzioniranje čeličnog priključka stup-temelj

Sažetak:

U čeličnim konstrukcijama temeljni stupovi imaju važnu ulogu i način na koji su spojeni sa temeljnom konstrukcijom ima velik utjecaj na stabilnost i krutost, kako stupa tako i ostatka konstrukcije. Ovakva vrsta priključka dimenzionira se pomoću metode komponenata koja je detaljno opisana u Eurocode-u, a kratak opis prikazan je u ovom radu. Također, za modeliranje ovakvih vrsta spojeva sve se više koriste softveri, čiji se proračuni uglavnom temelje na navedenoj metodi komponenata ili FE analizama.

Glavni cilj ovog rada je provjeriti točnost softverskih rezultata dobivenih analizom spoja čija konfiguracija odgovara spoju neke konstrukcije u realnosti, sa racionalnom geometrijom i propisanim opterećenjem. Nakon što je modeliran i proračunat 3D model konstrukcije u softveru „*SCIA Engineer* “, pokazalo se da je HEA 200 najprikladniji poprečni presjek za temeljne čelične stupove, sa zadovoljavajućim faktorom iskoristivosti. Preko BIM veze, spoj je izvezen u softver za proračun spojeva - *IDEA StatiCa*, gdje je priključak i dizajniran. Isti postupak proveden je u *Autodesk Robot Structural Analysis Professional*, koji ima mogućnost izračuna spoja unutar softvera, kao poseban način analize. S obzirom da se prilikom dimenzioniranja konstrukcije čelični profil HEA 200 pokazao kao idealan za temeljni stup, konfiguracija spoja napravljena je da odgovara uzorku koji je eksperimentalno i numerički ispitivan u *Seco, 2019*, gdje je korišten isti poprečni profil stupa.

Da bi se izvela pravilna numerička analiza, nepohodno je bilo opteretiti navedene spojeve kombinacijom uzdužne sile i momenta u smjeru jače osi, slabije osi ili dvoosnog savijanja. Iteracijskim postupkom dobiven je maksimalni moment savijanja za svaku kombinaciju opterećenja. Analitički model temeljen na metodi komponenata koji je predložila *Seco, 2019* (a koji je sa zadovoljavajućim rezultatima verificiran iznad spomenutim numeričkim i eksperimentalnim ispitivanjima) prilagođen je i pripremljen za analizu koju ova teza zahtijeva, a sve to s ciljem adekvatnog uspoređivanja softverskih rezultata s analitičkim.

Nadalje, provedeno je parametarsko ispitivanje kako bi se ispitao utjecaj određenih parametara na otpornost spoja. Za svaki promijenjeni parametar dobivene su interakcijske krivulje i zapisane su napomene o ponašanju pojedinog spoja.

Nakon više od dvije tisuće numeričkih pokušaja, iteracijski je izračunato oko četiri stotine graničnih momentnih otpora i zapisano je preko petsto zabilješki o rezultatima i ponašanju spoja, te su glavni zaključci prikazani u petom i kratko sažeti u šestom poglavlju. Ovo istraživanje rezultiralo je raznim zanimljivim činjenicama i idejama koje bi mogle biti dodatno analizirane i istraživane, ali se iz vremenskih ili kapacitetskih razloga nisu mogle uklopiti u ovu tezu te bi mogle biti dobra podloga za daljnji rad.

Ključne riječi: čelični priključak stup-temelj; dvoosno savijanje; softver; moment otpora

Design of column bases in buildings

Abstract:

In steel structures, column bases have an important role, and the way connection between column base and a concrete foundation is designed has a major influence on the stability and stiffness of the column and rest of the structure. This kind of connection is designed with the component method provided by Eurocode and described shortly in this work. Besides that, software solutions are becoming more common, which are in general also based on the component method or FE analysis.

The main goal of this work is to check the accuracy of software calculations performed on a connection design that would be appropriate for a building that is subjected to realistic dead and live load. Thus, *SCIA Engineer* software is used for establishing the structural geometry and for the analysis. HEA 200 turned out to be the most appropriate cross-section for column bases, with a satisfactory utilization ratio. Via BIM link, the connection was exported to *IDEA StatiCa*, where the connection was designed. The same procedure was adapted with *Autodesk Robot Structural Analysis Professional*, which has an option of calculating the connections inside the software, as a special analysis mode. For both software, the configuration of the connection was conceived to match the specimen that was experimentally and numerically studied in *Seco, 2019.*

To perform proper numerical analysis, those connections were subjected to a combination of axial force and in-plane, out-of-plane, or biaxial bending moment, and by iteration procedure, the maximum bending moment was obtained for each loading condition. The component method based analytical model proposed by Seco (which was verified with the abovementioned numerical and experimental tests with very satisfactory results) was adapted and prepared for analysis that this thesis requires with the intention to compare software results against those obtained analytically.

Furthermore, the parametric study was performed to investigate the influence of several parameters on the connection resistance. Moment resistance curves and notes about the behavior of the connection were obtained for change of each parameter.

After roughly four hundred runs performed in software and over five hundred recorded notes and comparison of the results against one obtained analytically, the main conclusions are represented in Chapter 5 and shortly summarized in Chapter 6. Investigating the behavior of the connection resulted in other interesting facts that should be analyzed, and ideas that could be implemented but could not fit in this thesis and perhaps can be a good basis for further work.

Keywords: Column base connections; biaxial bending; software; moment resistance

SVEUČILIŠTE U SPLITU
FAKULTET GRAĐEVINARSTVA, ARHITEKTURE I GEODEZIJE

STUDIJ:	**DIPLOMSKI SVEUČILIŠNI STUDIJ GRAĐEVINARSTVA**
KANDIDAT:	Filip Omazić
BROJ INDEKSA:	762
KATEDRA:	**Katedra za Metalne i drvene konstrukcije**
PREDMET:	Metalne konstrukcije 2

ZADATAK ZA DIPLOMSKI RAD

Tema: Dimenzioniranje čeličnog priključka stup-temelj

Opis zadatka: Cilj ovog zadatka je analiza točnosti softverskih rješenja po pitanju dimenzioniranja čeličnog priključka stup-temelj. Kako bi se ispitala točnost softverskih rezultata, prije svega je potrebno napraviti model realne konstrukcije, propisno nanijeti opterećenja te odabrati potreban profil poprečnog presjeka. Potom je potrebno modelirati spoj u softverima za proračune spojeva, ispitati njihovo ponašanje te iteracijskim putem dobiti granične momente nosivosti. Dobivene rezultate usporediti sa eksperimentalnim rezultatima i rezultatima analitičkog modela koji su opisani u *Seco, 2019*. Analitički model neophodno je prilagoditi ovakvoj vrsti ispitivanja. Nakon provođenja numeričke analize potrebno je napraviti parametarska ispitivanja i provjeriti utjecaj pojedinih parametara na ponašanje spoja. Sve rezultate obrazložiti i grafičkiprikazati.

U Splitu, 25/02/2020.g.

Voditelj Diplomskog rada:

Izv.prof.dr.sc. Neno Torić

Predsjednik Povjerenstva
za završne i diplomske ispite:
Doc. dr. sc. Ivo Andrić

This thesis was prepared and defended at the Faculty of Sciences and Technology at the University of Coimbra, and afterward, it was upgraded and prepared for the defense at the University of Split, Croatia.

UNIVERSIDADE D
COIMBRA

Design of column bases in buildings

Dissertation submitted in fulfillment of the requirements for the degree of Master in Civil Engineering – Specialization in Structural Engineering

Author:

Filip Omazić

Supervisors:

University of Coimbra:

Luís Filipe Costa Neves
Laura da Silva Seco

University of Split:

Neno Torić

Ivica Boko

Coimbra, July 2020.

ACKNOWLEDGEMENTS

With this thesis, I am concluding my five years of study, which turned out to be a beautiful and very educational stage of my life. Completing this work and overcoming the obstacles I encountered in my academic journey, and during the process of writing this paper, would not have been possible without some people to whom I would like to dedicate a few words.

First, I would like to thank my supervisor at the *University of Coimbra*, prof. Luís Filipe da Costa Neves, for encouraging me to embrace this project. Without guidance, expert advice, and an accessible attitude that he ensured me, realizing this project would not have been possible.

Special thanks to my co-supervisor at host university, Laura da Silva Seco, for authorizing me to use her work in this thesis and introducing me with all its parts. Patience, knowledge, and constructive criticism that she provided me had a huge impact on this thesis.

I would like to express my gratitude to my supervisors at the *University of Split*, prof. Neno Torić and prof. Ivica Boko, who gladly accepted this role and provided me knowledge acquired with years of work experience in this field. The answers to all my doubts, together with the expert comments given to me by Prof. Torić, meant a lot to me and had a major influence on this thesis.

A word of gratitude to all professors I met during my studies at the University of Split, who had a positive impact on me, not only in the mean of gained knowledge but also in a way how their kindness and accessibility influenced me as a person. I have never been able to thank some of them and I would like to do it this way.

I would like to thank the Scorpus7 d.o.o. design office, where I had the opportunity to work during my graduate studies. All employees, headed by Antonio Martić, helped me to upgrade my academic knowledge with practical work in a very professional way. Their friendly approach, knowledge transferred on me, and shown understanding towards my academic obligations is something I will always appreciate.

Finally, I must express my very profound gratitude to my family and loved ones, who provided me with unfailing support and continuous encouragement throughout my years of study and through the process of researching and writing this thesis. This accomplishment would not have been possible without them. Thank you.

CONTENTS

1 INTRODUCTION

1.1 Scope of the dissertation

There is a high level of steel use in the structure designs nowadays. Since the steel resistance is very high, both for compressive and tensile forces, this material is suitable for various types of constructions. Besides that, steel can be well recycled, prefabricated and designed in various shapes, easily transported and built quickly. In addition to all other structures, steel is very common in the construction of buildings and halls, either in the structures that are made only of steel or as a composite with other materials. Column bases are very important elements of all steel structures, and the way they are connected to the concrete foundation greatly influences the strength and behavior of the column and rest of the structure. They should be designed properly since all forces from the structure are transferred to the ground through them. Despite the importance of this kind of connection, a much smaller number of studies and researches has been done on this topic compared to other types of steel joints.

It is inevitable that in most constructions the column base will be exposed to a combination of axial force and bending moment in a particular direction, and the component method is used for analyses of these types of connections, as described in EN 1993-1-8. The focus is mostly on analyzing the behavior of the connection when it is subjected to an in-plane bending (bending over the stronger axis). However, there is no method that provides the mechanical properties of the joint when subjected to weak axis bending or biaxial bending *(Amaral, 2014).*

Recently, *Seco (2019)* proposed an analytical model that is a significant advance in the design and analysis of column bases, since it copes with combinations of axial force and biaxial bending moment. One of the main goals of this thesis is to compare the results from this novel analytical model to the results provided by an analysis of the software commonly found in practice.

For this type of connection, many computer programs have already been developed. It is expected that structural engineering will progress over time and software use will be even more frequent, so it is necessary to ensure that these structural solutions are accurate, without major errors in the field of statics, and not to cause unnecessary economic losses.

1.2 Objectives

The main goal of this paper is to analyze and determine the accuracy of the solutions, in terms of column base connections, offered by some of today's most used structural analysis software. The design of the connection will be determined according to the needs of a structure with some realistic geometry and loads selected according to the standards such as Eurocode, and all of that will be modeled in software. After dimensioning of the structure and selecting the appropriate steel column profile, the connection will be exported via BIM link to connection design software designed in a way that the steel column is welded to a column base plate, which is connected to the concrete block by means of four anchor bolts. It will be subjected to a combination of axial force and bending moment in each direction (in-plane, out-

of-plane, and biaxial). Its behavior will be analyzed and the results will be compared to the ones obtained with the analytical model proposed by *Seco (2019).*

The *Seco*'s component method based analytical model was validated in a numerical and experimental way, as described in her work. In order to be able to use the mentioned analytical model for the form of analysis required for this work, the model had to be rearranged and adapted.

1.3 Chapter organization

This dissertation is organized into six chapters described as follows:

- Chapter 1 – Introduction: short lines about the thesis, main objectives and a short description of each chapter,
- Chapter 2 – State of the art: in this chapter the main parts of the column base connection are carried out, as well as the previous work based on this kind of connection. At the end of the chapter the component method, which is currently used for column base connections analysis, is shortly presented.
- Chapter 3 – Primary reference – *Seco*'s model: this chapter focuses on work and main conclusions carried out by *Seco (2019)*, whose analytical model is used in this dissertation,
- Chapter 4 – Software tools: list of the software used for column base connection analysis and a brief overview of the methodology used to approach the analysis,
- Chapter 5 – Analysis and comparison of the results: numerical analysis and parametric study are carried out in this chapter, as well as their comparison against the analytical model,
- Chapter 6 – Conclusions: summary of the work, as well as some main conclusions and recommendations are carried out.

2 STATE OF ART

2.1 Introduction

The present chapter contains the most common design of column bases as well as a short description of the main numerical and experimental works carried out previously.

2.2 Design of the column bases

The two most common types of column base connections are exposed column base (see Figure 2.1a) in which different configurations can be considered (number and position of anchor bolts, stiffeners, wedges, etc.), and the column base connections embedded in the concrete (see Figure 2.1b). This dissertation will focus on rigid/semi-rigid connections as in Figure 2.1a, with two outer anchor bolt rows.

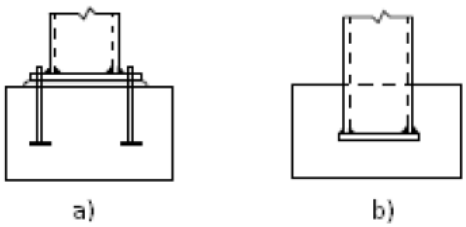

Figure 2.1: Types of column base: a) Exposed column base, b) Embedded column (Horova, 2010)

The main elements of exposed column base plates are (see Figure 2.2):

- stiffened/unstiffened steel column (HEA, HEB, IPE steel profiles)
- base plate welded to the column foot
- mortar (grout) layer
- anchor bolts
- concrete block (foundation).

As mentioned before, connection can be reinforced using stiffeners or wedges. Additionally, if necessary, the connection could be modeled with a shear resisting key (shear lug).

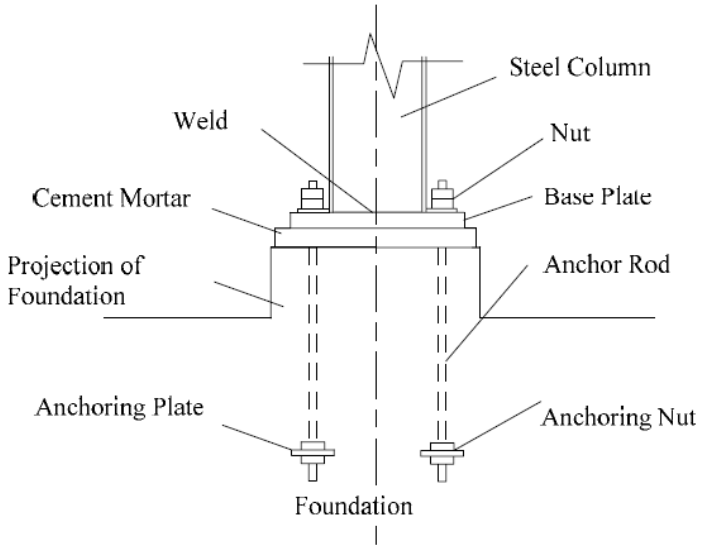

Figure 2.2: Elements of exposed column base (Grauvilardell et al., 2014)

2.2.1 Base plate

The main function is to increase the contact area between the column and the concrete block, allow a better stress distribution in the compressive side and prevent the crushing of the concrete. Another function is to transfer the possible tension in the column to the anchor bolts *(Amaral, 2014)*.

2.2.2 Grout layer

The contact between the base plate and the concrete block can be provided by the grout layer allowing the transition of shear forces from the column to the concrete footing by the friction between themselves. The grout layer also fills the void spaces in the concrete surface for increasing the friction between the steel plate and concrete foundation. Correct execution of the grout provides a full contact between base plate and footing for transferring the normal and lateral forces that might have an effect on the behavior of the column base connection.

2.2.3 Concrete foundation

The concrete block is the foundation of the column whose function is to transfer the loads to the ground, and foundations are dimensioned according to specific soil conditions. All the rules that apply during the design of any structure should be taken into account, such as laying the bottom of the foundation at a level below the freezing zone, the calculation of the overturning of the foundation, etc.
Also, the concrete class and reinforcement should be chosen according to expected loads and coordinated with other parts of the connection, and aim that failure occurs at the same time as it occurs for other elements.

The design is based on the calculation of an effective rigid area under the flexible plate. The bearing strength of concrete is recalculated into the design value of compressive strength, f_{cd} *(Horova, 2010),* since it can happen that it is not the same as the strength of tested compressive cube.

2.2.4 Anchor bolts

Anchor bolts connect the column, base plate and foundation, and their main purpose is transferring the tensile loads to the corresponding foundation. These loads may appear in form of pure tension or tension due to uni-axial or bi-axial bending moment or even shear forces.
There are various types of anchor bolts, as shown in Figure 2.3, and they should be chosen according to the corresponding conditions. The most common ones are the cast-*in-situ* anchor bolts and hooked bars since they are the most economic ones *(Amaral, 2014),* which are also considered as the simplest option as they don't need specific devices or technical workmanship. Anchoring to grillage beams embedded in the concrete foundation is designed only for column bases loaded by large bending moment because it is very expensive.

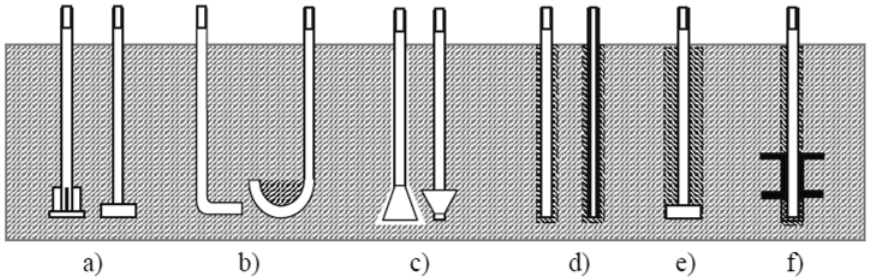

Figure 2.3: Types of anchor bolts: a) cast-in-situ anchor bolts, b) hooked bars, c) undercut anchor bolts, d)bonded anchor bolts, e) grouted anchor bolts, f) anchoring to grillage beams (Abejide, 2007)

The bolt resistance is easy to define with the standards given in the Eurocode (check *EN 1993-1-8*) but the anchoring resistance calculation is complex to determine and it is not convenient for practical design *(Amaral, 2014).*

2.3 Previous studies

Current guidelines neglect the effect of bending moment applied on the minor axis, focusing on the design of connections subjected to a bending moment applied on the direction of the major axis. The out-of-plane/biaxial bending moment is inevitable in most constructions and should be taken into account, due to the fact that effect can lead to serious stability risks.

Also, test campaigns were carried out on column base plates to have a better understanding of the behavior of such connections subjected to different loading conditions. In some cases, experimental tests represented the starting point to the development and validation of a new calculation procedures. Comparisons between the existing component method and experimental laboratory tests on column base plates are also done and presented in this section *(Seco, 2019).*

2.3.1 In-plane bending studies

The first studies were carried out in 1985 at the University of Laval in Canada. In order to estimate the behavior of column base plates, Picard and Beaulieu (1985) developed an experimental investigation on column base plates in order to estimate their mechanical properties when subjected to a combination of an axial force and in-plane bending moment.

In presence of large eccentricities, Picard and Beaulieu (1985) proposed the equation for the ultimate bending moment resistance and concluded that the existing theoretical relation for calculation of moment resistance was conservative.

Another work, by Ermopolous and Stamatopoulos (1996), aimed to develop a relationship between the bending moment and the rotation for different types of connections (size and thickness of the base plate; size, length and location of the anchor bolts; material properties of the different elements; geometry of the concrete block; a level of the applied axial load).

The design procedure for the calculation of the rotation, for a given combination *M+N* (bending moment and axial force), is characterized by an iterative calculation to obtain the neutral axis position and then, the stress distribution. Then, the rotation can be calculated, allowing us to obtain any point from the moment-rotation curve. This calculation procedure is divided into three models, according to the level of the concrete stresses that are developed under the base plate (see Figure 2.4) *(Seco, 2019)*.

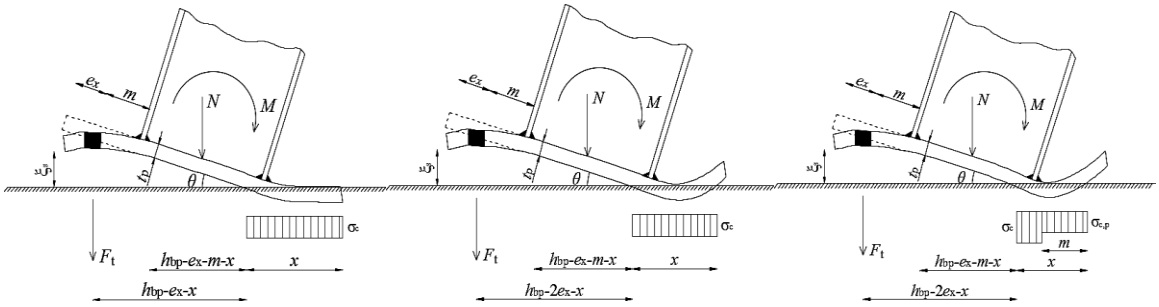

Figure 2.4: Distribution of the stresses for Type models I, II and III *(Seco, 2019)*

Great progress in the study of column base plates subjected to bending moment in major axis direction was made by Jaspart and Vandegans (1998) that proposed a mechanical model to accurately calculate the moment-rotation relationship.

The model was validated against the results obtained from an experimental program carried out at the University of Liège. Test set-up consisted of a steel column welded to a steel base plate, with two different thicknesses, and connected to a concrete block by means of two or four anchors.

To guarantee good contact, a thin layer of the grout was placed between the base plate and the concrete. Specimens were loaded with a combination of a compressive axial force and a bending moment in the direction of a stronger axis.

In the following Table 2.1 the used tests and respective parameters are summarized.

Table 2.1: Test designations (Jaspart and Vandegans, 1998)

Specimen	Number of anchor bolts	Base plate thickness (mm)	Normal force (kN)
PC2.15.100	2	15	100
PC2.15.600	2	15	600
PC2.15.1000	2	15	1000
PC2.30.100	2	30	100
PC2.30.600	2	30	600
PC2.30.1000	2	30	1000
PC4.15.100	4	15	100
PC4.15.400	4	15	400
PC4.15.1000	4	15	1000
PC4.30.100	4	30	100
PC4.30.400	4	30	400
PC4.30.1000	4	30	1000

Moment-rotation curves for different test variations are depicted in the following figures:

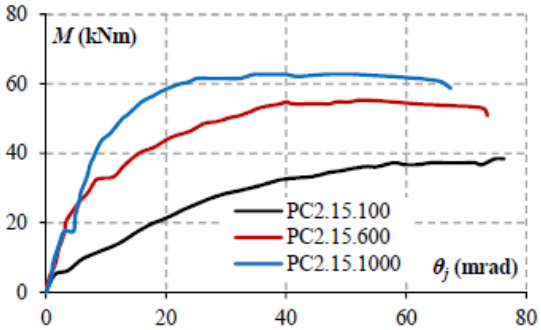

Figure 2.5: Moment-rotation curves for PC2.15 tests *(Seco, 2019)*

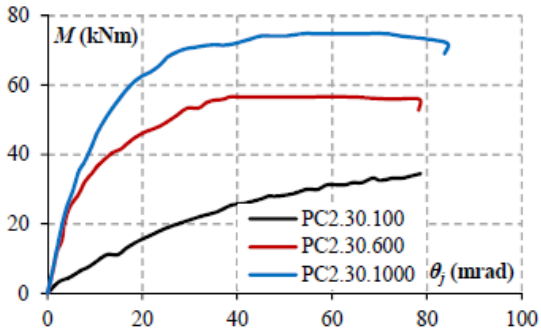

Figure 2.6*:* Moment-rotation curves for PC2.30 tests *(Seco, 2019)*

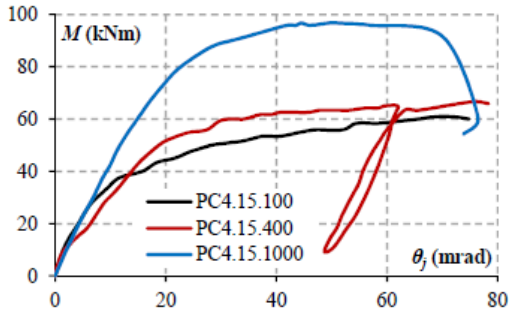

Figure 2.7: Moment-rotation curves for PC4.15 tests *(Seco, 2019)*

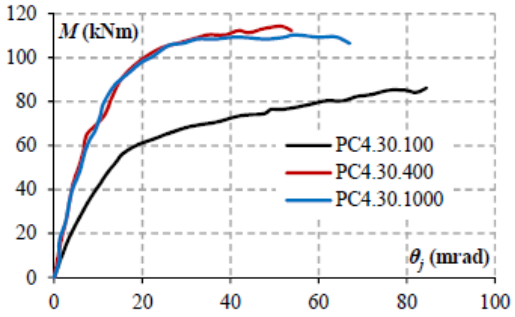

Figure 2.8: Moment-rotation curves for PC4.30 tests *(Seco, 2019)*

From the figures above can be spotted that the bending moment resistance is higher as the compressive force increases. Also, a higher load level means less base plate deformation and thus delaying the failure of the anchor bolts. Tests PC2.30 showed that a thicker base plate leads to higher ultimate resistance of the connection. An important note is that increase of axial force does not always result in higher values of resistance and can also lead to local buckling of a column.

The most rigid and resistant column base plates turned out to be the ones in which applied compressive force is higher as long as the failure occurs on the connection. When yielding/buckling occurs on the column itself, then resistance can decrease as the compression force increases. Results also indicated that column base plates have a high semi-rigid behavior, even when dealing with classical pinned connections, which is positive for the design of building frames.

As previously mentioned, Jaspart and Vandegans (1998) developed an analytical model to predict the resistance of this type of connection. This model was based on the component method (method will be shortly described later in this thesis).

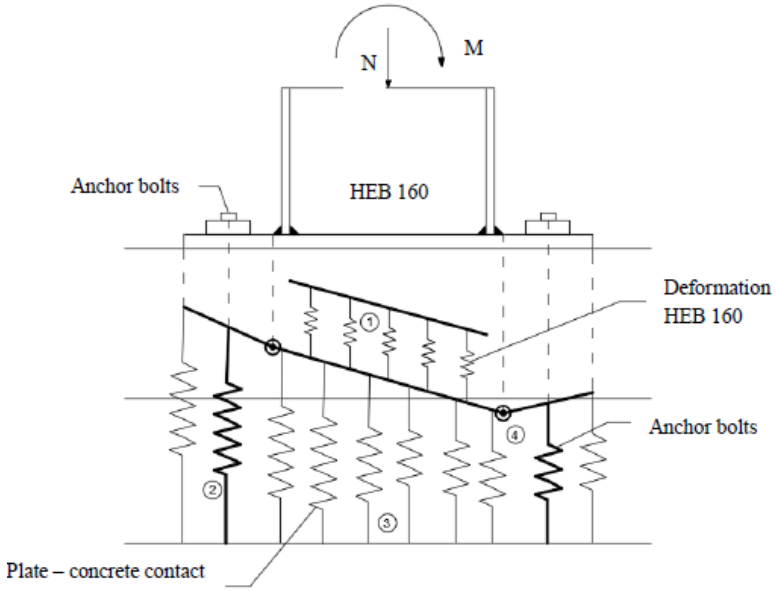

Figure 2.9: Modelling of column bases *(Jaspart and Vandegans, 1998)*

Figure 2.9 represents the model considering the observations made from the experimental results. In the model, springs replace the main components and this model does not take into account the buckling of the flanges and web of the column that might develop.

The moment rotation curves, presented in Figure 2.10 and Figure 2.11, were obtained by the refined model and experimental tests. Although the ultimate bending resistance is accurately estimated by the model, the curves are also satisfactory, especially for PC4.30.400. As can be seen, the rotational stiffness of the connection PC4.15.400 is different from the test. This component is modeled in a simplified way considering Annex J of ENV 1993, the rotation capacity of the connection was not considered either and the modeling of the concrete in compression could probably be improved.

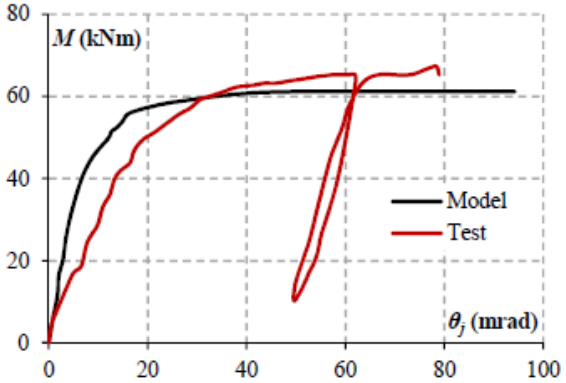

Figure 2.10: Moment rotation curves of PC4.15.400 *(Seco,2019)*

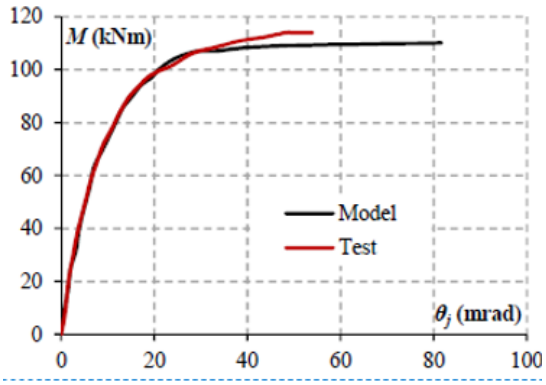

Figure 2.11: Moment rotation curves of PC4.30.400 *(Seco,2019)*

G.N Stamatopoulos and J.Ch. Ermopoulos (2011) carried out the eight specimens and tested them for an in-plane bending moment with a change in a compressive force, and also they made the 3D FEM models of the test specimens that were simulated. A correlation was performed between the experimental and finite element results with the analytical formula proposed by the authors, to verify the accuracy of the obtained analytical results.

The experimental curves were compared against the numerical and analytical ones in order to validate the analytical formula proposed by the authors that relates the moment *M* with the rotation of the connection θ_j.

In Figure 2.12 is shown that the proposed formula is in good agreement with the curves obtained experimentally and by FEM models, for different values of axial force.

The model requires to predefine the value of the rotation θ_j from an iterative procedure presented in Ermopolous and Stamatopoulos (1996), in which the position of the neutral axis must be first calculated. This required pre-calculations are considered as disadvantage of the model.

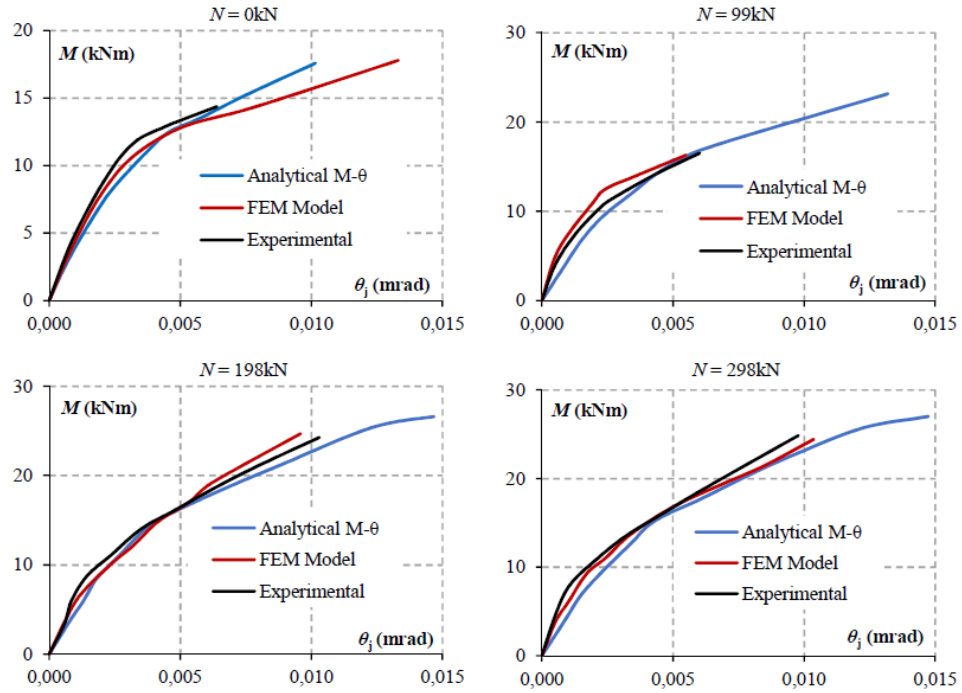

Figure 2.12: Experimental, numerical and analytical moment-rotation curves (SP1 tests) *(Seco, 2019)*

Based on the mentioned studies, Abdollahzadeh and Ghobadi *(2013)* proposed a similar nonlinear model. The existing data was used to compare and validate the model. Figure 2.13 shows the results of the model compared against the experimental and FEM results presented in Stamatopoulos and Ermopolous *(2011).*

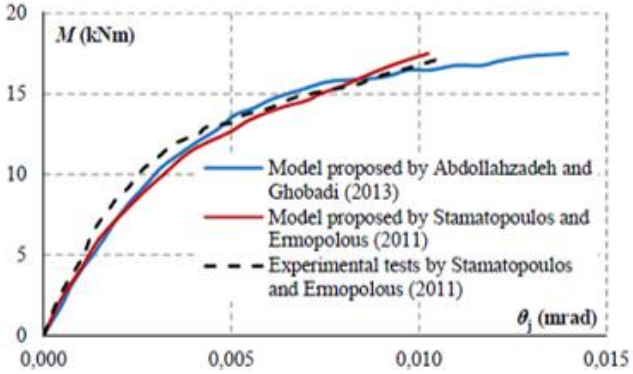

Figure 2.13: Comparison of the moment-rotation curves for test *SP1 (Seco,2019)*

2.3.2 Out-of-plane bending studies

Not so many researches have been made when it comes to a column base connection subjected to an out-of-plane bending moment. The first significant experimental and numerical studies were made by *Lee et al. (2008a)*. Evaluating the *Drake & Elkin* method numerically was the first step, as so as investigating the effects of the relative strength ratio among the connection elements. The experimental study was also

conducted to evaluate the D&E method and to verify the major findings from the numerical study. In the direction of the weak axis, four exposed-type column-base plate connections (two 6-bolt connection and two 4-bolt connection) were produced using notch-tough filler metals (SAC,1997). The effects of shear force and bending moment were also considered.

In short, the conclusion was that the lower values for the strength and rotation capacity were observed for the most flexible base plate due to the early yielding of the base plate. Another conclusion was that the initial rotational stiffness was strongly related to the influence of anchor bolts. Furthermore, another conclusion was that although the D&E method is highly sensitive to the grout compressive strength (f_c), this parameter had no big influence on the variation of the resultant bearing force, later being more dependent on parameters such as the base plate thickness and anchor bolt stiffness.

Build on this work, the University of Michigan conducted an additional test campaign on four exposed-type column base plates to compare and evaluate results obtained from the D&E method, as well as the validity of the numerical parametric study. Unlike the previous method, in this one the influence of anchor bolts, relative strength between the base plate and the anchor bolts, and different filler metal and welding detail was also investigated. The mechanical and geometrical characteristics of specimens tested and calculated numerically are similar (see Table 2.2).

Table 2.2: Tests characteristics (*Lee, Goel and Stojadinovic, 2008b*)

	6-bolt specimen		4-bolt specimen	
	SP 6-1	SP 6-2	SP 4-1	SP 4-2
Number of anchor bolt	6	6	4	4
Base plate thickness (mm)	57	57	57	57
Weld yield strength (N/mm^2)	440	475	440	475
Weld tensile strength (N/mm^2)	525	593	525	593

In Figure 2.14 and Figure 2.15, a comparison between the numerical and experimental lateral force-drift curves is represented. Furthermore, from Figure 2.16 and Figure 2.17 can be concluded that higher stiffness of the anchor bolts from four-bolt tests, led to higher values of tensile bolt forces.

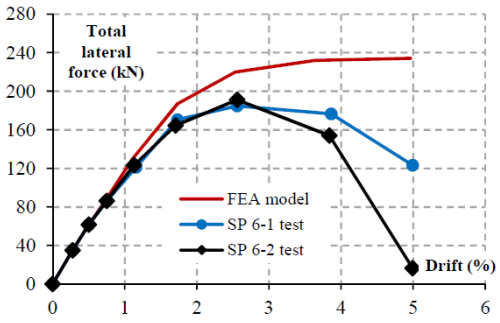

Figure 2.14: Lateral force–drift curve SP6 *(Seco, 2019*

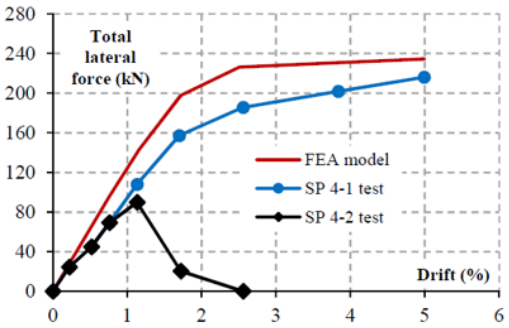

Figure 2.15: Lateral force–drift curve SP4 *(Seco, 2019)*

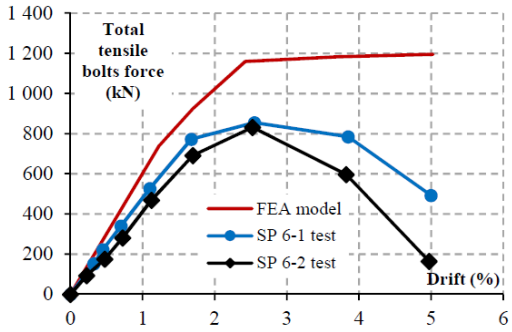

Figure 2.16: Total anchor bolt forces *(Seco, 2019)*

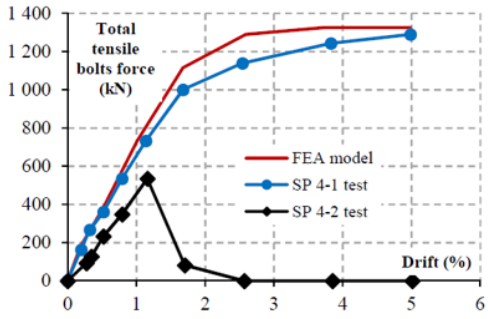

Figure 2.17: Total anchor bolt forces *(Seco, 2019)*

Considering the previous analyzes, it can be concluded that the Drake and Elkin method is not appropriate for predicting the behavior and performance of the column base plate subjected to out-of-plane bending moment.

2.3.3 Biaxial bending studies

An experimental program on column base plates subjected to combination of compressive force and uniaxial/biaxial bending was performed at the Brno University of Technology. The configuration was set-up on a way that column base plates were fixed to the reinforced concrete foundation by means of four anchor bolts. A grout layer was considered between the base plate and the concrete surface and a shear lug was welded to the bottom of the base plate. As shown in Table 2.3, the four specimens had the same geometrical characteristics.

Table 2.3: Adopted geometry and materials for tests *(Seco, 2019)*

Column	HEB 240 $L = 2020$ mm
Base plate dimensions (mm)	440×330×20
Steel grade (column, base plate)	S235
Concrete dimensions (mm)	1500×1000×400
Concrete grade	C16/20
Anchor bolts	M20 8.8
Shear lug	IPE 100 $L = 100$ mm
w^*	160 mm
p^*	340 mm

*w, p – distance between the centre line of the anchor bolts in the yy' and zz' axis direction, respectively.

Primary, the failure occurred due to anchor bolts in tension and yielding of the base plate in bending. Superficial cracks could also be observed on the concrete foundation. The moment-rotation curves are plotted in Figure 2.18 (the curve from Eurocode 3 for the in-plane bending moment is added) and Figure 2.19.

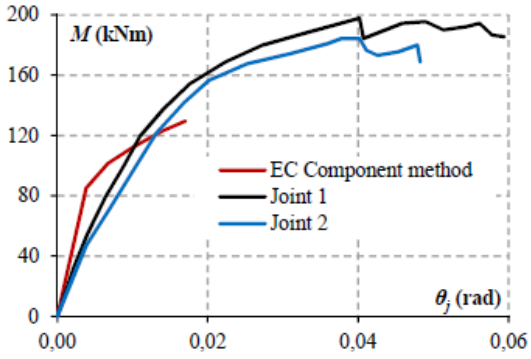

Figure 2.18: Moment-rotation curves M0 *(Seco, 2019)*

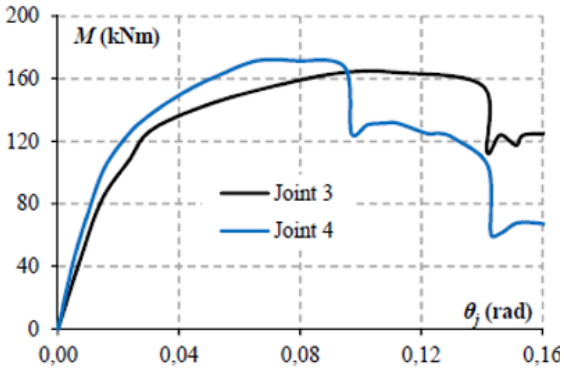

Figure 2.19: Moment-rotation curves M45 (26,56º) *(Seco, 2019)*

Observing the Figure 2.18 it can be seen that the moment-rotation curve of the EC Component method is above the connections curves, which means that the Eurocode approach overestimates the stiffness of column bases until the level of in-plane bending moment reaches the value of 110 kNm, after that point EC3 approach starts to show underestimated resistances. When it comes to the biaxial bending moment, the rotation capacity of the two mentioned specimens is a bit different due to material variability (Figure 2.19).

The numerical study was carried out by Amaral (2014) at the University of Porto, with the primary objective to evaluate the structural behavior of column bases under biaxial loading conditions, and the results were compared with the experimental results presented by *Bajer et al.* (2014).

The comparison of the results was quite satisfactory for both in-plane and biaxial bending. The analytical model based on the component method was proposed, modified on a way that the effective length was chosen as the smallest value of the effective lengths of each possible mechanism for the different available failure modes.

The location of the neutral axis, where the tensile part develops, should be calculated first. Also, the premises are that the anchor bolts row develop its full resistance, the effective area around the web is not taken into account for the compressive resistance, the area under compression cannot cross the *z*-xis of the connection.

For more detail check *Amaral, 2014.*

Afterward, for the resistance under biaxial bending moment, the elliptical curve is proposed (equation 2.1 and Figure 2.20):

$$\left(\frac{M_{j,op}}{M_{j,op,u}}\right)^2 + \left(\frac{M_{j,ip}}{M_{j,ip,u}}\right)^2 = 1 \qquad (2.1)$$

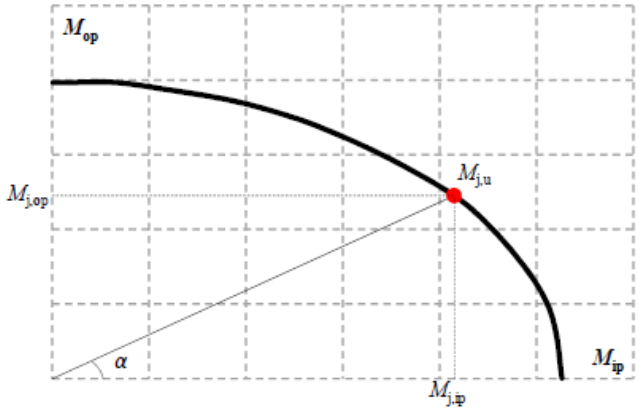

Figure 2.20: Determination of the design moment resistance *M*j,u *(Seco,2019)*

Even though this was a big step forward in researching this area, this approach has proven to be a bit conservative and there is a space for improvement. This model is based on the methodology of Eurocode, and although it has some limitations, it makes it easier and more familiar for engineers to use it *(Seco, 2019)*.

Fasaee *et al.* (2018) carried out the analytical study to address the biaxial capacity and minor-axis capacity of column base connections. Also, a numerical model validated was proposed and validated against experimental results presented in Gomez et al. (2010). Geometry and configuration are presented in Table 2.4.

Table 2.4: Material properties and results of the tests (Fasaee *et al.*, 2018)

Test	Column size[b]	Plate size	Base plate material		Rod material[a]		Axial load	M_{test}	M_{FEM}	M_{FEM}/M_{test}
		b_{bp}, h_{bp}, t_p (mm)	$f_{y,bp}$ (MPa)	$f_{u,bp}$ (MPa)	$f_{y,b}$ (MPa)	$f_{u,b}$ (MPa)	N (kN)	(kNm)	(kNm)	
1	W200×71	356×356×25	278	473	786	1010	0	123	125	1,02
2	W200×71	356×356×25	278	473	786	1010	0	123	125	1,02
4	W200×71	356×356×38	255	468	335	492	411	127	121	0,95
5	W200×71	356×356×25	278	473	786	1010	411	167	169	1,01
6	W200×71	356×356×51	265	497	786	1010	411	187	200	1,07
7	W200×71	356×356×25	278	473	786	1010	690	196	197	1,01
Mean										1,01
COV (coefficient of variation = standard deviation/mean)										0,04

b_{bp}, h_{bp}, t_p = width, height and thickness of the base plate;
f_y, f_u = yield strength and ultimate strength;
M_{test}, M_{FEM} = measured and calculated moment capacities, respectively.

[a] All anchor rods were 19 mm in diameter and placed at 38 mm from the edge of the plate.
[b] The column was fabricated from steel A992.

After validating the numerical models, the study of the behavior under biaxial bending for models corresponding to Tests No. 1 (including Tests No.5 and 7), 4 and 6 was performed. A horizontal displacement was applied at the top of the column with different inclinations: 0º for strong axis bending, 30º, 45º and 60º for biaxial bending, and 90º for weak axis bending (Seco, 2019).

The numerical results were normalized with respect to the uniaxial moment resistances in interaction curves and highlight an elliptical shape that was proposed in the interaction relationship of Equation (2.2).

$$\left(\frac{M_x}{M_{ux}}\right)^2 + \left(\frac{M_y}{M_{uy}}\right)^2 = 1 \tag{2.2}$$

where:

M_x and M_y: the applied in-plane and out-of-plane bending moments and

M_{ux} and M_{uy}: in-plane and out-of-plane bending moment resistances.

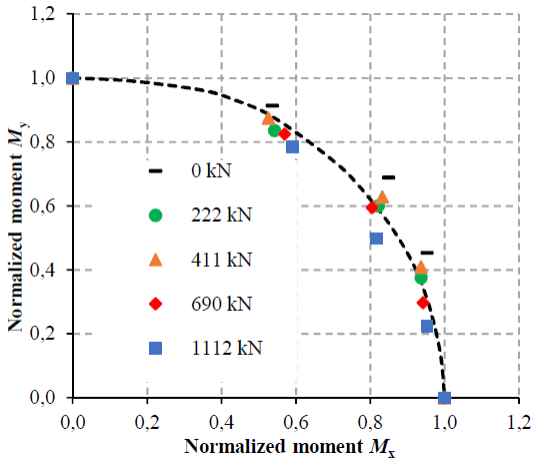

Figure 2.21: Proposed elliptical curve (*Fasaee et al., 2018)*

In conclusion, the model accuracy proved to be good, and the model showed satisfactory results when compared to the numerical and experimental analysis.

2.4 Component method

Studies in the past, as so as the evolution and progress of researchers, have resulted in different calculation methods for predicting the behavior of steel structures. In this sub-chapter only the most common design method nowadays will be presented – the Component method, which is the current design procedure of EN 1993-1-8. Also, the calculations of many software are based on this method.

This method still has some space for improvements such as calculation guidelines for the column base plates subjected to bending moment over a minor axis or especially biaxial bending moments. In this method, the first step is to identify basic components in order to characterize the mechanical properties of each one. After that, it is necessary to assembly component properties to obtain the properties of the whole connection. The final step is the classification of the joint. The components are identified by the loading type (tension, compression, shear) and they are independent of each other behavior.

The main components are:

- base plate in bending and anchor bolts in tension,
- base plate in bending and concrete block in compression,
- the anchor bolts in shear,

- column web and flange in compression.

Resistance F_{rd}, initial stiffness, $S_{j,ini}$, and deformation capacity δ_{Cd}, are the most relevant mechanical properties of the components and they allow to characterize the behavior of the connections (see Figure 2.22).

Depending on the value of $S_{j,ini}$, the joint is classified with the purpose of simplification of the joint behavior under the frame analysis. When the column base is loaded with a bending moment, the anchor bolts in the tensile zone are activated to transfer the applied force and the column base plate is deformed. This deformation consists of the elongation of the anchor bolts and the bending of the base plate. Failure of the tensile zone can be caused either by yielding of the base plate, failure of anchor bolts, or their combination.

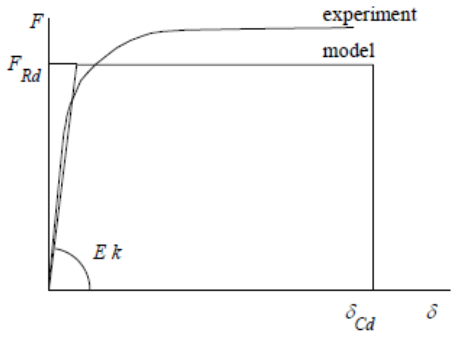

Figure 2.22: Characteristics of the component *(Sokol and Wald, 2000)*

Base plate in bending under tension

The tensile part is replaced by a T-stub, in order to describe its behavior. The T-stub model is based on the similar assumptions as used in beam-to-column connections, with width equal to the effective length l_{eff} in order to create a T-section with the same resistance as the component (see Figure 2.23).

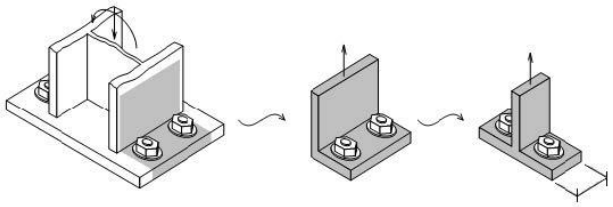

Figure 2.23: Tensile zone and equivalent T-stub for bending moment in strong axis *(Sokol and Wald, 2000)*

When the base plate is thin and more flexible, contact between the edge of the base plate and concrete can occur leading to prying forces, resisted by anchor bolts (see Figure 2.24).

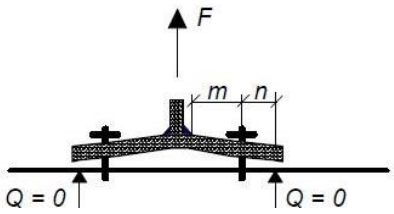

Figure 2.24: Forces applied on the T-stub in tension *(Wald et al., 2014)*

According to the *EN 1993-1-8*, if active length of the anchor bolt (L_b) is smaller than a L_b* (see equation 2.3), prying forces must be taken into account. Otherwise, calculation is done without influence of the prying effect.

$$L_b^* = \frac{8{,}8m^3 A_s n_b}{\sum l_{eff,1} t_{bp}^3} \tag{2.3}$$

Where

m: distance represented in Figure 2.24,
A_s : threaded area of the anchor bolt,
n_b : number of activated anchor bolts rows,
S$l_{eff,1}$: effective length of the T-stub,
t_{bp} : base plate thickness.

And then L_b can be calculated as:

$$L_b = L_{be} + L_{bf} = 8d + L_{bf} \tag{2.4}$$

In Figure 2.25 lengths of *d* and L_{bf} are defined:

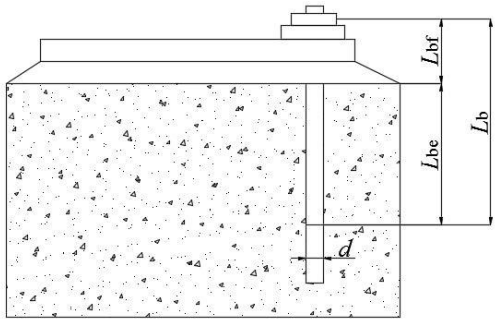

Figure 2.25: Anchor bolt equivalent length *(Seco, 2019)*

Design resistance – $F_{T,Rd}$

The value of the resistance depends on the failure mode of the T-stub. Three collapse mechanisms are possible (see Figure 2.26).

For flexible plate and high resistance of anchor bolts, mode 1 will occur (yielding of the base plate). Mode 2 will occur as a combination of anchor bolts failure and base plate yielding in presence of prying forces. For thick base plates and low anchor bolts resistance, mode 3 should occur. The calculation of the resistance provided by the *EN 1993-1-8* is presented in Table 2.5.

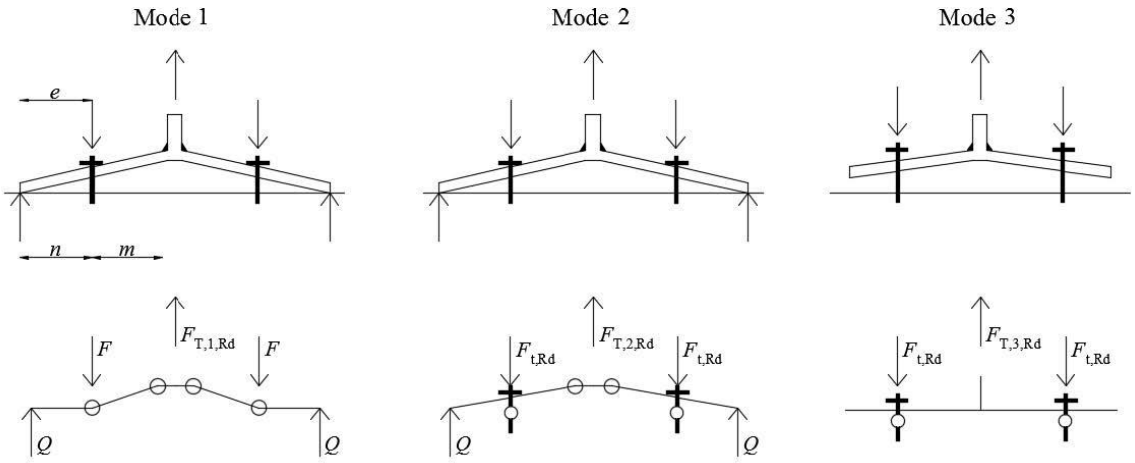

Figure 2.26: Available failure modes for a T-stub in tension (Seco, 2019)

Table 2.5: Design resistance of a T-stub *(Seco,2019)*

	Prying forces ($L_b \leq L_b^*$)		No prying forces
Mode 1	Method 1	Method 2 (alternative)	
	$F_{T,1,Rd}=\frac{4M_{pl,1,Rd}}{m}$	$F_{T,1,Rd}=\frac{(8n-2e_w)M_{pl,1,Rd}}{2mn-e_w(m+n)}$	$F_{T,1\text{-}2,Rd}=\frac{2M_{pl,1,Rd}}{m}$
Mode 2	$F_{T,2,Rd}=\frac{2M_{pl,2,Rd}+n\sum F_{t,Rd}}{m+n}$		
Mode 3	$F_{T,3,Rd}=\sum F_{t,Rd}$		
m and n : distances taken from Figure 2.46 e_w : $d_w/4$ with d_w equal to the diameter of the nut			

The effective length of the T-stub should be chosen according to its failure mode, which is divided into two groups – circular and non-circular patterns (see Table 2.6).

Table 2.6: Effective lengths of a T-stub subjected to strong axis bending *(Seco, 2019)*

	Yield pattern	Effective length
Circular patterns	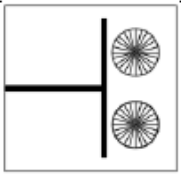	$l_{cp,1}=2\pi m_x$
	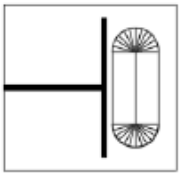	$l_{cp,2}=\pi m_x+w$
	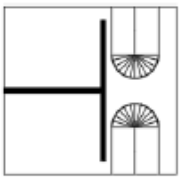	$l_{cp,3}=\pi m_x+2e$

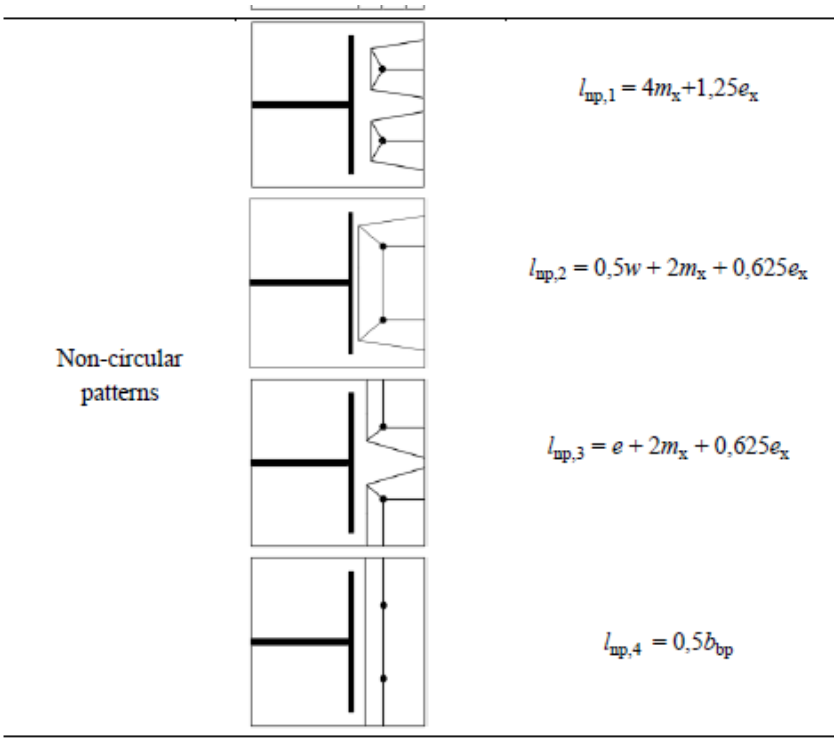

where:

m_x: distance from the center line of the anchor bolt to the flange,
w: the distance between the center line of both anchor bolts in the same row,
e: distance from the center line of the anchor bolts to the edge of the base plate,
e_x: distance from the center line of the anchor bolts to the edge of the base plate,
b_{bp}: base plate width.

Component stiffness – k_T

Again, the stiffness calculation depends on the presence of prying effect, and according to the *EN 1993-1-8*, the stiffness coefficient of an anchor bolt row is:

$$k_T = \frac{1}{\frac{1}{k_{15}} + \frac{1}{k_{16}}} \tag{2.5}$$

And stiffness coefficients can be calculated from:

Presence of prying effect:

$$k_{15} = \frac{0{,}85\, l_{eff}\, t_{bp}^3}{m^3} \tag{2.6}$$

$$k_{16} = 1{,}6\, A_s / L_b \tag{2.7}$$

Absence of prying effect:

$$k_{15} = \frac{0{,}425 l_{\text{eff}} t_{\text{bp}}^3}{m^3} \tag{2.8}$$

$$k_{16} = 2{,}0\, A_s / L_b \tag{2.9}$$

Concrete and grout in compression

The resistance of the compressive area depends mainly on the bearing strength of concrete. For this case, an equivalent T-stub model in compression is used to obtain the resistance values for the combination of the following components (*Seco*, *2019*):

- steel base plate in bending under the bearing pressure of the foundation,
- concrete and/or grout in bearing.

Design resistance – $F_{c,Rd}$

According to the *EN 1993-1-8* the design resistance of the T-stub flange in compression can be calculated with:

$$F_{c,Rd} = f_{jd}\, b_{\text{eff}}\, l_{\text{eff}} \tag{2.10}$$

with

f_{jd}: design bearing strength of concrete,
b_{eff}: effective width of the T-stub,

$$b_{\text{eff}} = \begin{cases} t_f + 2c & \text{for large projection} \\ \frac{h_{bp} - h_c}{2} + t_f + c & \text{for short projection} \end{cases}$$

l_{eff} : effective length of the T-stub.

$$l_{\text{eff}} = \begin{cases} b_c + 2c & \text{for large projection} \\ b_{bp} & \text{for short projection} \end{cases} \tag{2.11}$$

c: additional bearing width:

$$c = t_{bp} \sqrt{\frac{f_{yd}}{3 f_{jd}\, \gamma_{M0}}} \tag{2.12}$$

t_{bp}: thickness of the base plate,
$f_{y,bp}$: yield strength of the base plate,
γ_{M0} : safety coefficient, taken equal to 1.

The flexible base plate was replaced by an equivalent rigid plate under the flange in compression with dimensions b_{eff} and l_{eff} in order to model the behavior of the component (Equation (2.10). The pressures transferred to the T-stub are assumed to be uniformly distributed on the equivalent area of the T-stub in compression as shown in Figure 2.27 (*Seco*, *2019*):

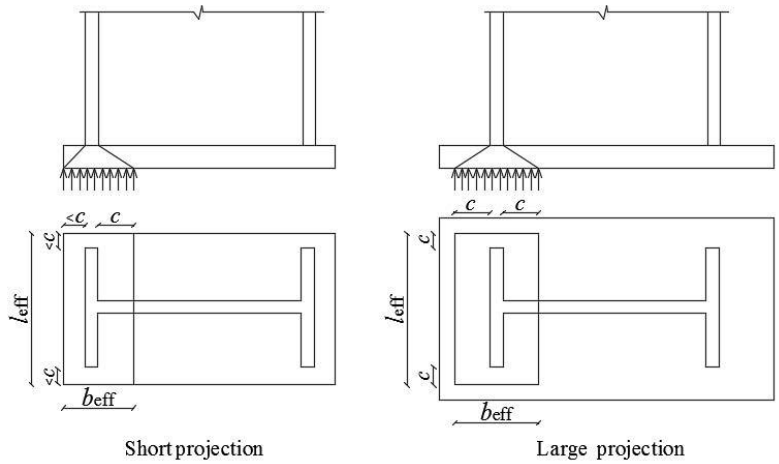

Figure 2.27: Equivalent area of a T-stub in compression *(EN 1993-1-8)*

The pressure on the effective bearing area should not be higher than the design bearing strength (f_{jd}):

$$f_{jd} = \beta_j \alpha_{bf} f_{cd} \tag{2.13}$$

with

βj : foundation joint material coefficient, equal to 2/3 when the characteristic strength of the grout is not less than 0,2 times the characteristic strength of the concrete foundation and the grout thickness is not greater than 0,2 times the smallest width of the steel base plate. For cases where the thickness of the grout is more than 50 mm, the characteristic strength of the grout should be at least the same as that of the concrete block,

and:

$$\alpha_{bf} = \min\left[1+\frac{d_f}{\max(h_{bp},b_{bp})};1+2\frac{e_h}{h_{bp}};1+2\frac{e_b}{b_{bp}};3\right] \tag{2.14}$$

$$f_{cd} = \frac{\alpha_{cc} f_{ck}}{\gamma_c} \tag{2.15}$$

where

α_{cc}: is considered equal to 1,

γ_c: is equal to 1,5

d_f: is the depth of the concrete foundation

e_h and e_b: are the distances from edge of the concrete foundation until the edge of the base plate in two opposite directions.

Component stiffness -k_C

The compression stiffness coefficient and stiffness coefficient k_{13} should be taken as equal according to the *EN 1993-1-8*, then:

$$k_C = k_{13} = \frac{E_c \sqrt{b_{eff}\, l_{eff}}}{1{,}275E} \tag{2.16}$$

where

E_c : concrete elastic modulus,
E : steel elastic modulus,
b_{eff} : effective width,
l_{eff} : effective length.

Column flange and web in compression

The design resistance of the column flange and web in compression can be calculated from:

$$F_{c,fc,Rd} = \frac{M_{c,Rd}}{(h_c - t_{fc})} \tag{2.17}$$

with

$M_{c,Rd}$: design moment resistance of the column cross-section that in presence of class 1 can be taken as:

$$M_{C,Rd} = M_{pl,Rd} = \frac{W_{pl,y} f_y}{\gamma_{M0}} \tag{2.18}$$

h_c : column cross section height
t_{fc} : column flange thickness,
$W_{pl,y}$: column plastic section modulus (strong-axis).

Besides that, the resistance of column bases under pure compression is obtained according to cl. 6.2.8.2. of the *EN 1993-1-8*. The model assumes that the design resistance $N_{j,Rd}$ is equal to the sum of the design resistance given by three equivalent T-stubs that do not overlap each other (see Figure 2.28).

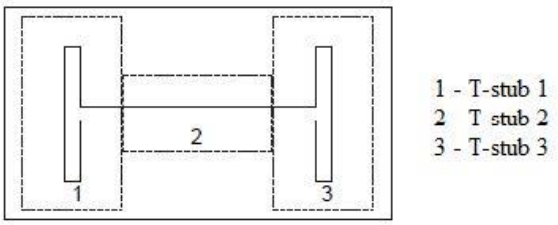

Figure 2.28: T-stubs under compression *(EN 1993-1-8)*

$$N_{j,Rd} = F_{C,Rd,1} + F_{C,Rd,2} + F_{C,Rd,3} \quad (2.19)$$

Firstly, the design resistance and stiffness of each mentioned component should be calculated, and after that calculation proceeds with the assembly of the mechanical properties to obtain the overall properties of the connection. For the design of the column base, $M_{j,Rd}$, the loading case must be defined within the following considered cases:

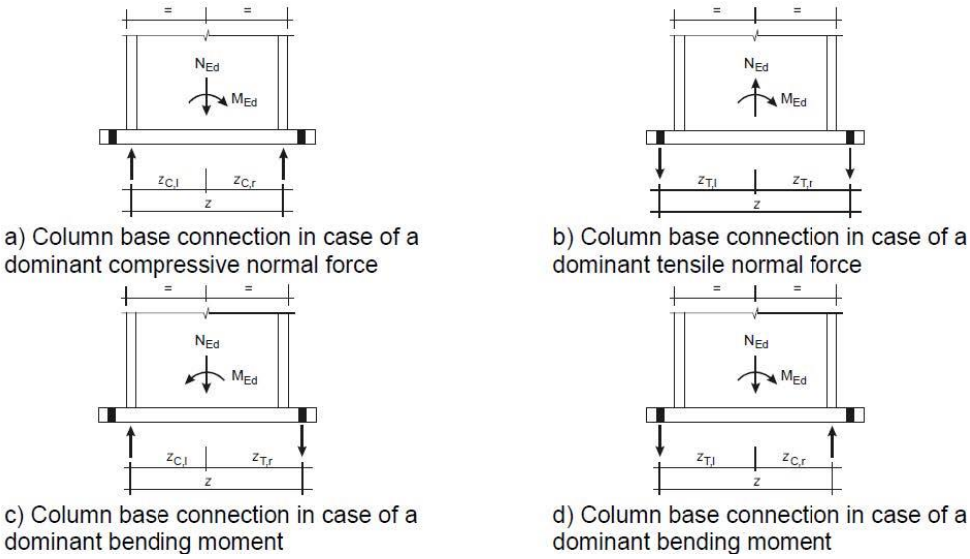

Figure 2.29: Mechanical models of resistance for bending about the strong axis *[EN 1993-1-8]*

For the represented cases in Figure 2.29, failure occurs due to:

a) – The collapse of the connection is due to the concrete failure (axial force only).

b) – Dominant tension axial force which leads to tension in both rows of anchor bolts. Failure occurs due to yielding of the bolts or because of a plastic mechanism in the base plate

c) & d) – Dominant bending moment leading to tension in one anchor bolts row and the compression in the concrete. The failure occurs due to yielding of the bolts or due to a plastic mechanism in the base plate

Thus, when calculating $M_{j,Rd}$, the absence of prying forces should be considered when calculating $F_{T,Rd}$, and $F_{C,Rd}$ is equal to the minimum value of $F_{C,Rd}$ and $F_{c,fc,Rd}$.

From EN 1993-1-8, the following Table 2.7 summarizes the calculation of the design moment resistances for the available cases:

Table 2.7: Design moment resistance of column base plates

Loading	Lever arm z	Design moment resistance $M_{j,Rd}$	
Left side in tension Right side in compression	$z = z_{T,l} + z_{C,r}$	$N_{Ed} > 0$ and $e > z_{T,l}$ The smaller of $\frac{F_{T,l,Rd}z}{z_{C,r}}+1$ and $\frac{-F_{C,r,Rd}z}{z_{T,l}}-1$	$N_{Ed} \leq 0$ and $e \leq -z_{C,r}$
Left and right side in tension	$z = z_{T,l} + z_{T,r}$	$N_{Ed} > 0$ and $0 < e < z_{T,l}$ The smaller of $\frac{F_{T,l,Rd}z}{z_{T,r}}+1$ and $\frac{F_{T,r,Rd}z}{z_{T,l}}-1$	$N_{Ed} > 0$ and $-z_{T,r} < e \leq 0$ The smaller of $\frac{F_{T,l,Rd}z}{z_{T,r}}+1$ and $\frac{F_{T,l,Rd}z}{z_{T,l}}-1$
Left side in compression Right side in tension	$z = z_{C,l} + z_{T,r}$	$N_{Ed} > 0$ and $e \leq -z_{T,r}$ The smaller of $\frac{-F_{C,l,Rd}z}{z_{T,r}}+1$ and $\frac{F_{T,r,Rd}z}{z_{C,l}}-1$	$N_{Ed} \leq 0$ and $e > z_{C,l}$
Left and right side in compression	$z = z_{C,l} + z_{C,r}$	$N_{Ed} \leq 0$ and $0 < e < z_{C,l}$ The smaller of $\frac{-F_{C,l,Rd}z}{z_{C,r}}+1$ and $\frac{-F_{C,r,Rd}z}{z_{C,l}}-1$	$N_{Ed} \leq 0$ and $-z_{C,r} < e \leq 0$ The smaller of $\frac{-F_{C,l,Rd}z}{z_{C,r}}+1$ and $\frac{-F_{C,r,Rd}z}{z_{C,l}}-1$
$M_{Ed} > 0$ is clockwise and $N_{Ed} > 0$ is tension $e = \frac{M_{Ed}}{N_{Ed}} = \frac{M_{Rd}}{N_{Rd}}$			

2.5 Concluding remarks

Looking at the provided materials, one can conclude there are big gaps in the design guidelines, especially when it comes to biaxial bending analysis.

The out-of-plane analytical models are based on the principles of the component method. The results obtained under these conditions turned out to be conservative.

The existing theoretical models for biaxial bending are based on a simplified approach, using an elliptical interaction curve.

In buildings, under 3D loading, column bases are commonly subjected to biaxial loading and more attention should be paid to this topic.

3 PRIMARY REFERENCE – *Seco's* model

Seco (2019) carried out the campaign of six experimental tests on steel column base plates connected to a concrete block, to study the behavior of this type of connection and validate the numerical and analytical model.

3.1 Experimental work

The experimental tests were done at the *Laboratoire de Génie Civil et Génie Mécanique* – INSA de Rennes. The main variables were the base plate thickness and the loading conditions: major/minor axis bending and biaxial bending moment. The base plates were in direct contact with the concrete block and connected to it using washer plates without any addition of grout or embedded plates (*Seco, 2019*).

3.1.1 Test set-up

All experimental tests used the same set-up. The column was positioned horizontally, working as a cantilever beam, fixed to a concrete block using four fasteners and loaded vertically by a load-jack at a distance of 1250 mm from the center of portal frame A (see Figure 3.1) (*Seco, 2019*). The concrete foundation was supported by two portal frames and at the level of the portal A it was placed on the top of two neoprene supports. Lateral torsional buckling was prevented by lateral supports located at mid-length of the column.

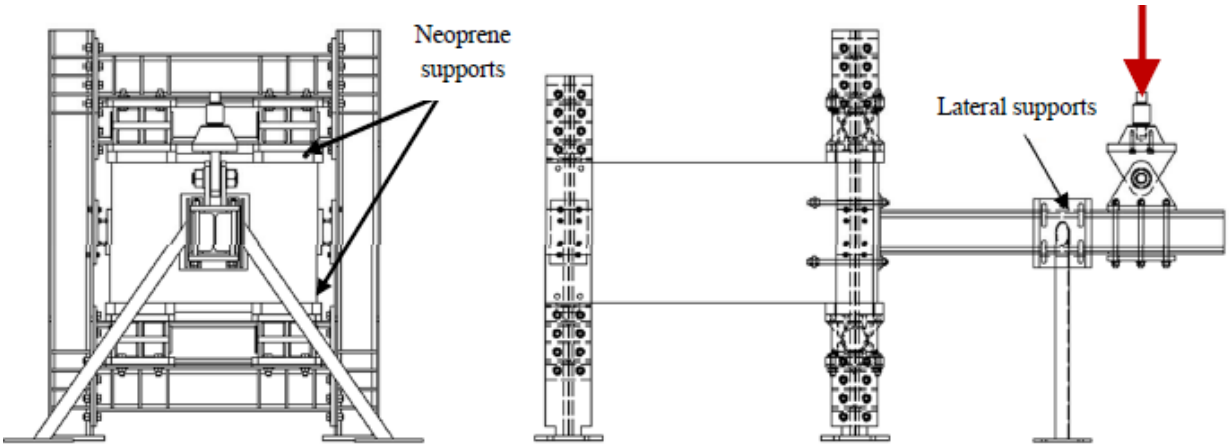

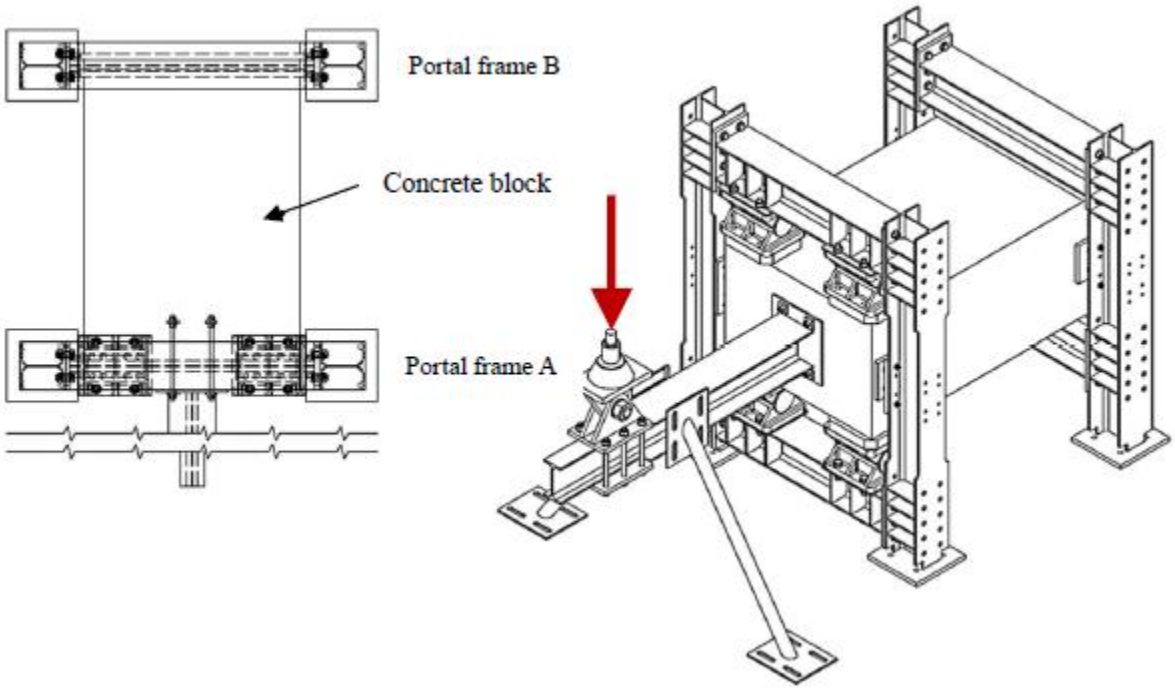

Figure 3.1: Test set-up for in-plane bending moment *(Seco, 2019)*

For the loading cases over the weaker axis and biaxial bending moment, the specific test set-up was used in which the column was divided into two parts. The parts of the column were connected by two bolted circular plates which allowed rotation of 90° and 45°degrees (see Figure 3.2 and see Figure 3.3-I) in order to simulate mentioned loading cases.

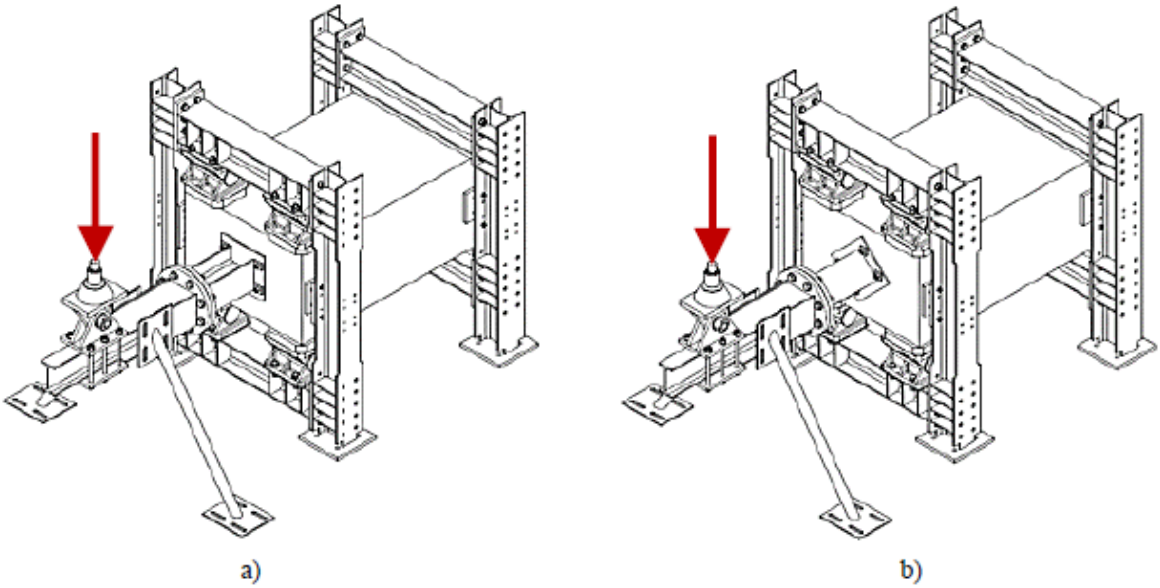

Figure 3.2: Test set-up for out-of-plane (a) and biaxial (b) bending moment *(Seco, 2019)*

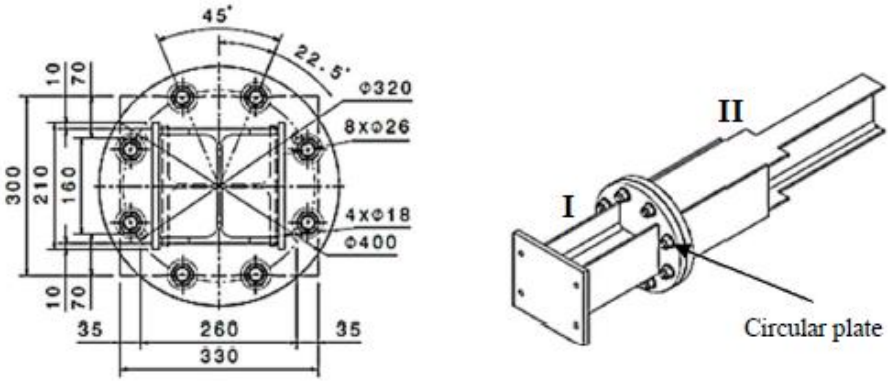

Figure 3.3: Assembly for out-of-plane and biaxial bending moment tests *(Seco, 2019)*

Specimens were loaded by a vertical force applied at the top of the column and increased until failure, generating a bending moment at the level of the connection (*Seco*, *2019*).

The configuration of the tested specimens is shown in detail in Figure 3.4 and the geometrical and mechanical characteristics are represented in Table 3.1.

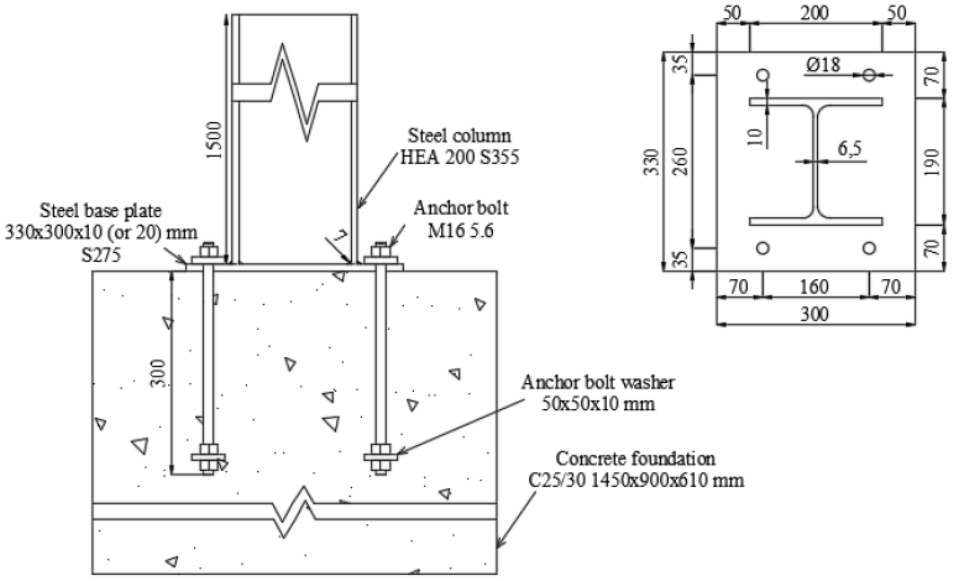

Figure 3.4: Tested column base plate configuration (dimensions in mm) *(Seco, 2019)*

Table 3.1: Identification of the column base plates test specimens (*Seco, 2019)*

Test ID	Loading conditions	Column profile	Column steel grade	Base plate thickness t_p (mm)	Base plate steel grade
SPE1-M0	In-plane bending	HEA 200	S355	10	S275
SPE2-M0	In-plane bending			20	
SPE1-M90	Out-of-plane bending			10	
SPE2-M90	Out-of-plane bending			20	
SPE1-M45	Biaxial bending			10	
SPE2-M45	Biaxial bending			20	

3.1.2 Instrumentation and materials

During the experimental tests, different measured values were monitored by LVDT's (linear variable differential transformer):

- vertical displacement of the column and the concrete block,
- horizontal displacement of the base plate,
- vertical force applied at the top of the column,
- axial strains at the base of the column steel profile.

Raw materials used for specimen fabrication have been tested in order to define its actual properties *(Seco, 2019).*

3.1.3 Testing procedure

Specimens were loaded by a vertical force, which was divided into elastic and plastic phases. The monotonic vertical force produced bending moment over the major and minor axis, as well as biaxial bending moment. For all specimens (two specimens with different base plate thickness for each loading type) the maximal forces applied during tests are shown in Table 3. 2.

Table 3.2: Maximal forces during tests (Seco, 2019)

Test ID	Applied vertical force (kN)		
	Elastic phase 1	Elastic phase 2	Plastic phase
SPE1-M0	7,5	15,0	37,6
SPE2-M0	10,0	25,0	42,1
SPE1-M90	6,0	12,0	28,9
SPE2-M90	8,5	20,0	35,0
SPE1-M45	7,5	15,0	34,2
SPE2-M45	10,0	20,0	41,1

3.1.4 Experimental results

The failure occurred due to the rupture of one or two activated anchor bolts in tension (see Table 3.3), while yielding of the base plate occurred only for specimens with a base plate thickness of 10 mm.

Table 3.3: Failure modes for SPE tests (*Seco, 2019*)

Test ID	Yielded elements	Failure mode
SPE1-M0	Anchor bolts/base plate	Anchor bolt (one)
SPE2-M0	Anchor bolts	Anchor bolts (two)
SPE1-M90	Anchor bolts/base plate	Anchor bolt (one)
SPE2-M90	Anchor bolts/column	Anchor bolt (one)
SPE1-M45	Anchor bolts/base plate	Anchor bolt (one)
SPE2-M45	Anchor bolts	Anchor bolt (one)

Figure 3.5 shows the curves of the forces applied by the load-jack as a function of the displacements measured for all tests.

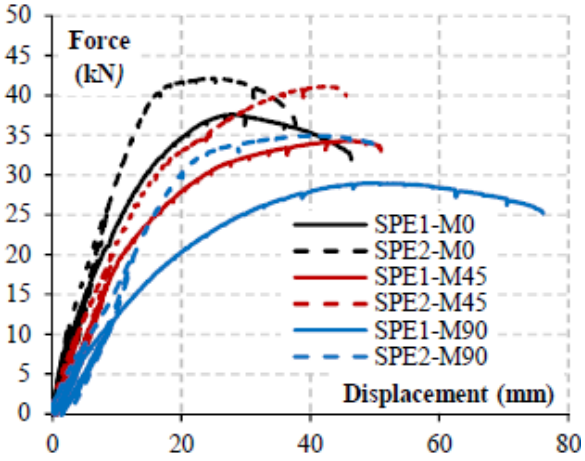

Figure 3.5: Force displacement curves for all tests *(Seco, 2019)*

These curves highlight the influence of the base plate thickness and the orientation of the applied bending moment on the deformability of the connection (*Seco*, *2019*). The maximum displacement is reached for thinner base plates (10 mm) because the yielding of the base plate occurs. When it comes to the direction of the applied load, the biggest displacement was observed in the M90 test series, also for the base plate thickness of 10 mm.

Also, the moment-rotation curves for all specimens were illustrated, where the rotation of the connection (θj) was calculated based on the displacements provided by LVDT's (see *Seco,2019* for more detail).

Resistance, initial stiffness and rotation capacities of SPE test series are summarized in Table 3.4, where the strong influence of base plate thickness can be seen for SPE2-M0 when it comes to Initial stiffness.

Table 3.4: Resistance, initial stiffness and rotation capacities of SPE test series *(Seco, 2019)*

Test	Plastic bending moment $M_{j,pl}$ (kNm)	Ultimate bending moment $M_{j,u}$ (kNm)	Initial stiffness $S_{j,ini}$ (kNm/rad)	Rotation capacity $\theta_{j,u}$ (mrad)
SPE1-M0	37,7	43,2	4117,4	44,7
SPE2-M0	42,9	48,5	7189,9	33,2
SPE1-M90	28,2	33,3	2028,7	69,5
SPE2-M90	35,9	40,2	3120,5	48,1
SPE1-M45	32,0	39,4	2440,5	62,7
SPE2-M45	36,6	47,3	3205,0	54,8

By increasing the base plate thickness, bending moment resistance, and the initial stiffness of the connection increases for all applied loads (especially when it comes to initial stiffness of SPE2-M0), but rotation capacity decreases and it affects the redistribution of the internal forces of the anchoring system as well. Bigger distance between the centers of compression and tension (z) also results in an increase of the initial stiffness and bending moment resistance of the connection.

The base plate thickness and the orientation of the bending moment have limited influence on the behavior of the connection after reaching the maximum force as the necking of the anchor bolts develops in these cases (*Seco, 2019*), and those parameters affect the spread of the compressive area.

3.2 Numerical work

The experimental results were compared against numerical ones, created with the Finite Element software ABAQUS. Also, the additional parametric studies were presented in order to investigate the influence of specific parameters.

3.2.1 Model definition

All connection components except the reinforcing bars were modeled as three-dimensional deformable solids using eight-node linear brick elements (*Seco, 2019*), while concrete reinforcement was modeled with two-node linear truss elements. The measured dimensions of the tested specimens were used in the numerical model.

The properties of the materials were adopted from the experimental stress-strain relationships which were obtained by laboratory tests.

3.2.2 Procedure

The load was applied in the two following steps. Firstly, the contact interactions between the elements and the boundary conditions needed to be set up. Secondly, the loading conditions from the experimental tests had to be reproduced.

For that, a displacement perpendicular to the center line of the column steel profile was applied at the location of the load-jack. Therefore, an increase of the bending moment at the column base plate with the direction of the applied displacement proceeded until failure.

The third step (the initial step) is necessary when models are subjected to a combination of axial force and bending moment in order to applicate axial force and displacement (bending moment) successfully.

Since the contact interactions between elements strongly affect the computing process and interactions in ABAQUS are characterized as step dependent, it must be defined correctly. To create it, a contact pair between two rigid or deformable three-dimensional surfaces had to be defined (*Seco, 2019*), so several contact interactions were defined in the models (see *Seco, 2019* for more detail).

According to the importance of the elements, different mesh sizes were adopted. Thus, anchor bolts, washers, embedded plates, base/end plates, the layer of concrete material in contact with the anchor bolts and welds were calculated with smaller mesh size, while for other elements coarser mesh was used during the calculation (see Figure 3.6)

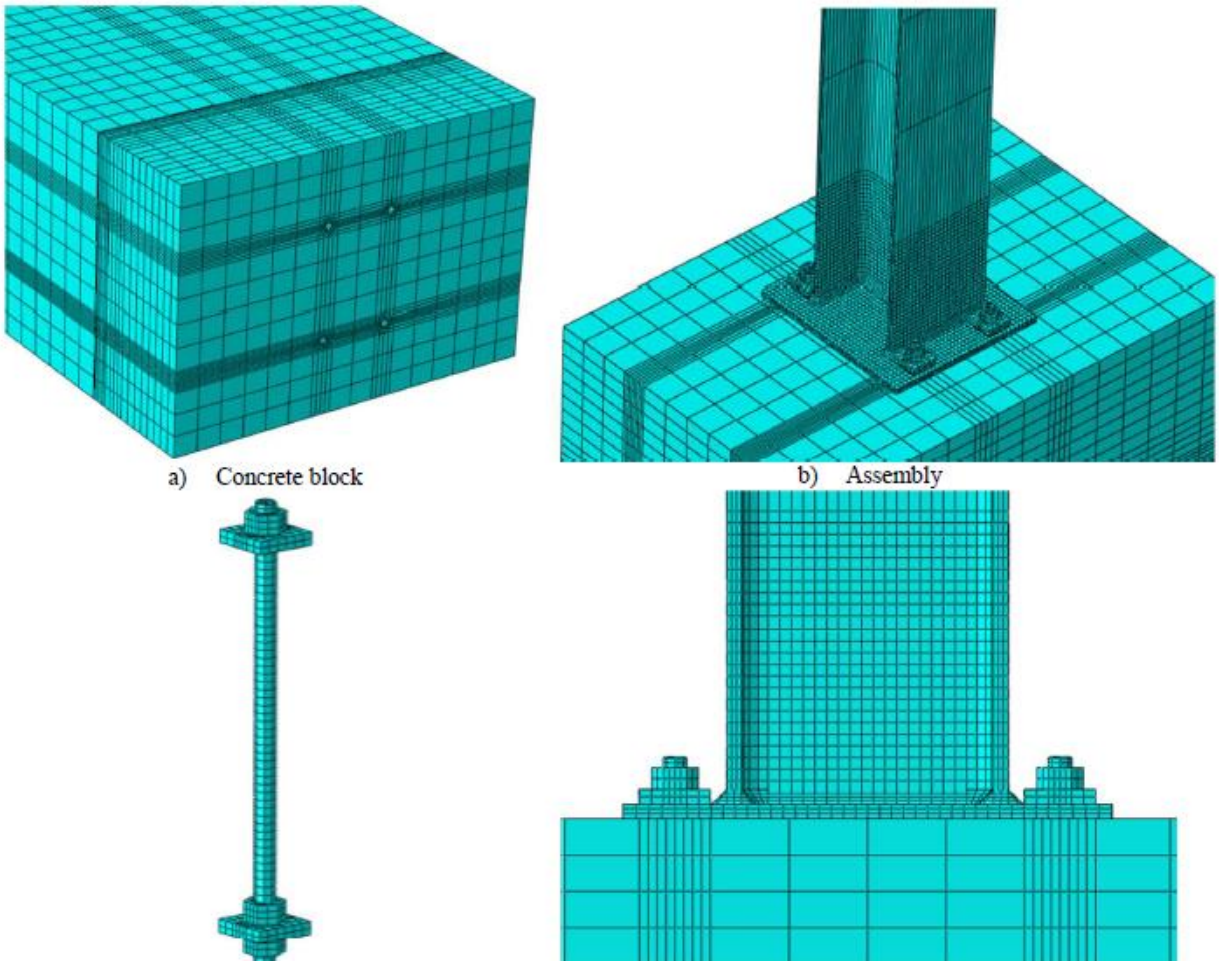

Figure 3.6: Meshing of the elements of the column base plate *(Seco, 2019)*

3.2.3 Comparing results

The comparison of the results is given in Table 3.5 and the numerical simulations are in good agreement with the experimental data for all specimens.

Table 3.5: Comparison of the plastic resistances and initial stiffness from the numerical models and experimental tests (Seco, 2019)

Test	Experimental		Numerical		Exp/Num	
	Initial stiffness $S_{j,ini,exp}$ (kNm/rad)	Plastic bending moment $M_{j,pl,exp}$ (kNm)	Initial stiffness $S_{j,ini,num}$ (kNm/rad)	Plastic bending moment $M_{j,pl,num}$ (kNm)	$S_{j,ini}$	$M_{j,pl}$
SPE1-M0	4117,4	37,7	4163	35,1	0,99	1,07
SPE2-M0	7189,9	42,9	7536	46,2	0,95	0,93
SPE1-M90	2028,7	28,2	2061	26,4	0,98	1,07
SPE2-M90	3120,5	35,9	2712	37,9	1,15	0,95
SPE1-M45	2440,5	32,0	2853	32,5	0,86	0,98
SPE2-M45	3205,0	36,6	4571	38,2	0,70	0,96

In Table 3.6 the comparison of the yielded elements and the failure modes obtained numerically and experimentally is represented.

Table 3.6: Comparison of the yielded elements and failure modes from the numerical models and experimental tests (*Seco*, 2019)

Test	Experimental		Numerical	
	Yielded elements*	Failure mode	Yielded elements*	Failure mode
SPE1-M0	AB/BP/W	AB	AB/BP/C/W	AB
SPE2-M0	AB	AB	AB/BP	AB
SPE1-M90	AB/BP/C/W	AB	AB/BP/C/W	AB
SPE2-M90	AB/C	AB	AB/BP	AB
SPE1-M45	AB/BP/W	AB	AB/BP/C/W	AB/W
SPE2-M45	AB	AB	AB/W	AB

***AB**: anchor bolts yielding due to tension and bending; **BP**: base plate yielding due to bending; **C**: column yielding due to bending; **W**: weld yielding due to bending.

Depending on the direction of the applied bending moment, it is concluded that for all specimens, the failure obtained numerically and experimentally is due to the rupture of one or two activated anchor bolts (*Seco, 2019*).

The comparison between numerical and experimental results, when it comes to bending resistance and the ultimate rotation capacity, is shown in Table 3.7. Despite the fact that the numerical model underestimates the ultimate rotation capacity and little deviations were observed in that area, results are in good agreement.

Table 3.7: Comparison of the numerical and experimental maximum bending resistances and rotation capacities *(Seco,2019)*

Test	Experimental		Numerical		Exp/Num	
	Maximum bending moment $M_{j,u,exp}$ (kNm)	Ultimate rotation capacity $\theta_{j,max,exp}$ (mrad)	Maximum bending moment $M_{j,u,num}$ (kNm)	Ultimate rotation capacity $\theta_{j,max,num}$ (mrad)	$M_{j,u}$	$\theta_{j,max}$
SPE1-M0	43,2	44,7	41,5	45,1	1,04	0,99
SPE2-M0	48,5	33,2	50,8	35,3	0,95	0,94
SPE1-M90	33,3	69,5	32,4	63,4	1,03	1,10
SPE2-M90	40,2	48,1	41,1	45,7	0,98	1,05
SPE1-M45	39,4	62,7	39,0	60,1	1,01	1,04
SPE2-M45	47,3	54,8	45,7	52,2	1,04	1,05

Furthermore, the axial strain obtained numerically was compared against the experimental measurements for specimens SPE1-M90 and SPE2-M90 with satisfactory results.

Finally, the conclusions were that the resistance, initial stiffness and rotation capacity predicted numerically are in good agreement with experimental results with deviations under 30%. The yielded elements and failure modes are similar and the strain distribution at the base plate of the column flanges for M90 specimens was correctly predicted by the numerical model.

3.3 Parametric studies

Several parameters were investigated to study their effect on the connection, such as base plate thickness, the column steel profile, the diameter and an arrangement of the anchor bolts. The connection was subjected to a combination of tensile/compressive axial force and bending moments over the major and minor axis, as well as biaxial bending moment.

Six configurations were studied, and their geometry is represented in Table 3.8. The nominal characteristics of the materials were used, with a weld throat thickness of 7 mm.

Table 3.8: Geometries of the parametric study (*Seco, 2019*)

Configuration	Column steel profile	Base plate thickness t_p (mm)	Anchor bolt diameter (mm)	e (mm)	e_x (mm)	p (mm)	w (mm)
P1	HEA 200	10	16	70	35	260	160
P2	HEA 200	20	16	70	35	260	160
P3	IPE 200	10	16	40	35	270	80
P4	IPE 200	20	16	40	35	270	80
P5	HEA 200	10	20	70	35	260	160
P6	HEA 200	20	20	70	35	260	160

Numerical analysis showed that the failure mode highly depends on the level of the applied axial force and the direction of the bending moment. The higher the axial force is, the higher is moment resistance and initial stiffness, no matter the orientation of the bending moment. The previous sentence is accurate only for axial forces lower than ≈0.5Nply. Also, a higher compressive axial force can cause local instabilities/yielding on the column flanges, which results in lower resistance and initial stiffness of the connection. Cross-sections whose geometry increases the lever arm, shows the higher moment resistance when it comes to dominant out-of-plane bending. Also, initial stiffness and the bending resistance of the connection is increased for higher anchor bolts diameters for the cases where failure mode happens due to anchor bolts in tension.

3.4 Analytical model

Seco, 2019 proposed an analytical model for column base plates connected to the base plate with four anchor bolts. The model is based on the Eurocode's Component Method and is compared to the abovementioned experimental and numerical results. Two variations of the model were presented – simplified and full analytical model (resistance in compression considers effective area around the column web). Equal to the Component Method, connection is considered as a set of basic components, and the calculation procedure consists in the following steps:

1. Identification of the individual components in tension and compression,
2. characterization of the individual resistance for each component,
3. assembly of the resistances of the components to calculate the overall resistance.

In the analytical model the sources of resistances are divided into two groups:

- the tensile components (the base plate in bending and the anchor bolts in tension),

- the components in compression (the concrete in compression, the base plate in bending under the bearing pressure on the foundation and the column in compression).

Depending on the load, the connections can work in two different modes, with a dominant bending moment and with dominant normal tensile/compressive force.

- bending moment is dominant: a tensile and a compressive area are identified and their behavior is modeled by T-stubs in compression/tension. For the full analytical model, the resistance of the web T-stub in compression is added *(Seco, 2019),*
- the normal tensile/compressive force is dominant: the connection is fully under compression or tension. The resistance of the connection is reached when either the T-stub in compression fails (for the full analytical model, a third T-stub is considered corresponding to the web of the column), or the resistance of the T-stub in tension is attained *(Seco, 2019),*

3.4.1 In-plane bending moment

The analytical model considers that the connections can work according to four distinct behavior types (see Figure 3.7), with certain differences between simplified and full analytical model. This allows to simplify the application of the calculation procedure and depending on the level of the applied axial force N, the model is divided as shown in the following figure.

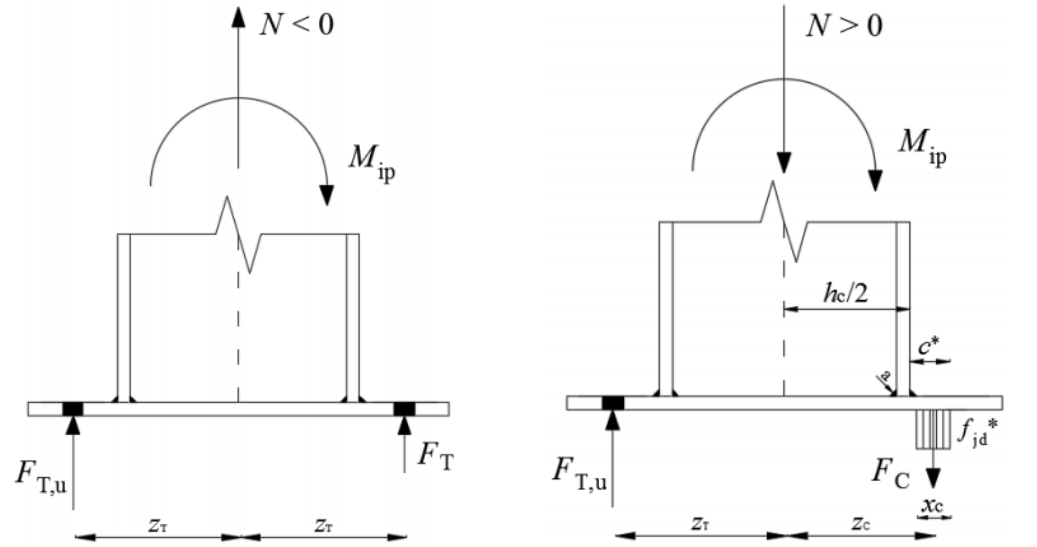

a) Dominant tensile force – behaviour type 1

b) Dominant bending moment with critical tensile force – behaviour type 2

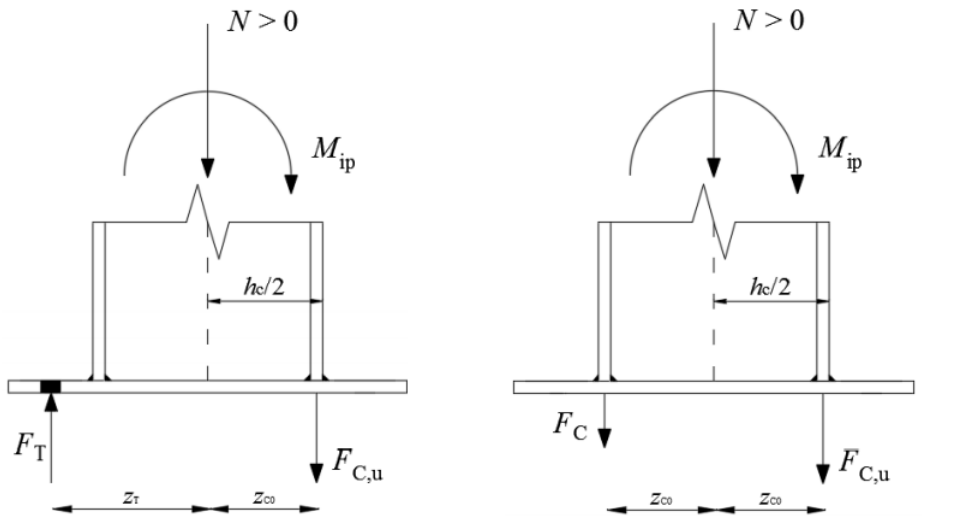

c) Dominant bending moment with critical compressive force – behaviour type 3

d) Dominant compressive force – behaviour type 4

Figure 3.7: Mechanisms considered in the full analytical model *(Seco, 2019)*

The validity domains of the abovementioned mechanisms are summarized below:

Table 3.9: Validity range of the mechanisms of the simplified analytical model (*Seco, 2019*)

Behaviour type	Loading	Range of validity
1	Dominant tensile force	$-N_{T,u} \le N \le N_1$
		$N_1 = -F_{T,u}$; $N_{T,u} = 2F_{T,u}$
2	Dominant bending moment with critical tensile force	$N_1 < N \le N_2$
		$N_2 = F_{C,u} - F_{T,u}$
3	Dominant bending moment with critical compressive force	$N_2 < N \le N_3$
		$N_3 = F_{C,u}$
4	Dominant compressive force	$N_3 < N \le N_{C,u}$
		$N_{C,u} = 2F_{C,u}$

In presence of dominant tensile force (Figure 3.7 a) the in-plane resistance is given by:

$$M_{j,ip,u} = 2z_T F_{T,u} + z_T N \tag{3.1}$$

Results of the analytical model were compared to the mentioned experimental tests by *INSA Rennes*, with a very satisfactory ratio (deviations are up to approximately 5%). When compared to numerical results and parametric study, the resistance obtained by the analytical model is lower than the numerical resistances and remains on the safe side.

with

$F_{T,u}$: resistance of the T-stub in tension according to 5.2.1,
N: axial force,
Z_T: lever arm (distance between the line of action of the anchor bolts and the center of the column).

In presence of dominant bending moment and critical tensile force (Figure 3.7 b) the in-plane bending resistance is:

$$M_{j,ip,u} = (z_T + z_C)F_{T,u} + z_C N \tag{3.2}$$

with

z_C: compressive lever arm (distance between the line of action of the resultant compressive force Fc and the center of the column):

$$z_C = \frac{h_c}{2} + c^* - \frac{x_c}{2} \leq z_{C0} \tag{3.3}$$

z_{C0}: compressive lever arm given by EC3-1-8 (distance between the action line of the resultant compressive force FC located at the column flange and the center of the column).

In presence of dominant bending moment and critical compressive force (see Figure 5.1 c) the in-plane bending resistance is determined according to Eurocode 3 part 1-8:

$$M_{j,ip,u} = (z_T + z_{C0})F_{C,u} - z_T N \tag{3.4}$$

with

$$F_{C,u} = b_{eff,c} l_{eff,c} f_{jd}^* \tag{3.5}$$

In presence of dominant compressive force (see Figure 5.1 d) two compressive forces F_C and $F_{C,u}$ are applied behind the column flange on the left and on the right sides, respectively (Seco, 2019). The ultimate bending moment resistance is calculated according to:

$$M_{j,ip,u} = 2F_{C,u} z_{C0} - z_{C0} N \tag{3.6}$$

The Full analytical model proposed by *Seco, (2019)* considers the additional resistance provided by the concrete around the column web in compression. The procedure is explained more in detail in *Seco, 2019*.

3.4.1.1 Comparison against experimental, numerical and parametric results

The bending moment resistances obtained by the presented analytical model were compared against the experimental tests shortly presented in sub-chapter 3.1. The results are very satisfactory, as well as failure modes (see Table 3.10).

Table 3.10: Comparison of the bending moment resistances obtained in analytical and experimental way (*Seco, 2019*)

Specimen	Experimental		Analytical		Ana/Exp
	Maximum bending moment $M_{j,u,exp}$ (kNm)	Failure mode	Maximum bending moment $M_{j,u,ana}$ (kNm)	Failure mode	$M_{j,u}$
SPE1-M0	43,2	Mode 2*	43,4	Mode 2	1,00
SPE2-M0	48,5	Mode 3	50,7	Mode 3	1,04

*During tests, prying effect did not develop due to initial imperfection. However, Mode 2 is still considered for this case, since the base plate yielded.

When compared to the numerical results, analytical models show lower resistance values that the numerical resistances, so the models can be used with confidence since results obtained analytically are mostly on the safe side.

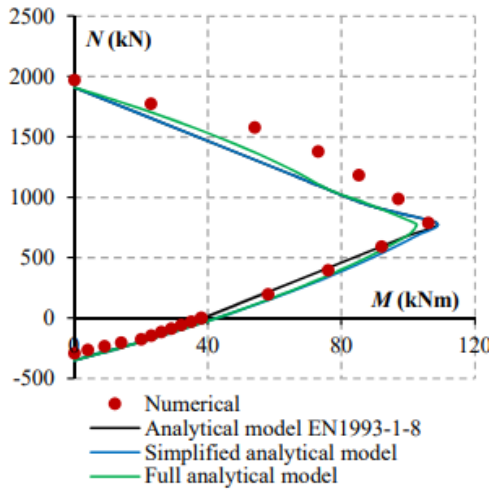

Figure 3.8: *M-N* interaction curves for P1 *(Seco, 2019)*

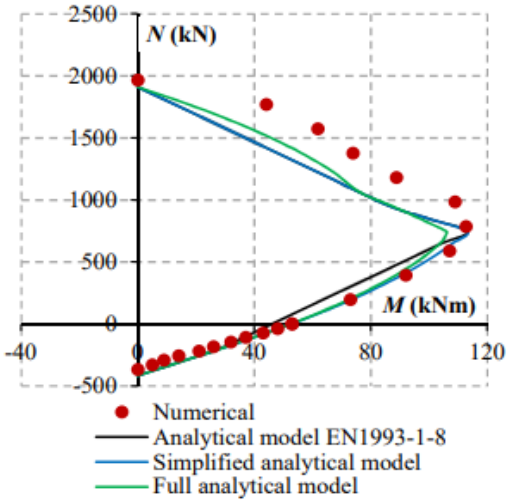

Figure 3.9: *M-N* interaction curves for P2 *(Seco, 2019)*

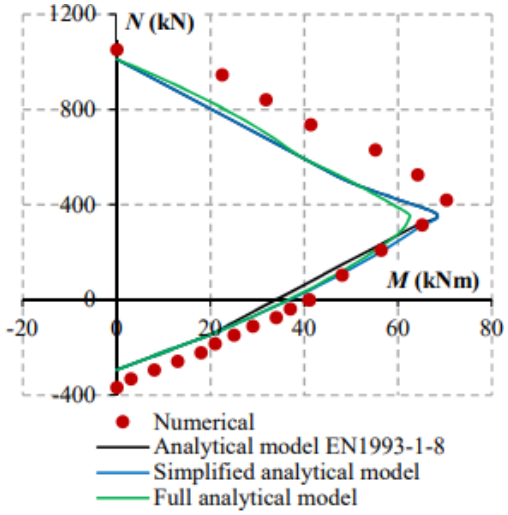

Figure 3.10: *M-N* interaction curves for P3 *(Seco, 2019)*

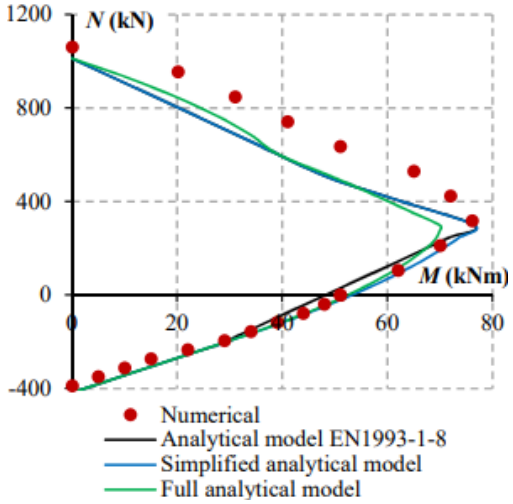

Figure 3.11: *M-N* interaction curves for P4 *(Seco, 2019)*

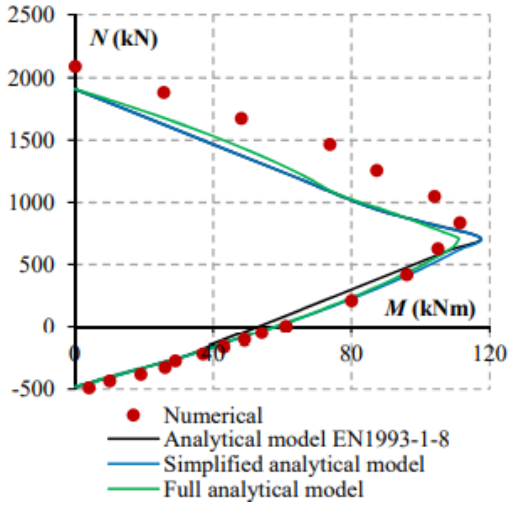

Figure 3.12: *M-N* interaction curves for P5 *(Seco, 2019)*

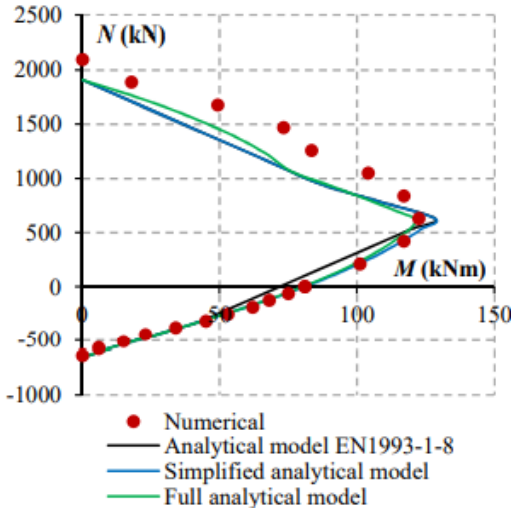

Figure 3.13: *M-N* interaction curves for P6 *(Seco, 2019)*

3.4.2 Out-of-plane bending moment

For calculation of the resistance of column base plates under axial force and bending moment over the minor axis, a simplified model is proposed based on the parabolic interaction suggested by the parametric study.

Before developing these equations, it is shown that with the force distribution presented in Figure 3.14, the parabolic interaction can be adequate *(Seco, 2019).*

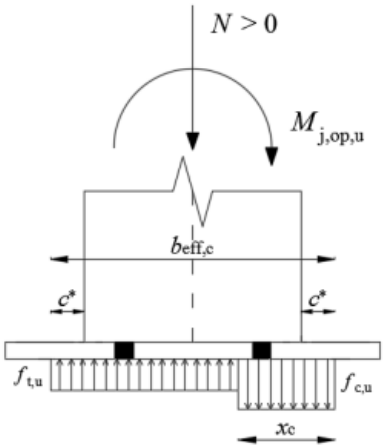

Figure 3.14: Mechanism of internal forces considered in the analytical model for out-of-plane bending moment *(Seco, 2019)*

The hypothesis seems rational for the compressive area, but for the tensile area, the lever arm can be underestimated or overestimated (depends on the anchor bolts displacement), and so the maximum bending moment. By determining the position of the neutral axis, the contribution of the compressive and tensile sides can be evaluated and after deriving the mathematical equations, the bending moment resistance $M_{j,op,u}$ is obtained from:

$$M_{\mathrm{j,op,u}} = M_{\mathrm{op,u,max}} \left[1 - \left(\frac{N - N_{\mathrm{Mmax}}}{N_{\mathrm{moy}}} \right)^2 \right] \tag{3.7}$$

with

$$N_{\mathrm{Mmax}} = \frac{N_{\mathrm{C,u}} - N_{\mathrm{T,u}}}{2} \tag{3.8}$$

$$N_{\mathrm{moy}} = \frac{N_{\mathrm{C,u}} + N_{\mathrm{T,u}}}{2} \tag{3.9}$$

$$M_{\mathrm{op,u,max}} = \frac{b_{\mathrm{eff,c}}}{4} \frac{N_{\mathrm{C,u}} + N_{\mathrm{T,u}}}{2} \tag{3.10}$$

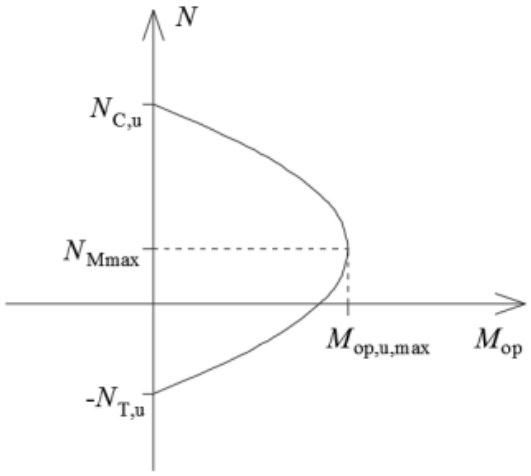

Figure 3.15: Parabolic interaction curve M-N *(Seco, 2019)*

To avoid an underestimating or overestimating of the lever arm and the maximum bending moment, the contribution of the tensile area to the maximum bending moment is evaluated considering that the tensile resistance develops at the anchor bolts location. The maximum bending moment becomes:

$$M_{op,u,max} = z_{T,op}F_{T,u} + z_{C,op}F_{c,f,u} \tag{3.11}$$

with

$$F_{c,f,u} = b_{eff,c}l_{eff,c}f_{id,max} \leq b_c t_{fc} f_{y,c} \tag{3.12}$$

Parameters $z_{T,op}$, $z_{C,op}$ are given by:

$$z_{T,op} = \frac{w}{2} \tag{3.13}$$

$$z_{C,op} = \frac{b_c}{4} + \frac{c^*}{2} \leq \frac{b_{bp}}{4} \tag{3.14}$$

3.4.2.1 Comparison against experimental, numerical and parametric results

Comparison against the experimental test results showed a slightly worse ratio with errors up to 8% on the safe side, which is still very satisfactory, while failure modes were the same as in the experimental tests.

Table 3.11: Comparison of the analytical results against the experimental tests for out-of-plane bending moment (*Seco, 2019*)

Specimen	Experimental		Analytical		Ana/Exp
	Maximum bending moment $M_{j,u,exp}$ (kNm)	Failure mode	Maximum bending moment $M_{j,u,ana}$ (kNm)	Failure mode	$M_{j,u}$
SPE1-M90	36,2	Mode 2	33,3	Mode 2	0,92
SPE2-M90	43,7	Mode 3	40,9	Mode 3	0,94

When compared to the numerical results, values predicted by the analytical models are in good agreement with the numerical models (*Seco, 2019*).

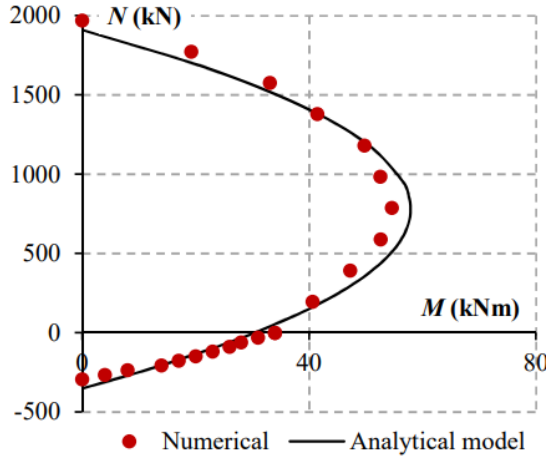

Figure 3.16: *M-N* interaction curves for P1 *(Seco, 2019)*

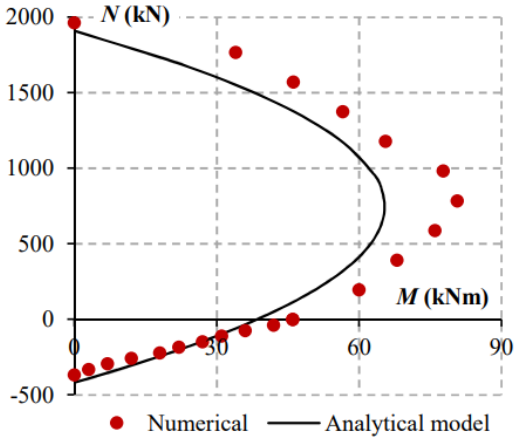

Figure 3.17: *M-N* interaction curves for P2 *(Seco, 2019)*

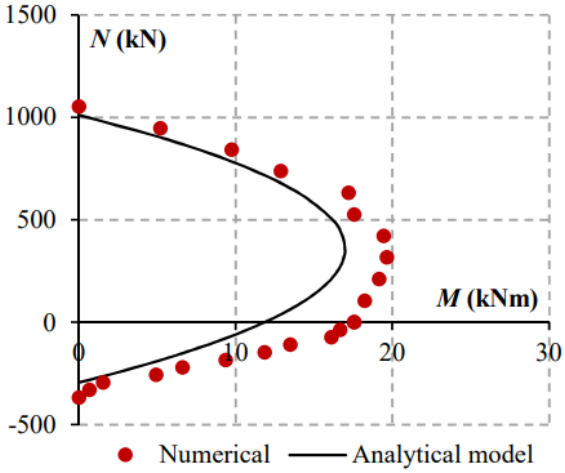

Figure 3.18: *M-N* interaction curves for P3 *(Seco, 2019)*

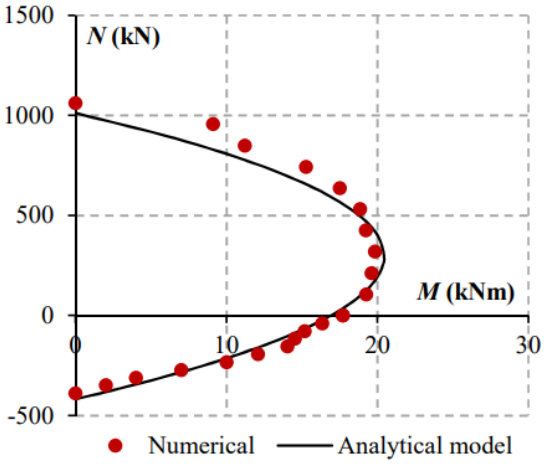

Figure 3.19: *M-N* interaction curves for P4 *(Seco, 2019)*

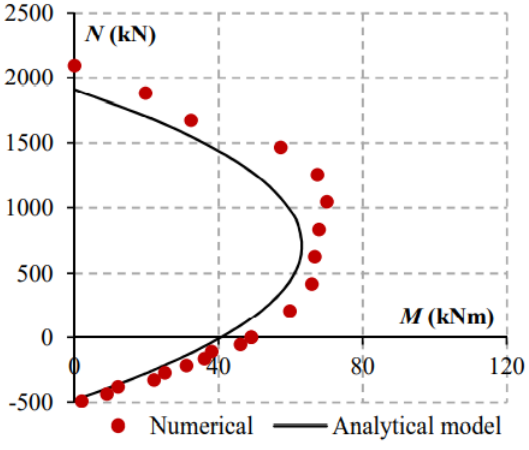

Figure 3.20: *M-N* interaction curves for P5 *(Seco, 2019)*

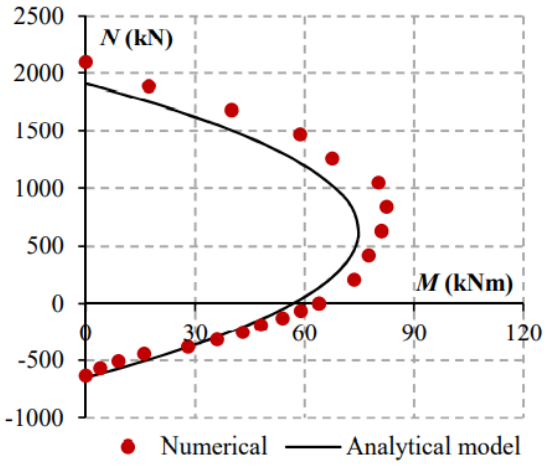

Figure 3.21: *M-N* interaction curves for P6 *(Seco, 2019)*

3.4.3 Biaxial bending moment

For the "I" profile steel columns, the elliptical interaction is quite conservative, whereas it becomes unsafe in presence of a dominant tensile force. For this reason a more rigorous model, based on a mechanical principles, is necessary for the evaluation of the interaction between in-plane and out-of-plane bending moments (*Seco, 2019*).

The analytical model presented here is divided into three cases depending on the axial force in the connection. The model is divided into dominant tensile force, dominant bending moment, and dominant compressive force as shown in the following figure:

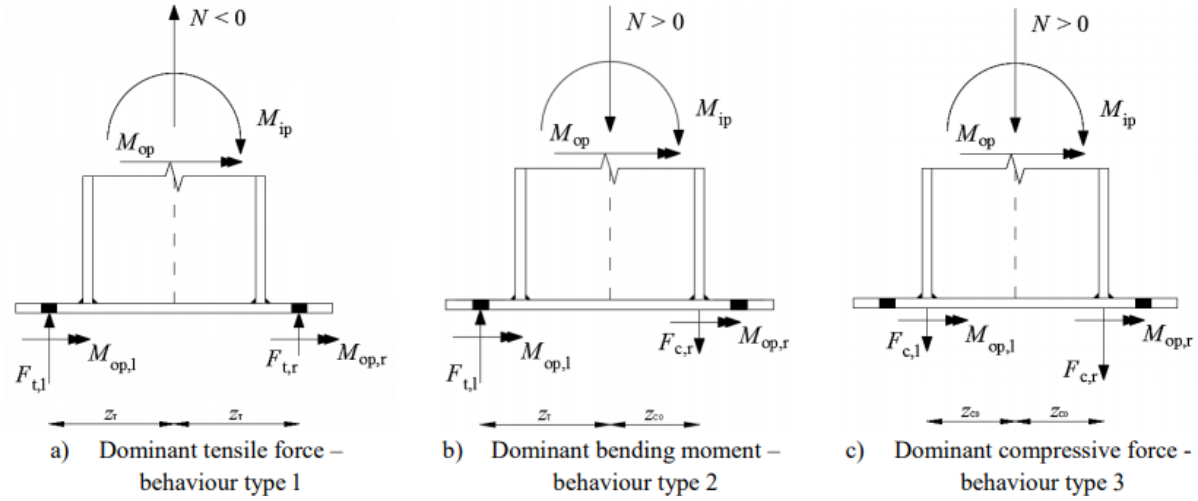

Figure 3.22: Mechanisms considered in the analytical model for biaxial bending moment (Seco, 2019)

The validity domains are determined with:

Table 3.12: Validity range of the mechanisms of the analytical model (*Seco, 2019*)

Behaviour type	Loading	Range of validity
1	Dominant tensile force	$-N_{T,u} \le N \le N_1$ and $M_{ip} \le 2z_T F_{T,u} + z_T N$ $N_1 = -F_{T,u}$; $N_{T,u} = 2F_{T,u}$
2	Dominant bending moment	$N_1 < N \le N_2$ and $M_{ip} \le \min\left((z_C+z_T)F_{T,u}+z_C N;(z_C+z_T)F_{C,u} - z_T N\right)$ $N_2 = F_{C,u}$
3	Dominant compressive force	$N_2 < N \le N_{C,u}$ and $M_{ip} \le 2z_C F_{C,u} - z_C N$ $N_{C,u} = 2F_{C,u}$

An expression for out-of-plane bending resistance for the case of dominant tensile force (Figure 3.21 a) is obtained with:

$$M_{op,u} = M_{op,u,max}\left[1 - \left(\frac{N - N_{Mmax}}{N_{moy}}\right)^2 - \left(\frac{M_{ip}}{z_T N_{moy}}\right)^2\right] \quad (3.15)$$

For specific case of a 45°biaxial bending where:

$$M_{op} = M_{ip} = M_{j,45,u} = \frac{M_{45}}{\sqrt{2}} \tag{3.16}$$

Resistance $M_{j,45}$,u is obtained by solving a quadratic equation as follows:

$$M_{j,45,u}{}^2 a_T + M_{j,45,u} b_T + c_T = 0 \tag{3.17}$$

with

$$\Delta_T = b_T^2 - 4 a_T c_T \tag{3.18}$$

$$a_T = \frac{1}{\left(z_T N_{moy}\right)^2} \tag{3.19}$$

$$b_T = \frac{1}{M_{op,u,max}} \tag{3.20}$$

$$c_T = \left(\frac{N - N_{Mmax}}{N_{moy}}\right)^2 - 1 \tag{3.21}$$

The positive solution of this equation is:

$$M_{j,45,u} = \frac{-b_T + \sqrt{\Delta_T}}{2 a_T} \tag{3.22}$$

In presence of dominant bending moment (see Figure 3.21 b) after applying tensile and a compressive force, inserting and solving equations, the total out-of-plane bending moment resistance is:

$$M_{j,op,u} = M_{op,u,max}\left[1 - \frac{1}{2}\left(\frac{\alpha_T N - N_{Mmax}}{N_{moy}}\right)^2 - \frac{1}{2}\left(\frac{\alpha_C N - N_{Mmax}}{N_{moy}}\right)^2 - \left(\frac{M_{ip}}{\bar{z} N_{moy}}\right)^2 - \frac{M_{ip}}{2\bar{z} N_{moy}{}^2} N(\alpha_C - \alpha_T)\right] \tag{3.23}$$

For the specific case of a 45°biaxial bending moment where:

$$M_{op} = M_{ip} = M_{j,45,u} = \frac{M_{45}}{\sqrt{2}} \tag{3.24}$$

Resistance $M_{j,45}$,u is obtained by solving a quadratic equation as follows:

$$M_{j,45,u}{}^2 a_M + M_{j,45,u} b_M + c_M = 0 \tag{3.25}$$

with

$$\Delta_M = b_M^2 - 4 a_M c_M \tag{3.26}$$

$$a_M = \frac{1}{\left(\bar{z}N_{moy}\right)^2} \tag{3.27}$$

$$b_M = \frac{1}{M_{op,u,max}} + \frac{N(\alpha_C - \alpha_T)}{\bar{z}N_{moy}^{\ 2}} \tag{3.28}$$

$$c_M = \frac{1}{2}\left[\frac{(\alpha_C N - N_{Mmax})^{\,2} + (\alpha_T N - N_{Mmax})^2}{N_{moy}^{\ 2}}\right] - 1 \tag{3.29}$$

The positive solution of this equation is:

$$M_{j,45,u} = \frac{-b_M + \sqrt{\Delta_M}}{2a_M} \tag{3.30}$$

In presence of dominant compressive force (see Figure 3.21 c) the total out-of-plane bending moment resistance is obtained as follows:

$$M_{j,op,u} = M_{op,u,max}\left[1 - \left(\frac{N - N_{Mmax}}{N_{moy}}\right)^2 - \left(\frac{M_{ip}}{z_C N_{moy}}\right)^2\right] \tag{3.31}$$

For the specific case of 45°biaxial moment where:

$$M_{op} = M_{ip} = M_{j,45,u} = \frac{M_{45}}{\sqrt{2}} \tag{3.32}$$

Resistance $M_{j,45,u}$ is obtained by solving a quadratic equation as follows:

$$M_{j,45,u}^{\ 2} a_C + M_{j,45,u} b_C + c_C = 0 \tag{3.33}$$

with

$$a_C = \frac{1}{\left(z_C N_{moy}\right)^2} \tag{3.34}$$

$$b_C = \frac{1}{M_{op,u,max}} \tag{3.35}$$

$$c_C = \left(\frac{N - N_{Mmax}}{N_{moy}}\right)^2 - 1 \tag{3.36}$$

The positive solution of this equation is:

$$M_{j,45,u} = \frac{-b_C + \sqrt{\Delta_C}}{2a_C} \tag{3.37}$$

3.4.3.1 Comparison against the experimental, numerical and parametric results

When compared to the experimental results, the analytical model gives satisfactory results. The resistance of specimen with 10 mm base plate thickness, subjected to axial force and biaxial bending moment, was overestimated by 5%, while the specimen with 20 mm base plate thickness was underestimated 2%.

Table 3.13: Comparison of the analytical results against the experimental tests for biaxial bending moment (*Seco, 2019*)

Specimen	Experimental	Analytical	Ana/Exp
	$M_{j,u,exp}$ (kNm)	$M_{j,u,ana}$ (kNm)	-
SPE1-M45	39,4	41,5	1,05
SPE2-M45	47,3	46,3	0,98

Comparison against the numerical results of the parametric study showed that the values obtained by analytical models underestimate the resistances obtained by the FE analysis.

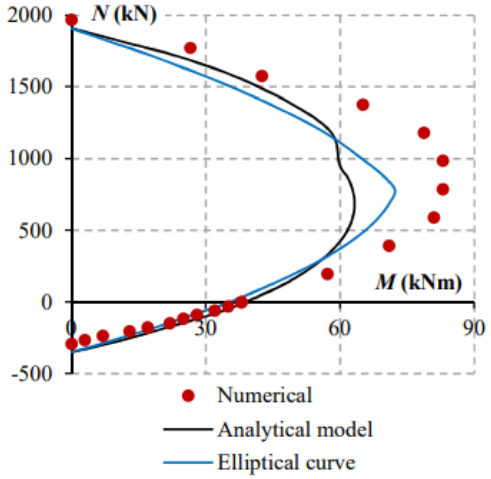

Figure 3.23: *M-N* interaction curves for P1 *(Seco, 2019)*

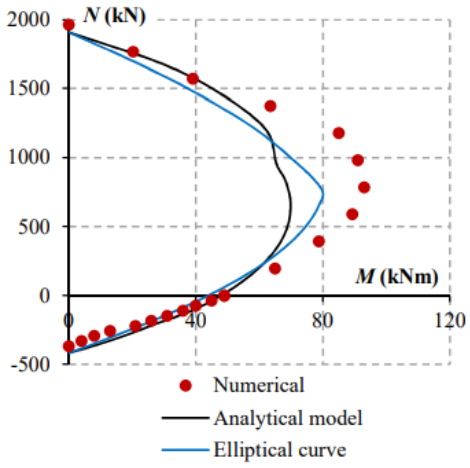

Figure 3.24: *M-N* interaction curves for P2 *(Seco, 2019)*

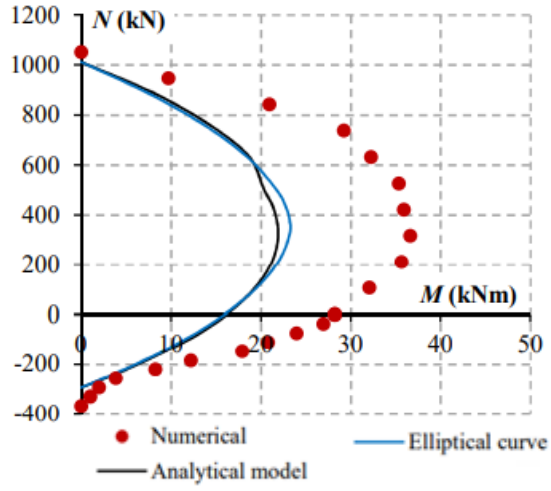

Figure 3.25: *M-N* interaction curves for P3 *(Seco, 2019)*

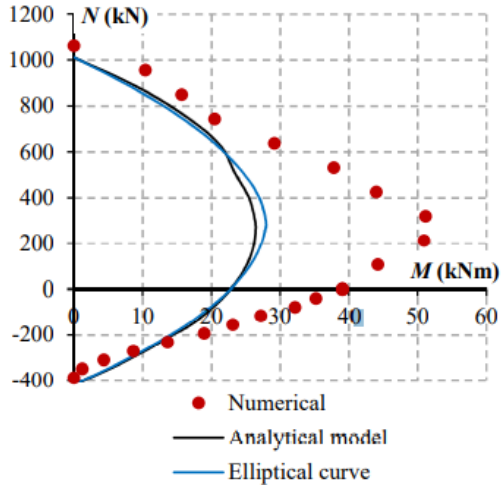

Figure 3.26: *M-N* interaction curves for P4 *(Seco, 2019)*

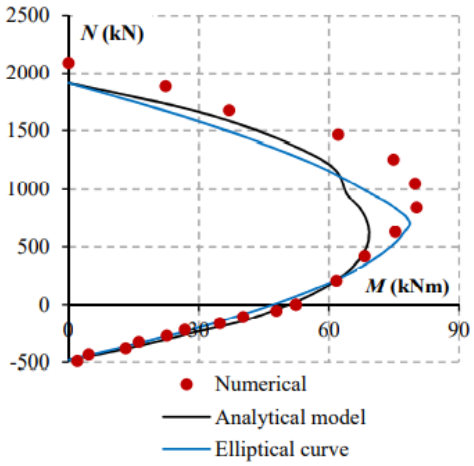

Figure 3.27: *M-N* interaction curves for P5 *(Seco, 2019)*

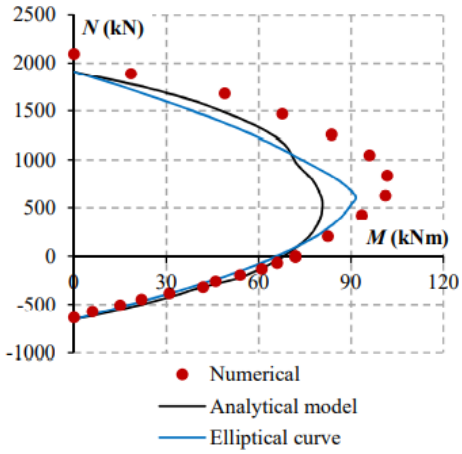

Figure 3.28: *M-N* interaction curves for P6 *(Seco, 2019)*

Analytical curves are generally circumscribed to the numerical curves, revealing a good accuracy of the obtained results with an acceptable safety margin, except for specimens P3 and P4 (*Seco, 2019*), that were mentioned in subchapter 3.2.4 in this thesis. When subjected to the tensile force, the model gives reliable results.

3.5 Concluding remarks

Even though the analytical model, in some cases, underestimates the resistance of the connection, it can be used with certainty since it remains on the safe side.

In some cases, an overestimation of the resistance was observed, although with an acceptable error. Due to its simplification, the analytical results for high levels of applied axial compressive force show less good agreement (*Seco, 2019*).

In general, this model has proven as a step forward in this field, and although there is always space for improvement, the behavior of such connections can be determined more accurately by using the abovementioned model.

4 SOFTWARE TOOLS

4.1 Autodesk Robot Structural Analysis

Various types of construction can be analyzed with *Autodesk Robot Structural Analysis* software. Among many types of structures and different kinds of connection, a fixed column base connection can be modeled in different ways with the possibility to modify all its elements. Thus, modification can be done on a concrete foundation, column base plate, anchor bolts, cross-section type, stiffeners, etc.

This thesis is focused on the "I" profile column bases, connected to the concrete block by means of four anchor bolts and base plate, which is welded to the steel column. During verification of the mentioned connection, the software applies the following code regulations:

- steel code for members EN 1993-1-1
- steel code for connections EN 1993-1-8
- CEB (COMITE EURO-INTERNATIONAL DU BETON) Guide – Design of Fastening in Concrete Thomas Telford 1997
- concrete code EN 1992-1
- The resistance of all components of a connection are checked during analysis, such as:
- bearing pressure resistance of foundation concrete $F_{,CRd}$ (EN1993-1-8 section 6.2.5.[3] and EN 1992-1[6.7.[2]),
- tensile resistance of an anchor $F_{T,Rd}$ which is equal to minimum value of resistance for:
- pull-out failure (EN 1992-1 point 6.4.2[2]),
- steel failure (EN1993-1-8 section 6.2.6.12 and Table 3.4.2)
- pull-out failure of concrete above the head (CEB Guide)
- concrete cone failure (CEB Guide)
- splitting failure (CEB Guide)
- anchor resistance for shear $F_{1vb,Rd}$ and for bearing pressure onto concrete $F_{2vb,Rd}$ (EN1993-1-8 section 6.2.2 [7,8] and Table 3.4)
- concrete cone resistance for pry out failure $F_{v,Rd,cp}$ (CEB Guide)
- resistance for concrete edge failure $F_{v,Rd,c}$ (CEB Guide)
- resistance of the base plate for shear with slippage $F_{f,Rd}$ – (EN1993-1-8 section 6.2.2 [6])
- resistance for bearing pressure of the wedge onto concrete $F_{v,Rd}$ – (EN1992-1)
- resistance of the column web in tension (EN1993-1-8 section 6.2.6.3)
- resistance of the column flange and web in compression (EN1993-1-8 section 6.2.6.7)
- resistance of the base plate subjected to bending in the tension zone (EN1993-1-8 section 6.2.6.11)

- resistance of welds between the column and the base plate, as well as vertical and horizontal welds connecting stiffeners – (EN1993-1-8 section 4.5.3)
- resistance of stiffeners (EN1993-1-1 section 6.2.1).

According to the *EN1993-1-8* section 6.2.8.2., the total resistance of a connection for simple compression is:

$$N_{j,Ed} / N_{j,Rd} \leq 1.0 \quad (4.1)$$

Also, according to the *EN1993-1-8* section 6.2.8.3 and Table 6.7, the total resistance of a connection subjected to bending and/or axial force $M_{j,Rd,}$ is calculated as:

$$M_{j,Ed,y} / M_{j,Rd,y} \leq 1.0 \quad (4.2)$$

or

$$M_{j,Ed,z} / M_{j,Rd,z} \leq 1.0 \quad (4.3)$$

Thus, the total resistance of a connection for biaxial bending moment and/or axial force is verified as:

$$M_{j,Ed,y} / M_{j,Rd,y} + M_{j,Ed,z} / M_{j,Rd,z} \leq 1,0 \quad (4.4)$$

For a connection subjected to shear force $V_{j,Rd,}$ total resistance, according to the *EN1993-1-8* section 6.2.2, is calculated as a sum of bolt resistances, slippage resistance, and wedge resistance:

$$V_{j,Ed,y} / V_{j,Rd,y} \leq 1.0 \quad (4.5)$$

or

$$V_{j,Ed,z} / V_{j,Rd,z} \leq 1.0 \quad (4.6)$$

The software also evaluates the stiffness of a connection and classifies a column base as rigid, semi-rigid, or pinned. The evaluated stiffness of a connection can be ascribed to a structure by defining additional elastic releases in the analyzed connection. Recalculation of the structure enables a more accurate estimation of loads acting on a connection *(Autodesk Robot Structural Analysis - User's Guide).*

Autodesk Robot Structural Analysis Professional 2017 v. 30.0.0.5913, with activated student license, was used for this thesis.

4.2 IDEA StatiCa

The theory of bar members is very common while designing steel structures, but for some cases, it is not valid (e.g., welded joints, bolted connections…) and structural analysis in such locations is difficult and

non-linear behavior must be considered. The component method (which is described in Chapter 2.4 of this thesis) is used very often and it calculates the joint as a system of interconnected components. The corresponding model is built per each joint type to be able to determine forces and stresses in each component (*IDEA StatiCa – Theoretical background*), as shown in Figure 4.1.

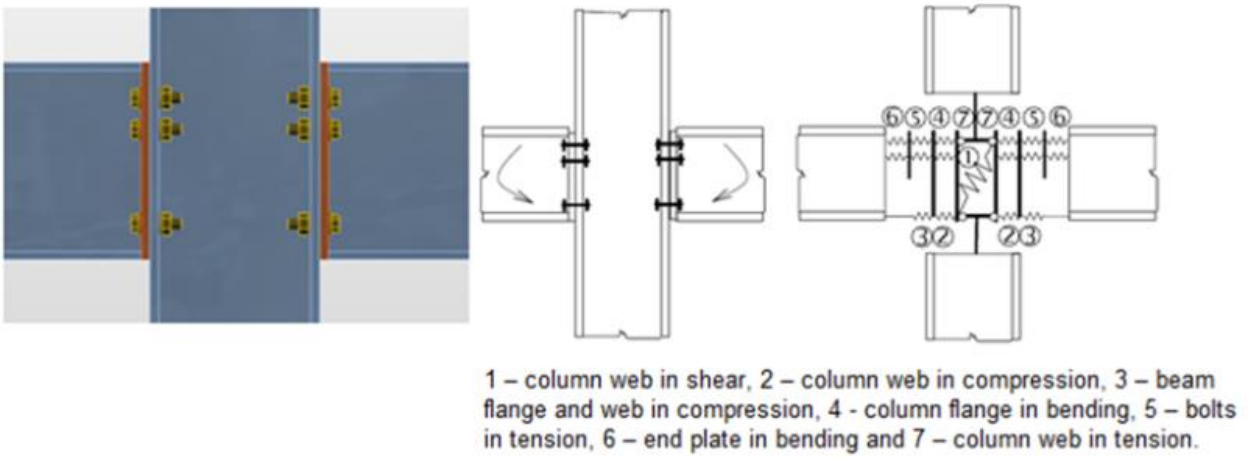

Figure 4.1: Example of a corresponding joint model with component method approach (*IDEA StatiCa – Theoretical background)*

IDEA StatiCa team, in cooperation with the Faculty of Civil Engineering in Prague and Brno University of Technology, developed a new Component Based Finite Element Model (CBFEM) method, for the advanced design of steel structural joints. Idea was that most of the useful parts of CM should be kept, while analyzing stresses of individual components (which is the weak spot of CM) were replaced by modeling and analysis using the Finite Element Method (FEM).

Check methods of specific components like bolts or welds are done according to the standard Component method (Eurocode), while for fasteners (bolts and welds) special FEM components had to be developed to model its behavior. There are a lot of guidance, for all types of joints, but this chapter will focus on elements that are contained in column base connections.

All parts of 1D members and all additional plates are modeled as plate/walls. These elements are made of steel and the behavior of this material is significantly nonlinear (*IDEA StatiCa – Theoretical background*). Thus, the real stress-strain steel diagram is replaced by the Ideal plastic material (Bilinear stress-strain diagram) for design purposes in building practice (see Figure 4.2).

The connection between the edge of one plate and the surface (or edge of the other plate) is ensured by additional special massless force interpolation constraints between the meshes. This calculation model obtains good results and the method is protected by patent.

The connection between the steel base plate and concrete foundation is modeled in a way that it resists compression fully, but it does not resist tension, as shown in Figure 4.3.

Welds are modeled by using a special elastoplastic element, which is added between the plates in order to eliminate the stress peaks that appear at the end of plate edges, in corners and rounding. Thus, the element takes into account the position, orientation and weld throat thickness.

The nonlinear material analysis is applied and elastoplastic behavior in equivalent weld solid is determined. The plasticity state is controlled by stresses in the weld throat section. The stress peaks are redistributed along the longer part of the weld length *(IDEA StatiCa – Theoretical background),* as shown in Figure 4.4.

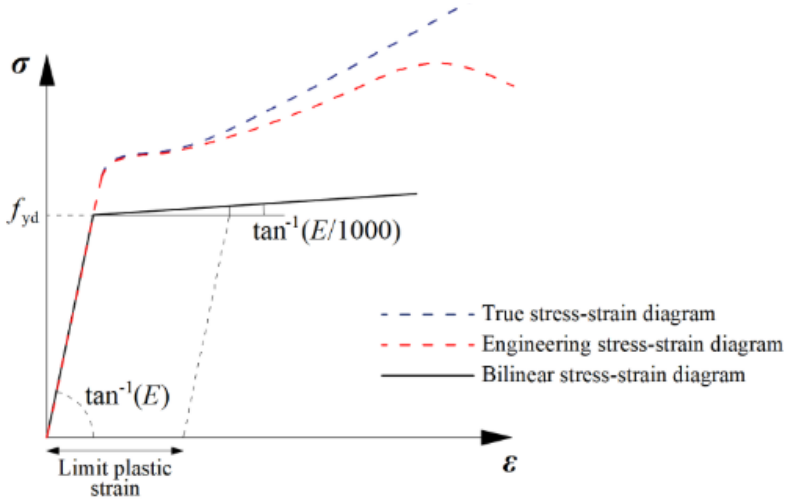

Figure 4.2: Material diagrams of steel in numerical models *(IDEA StatiCa – Theoretical background)*

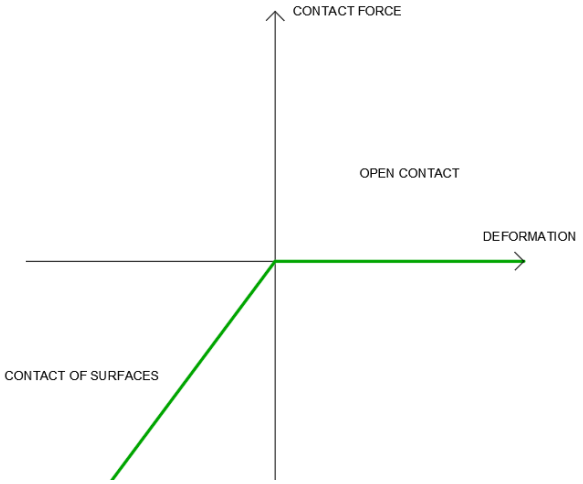

Figure 4.3: Stress-strain diagram of contact between the concrete block and the base plate

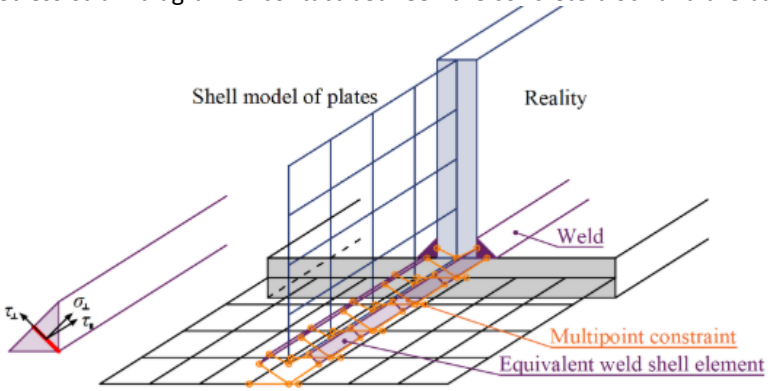

Figure 4.4: Constraint between weld elements and mesh nodes *(IDEA StatiCa – Theoretical background)*

Finally, the stress in throat section of fillet weld is calculated according to EN 1993-1-8 – Cl. 4.5.3.

When it comes to anchor bolts, as for the structural bolts, Component-Based Finite Element Method (CBFEM) describes its behavior with the dependent nonlinear springs.

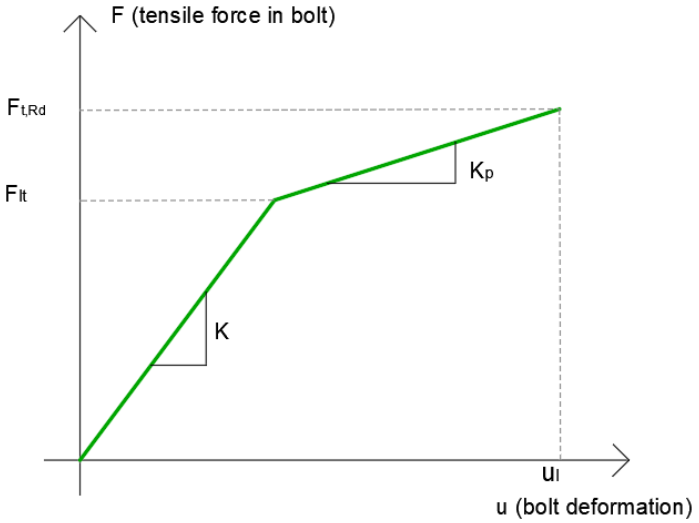

Figure 4.5: Load-deformation of the anchor bolt

The bolt behavior in *IDEA StatiCa* is modelled as represented in Figure 4.5, where:

K: linear stiffness of bolt,
K_p: stiffness of bolt at plastic branch,
F_{lt}: limit force for linear behavior of bolt,
$F_{t,Rd}$: limit bolt resistance,
u_l: limit deformation of bolt.

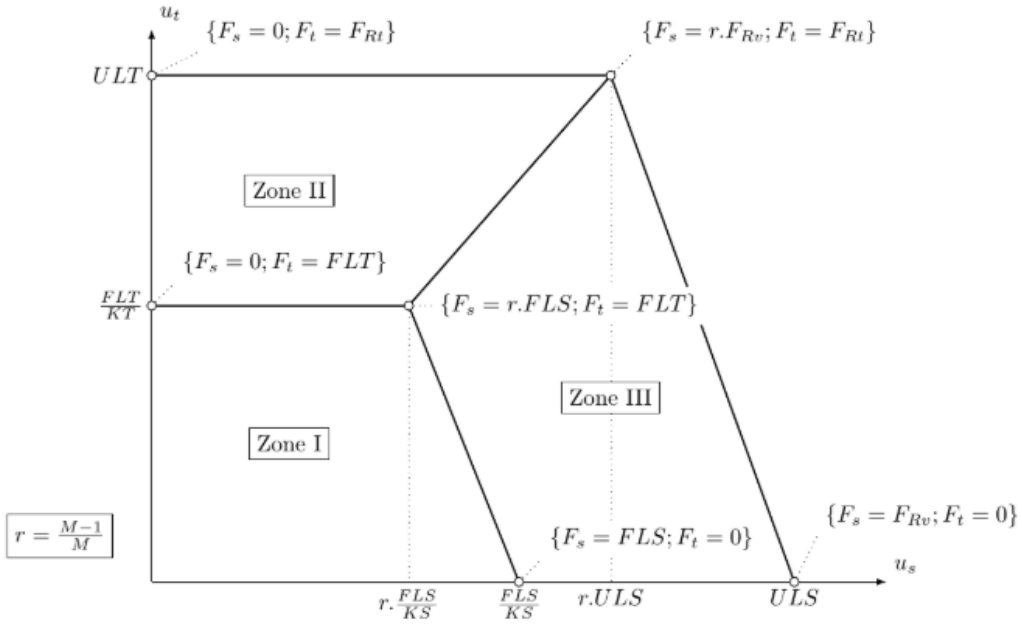

Figure 4.6: Example of interaction of axial and shear force (Eurocode)

All the formulas in detail can be checked in *IDEA StatiCa – Theoretical background* file.

Interaction of the axial and the shear force can be introduced directly in the analysis model. The distribution of forces reflects reality better (see Figure 4.6). As same as for the structural bolts, anchor bolts with a high tensile force take less shear force and vice versa *(IDEA StatiCa – Theoretical background).*

Concrete block is modeled in a way that connection between the concrete and the base plate resists only under compression, which is transferred with the Winkler-Pasternak subsoil model. Tensile forces are taken over by anchor bolts, while shear force is transferred by friction between the base plate and a concrete block, by shear key and by bending of anchor bolts and friction.

After applying loads, internal forces are analyzed using simple 1D members in the 3D model while considering the eccentricities of members caused by joint design (geometry of elements).

IDEA StatiCa Connection v. 10.1.117.55848 with activated students license was used for this thesis.

5 ANALYSIS AND COMPARISON OF RESULTS

5.1 Introduction

Most of the structural analysis nowadays are done through software tools, thus column base connections as well. It is expectable, as time goes on, that the software solutions will improve, and more types of analysis with more accurate results will be available. To achieve that, software methodologies and the newest studies should keep pace with each other. It has been proven that Eurocode methodologies still have space for improvement when it comes to column base connections subjected to in-plane, out-of-plane, and especially biaxial bending moment. Considering this fact, comparing the results obtained by programs whose approach is related to the component method described in Eurocode, against the results obtained by a previously verified analytical model, could give a better picture of how accurate the software analyzes are.

With intention to obtain a connection whose configuration is realistic and not randomly selected, a steel structure, with some rational spans and loads applied according to instructions such as those given in Eurocode regulations, is modeled in *SCIA Engineer* software. According to the results, the proper cross-section is selected, and the connection is designed in one of the commonly used software for structural analysis – *IDEA StatiCa* and *Robot* by *Autodesk*. Since she used the same column cross-section profile, the connection configuration is designed on a way it completely matches the specimen that was used in experimental, numerical and analytical analyzes described in *Seco, (2019)*. In this way, the comparison against those results will be more authoritative, and in some points, the results will be directly compared against experimental ones.

After numerical analyzes, a parametric study will be conducted to check how each parameter affects the software results, connection behavior and moment resistance capacity.

To achieve the desired results, more than two thousand iterative attempts resulted in roughly four hundred moment resistances of the connection and roughly five hundred recorded notes about behavior. In this way, a quality numerical and parametric research was conducted, and the behavior of the connection was studied all with the aim of checking the accuracy of the software results. Failure modes will be described in this chapter with marks as described in Table 5.1.

Table 5.1: Failure modes described

Failure modes	
Mark	Descritpion
CB	Concrete block
AB	Anchor bolts
CF	Column flange
BP	Base plate
W	Welds

5.2 Column base design in building

As mentioned before, in some rational constructions it is difficult to achieve that the column base is subjected only to bending moment load in the direction of the stronger or weaker axis. Usually, column base is, next to the axial force, subjected to biaxial bending moment, with an emphasis on one axis. To prove that and to obtain the connection configuration, which is suitable for use in real life, the rational steel construction is modeled in *SCIA Engineer* and *Robot Structural Analysis Professional*.

5.2.1 Structure geometry and loads

The geometry is chosen in a simple way in order to simulate the behavior of the most common steel structures, and on the other hand not to be related to some specific shape of structures or specific location. Thus, steel columns are arranged at spans of 4m in the shorter and 7m in the longer direction, and they are connected by horizontal beams. The structure consists of the one 3 meters high survey, so that wind and seismic loads affect the behavior of the construction in negligible values (see Figure 5.1). Other dead and live loads are applied following the guidance provided by Eurocode, in such a way that the load is selected to cover categories A, B and C (C1, C2, C3) which are described in the *EN 1991-1-1 6.3.1.2 [Table 6.2]*.

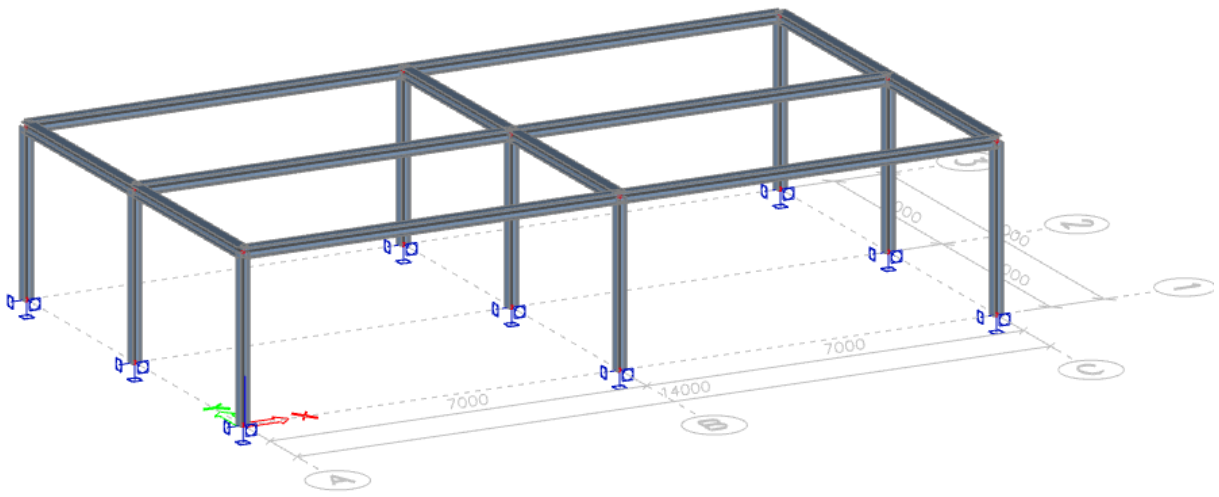

Figure 5.1: Geometry of the structure

5.2.2 Results and cross-section selection

After the construction was calculated in terms of linear analysis, satisfactory internal forces diagrams were obtained. Construction was subjected to ULS Check analysis which is part of *SCIA* software and is works on *EC-EN 1993* approach. After performed dimensional analysis, HEA 200 cross-section turned out to be the most relevant steel profile for this construction, with the utilization factor of 0.75 for corner columns (see Figure 5.2).

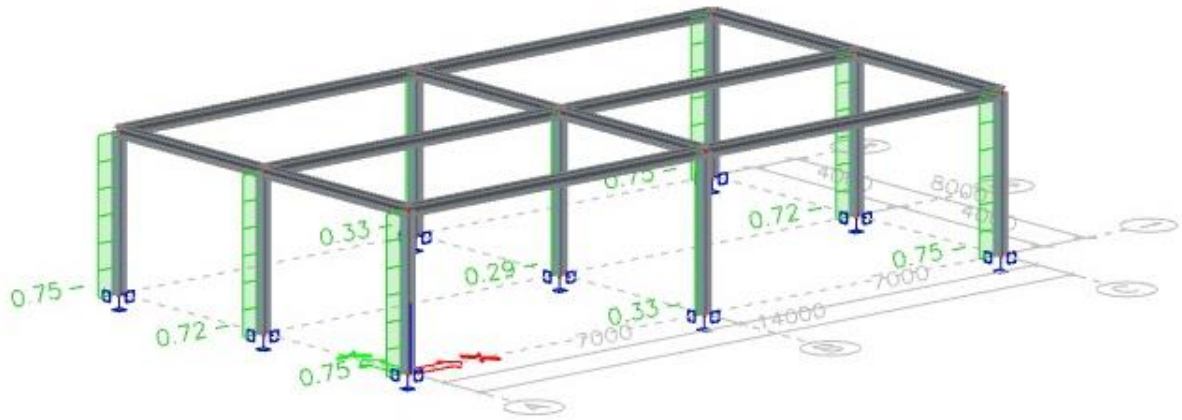

Figure 5.2: ULS Check factor for HEA200 steel column profile

The same procedure was done for Autodesk's *Robot*, and the similar results were obtained. Unlikely for *SCIA* whose connection had to be exported to IDEA StatiCa via BIM link to conduct connection analysis properly, *Robot* has an option to design and calculate connections in the specific program mode. After obtaining proper cross-section, the connection was exported from the structure into the connection design software mode, and the modeling could have started. The procedure will be presented in the following sub-chapters.

5.3 Numerical analysis

The same steel column profile as selected in the previous sub-chapter was examined on the experimental, numerical, and analytical way in *Seco (2019).* With aim to get the most relevant results for comparison, the rest of the connection set-up, modeled in *IDEA StatiCa* and *Robot*, was designed to match the one studied in *Seco (2019).*

5.3.1 Geometry and materials

The column base connection consists of a steel column HEA 200, which is welded by filled welds with 7 mm throat thickness, to a rectangular base plate of dimensions 330x300 mm. The base plate is fixed to a concrete block by means of four anchor bolts M16 class 5.6, which were embedded into the concrete block for a length of 300 mm with washers of dimensions 50x50x10 mm on top of it. The concrete block has dimensions of 1450x900x610 and class C25/30. The configuration is shown in Figure 3.4 of this thesis, and software designs are presented in Figure 5.3. The only difference in configuration is the column length, which is set-up to 3 m, instead of 1.5 m as it was considered in *Seco (2019)* because the length of 3 meters is closer to the design that will appear in actual constructions.

For all elements used in this test nominal values, defined by Eurocode, were selected for geometry (Table 5.2) and for the material properties (Table 5.3).

Table 5.2: Geometry of the observed connection

	Column steel profile		Base plate		Anchor bolts		Concrete	
Geometry	h_c (mm)	190	h_{bp} (mm)	330	d (mm)	16	h_f (mm)	610
	b_c (mm)	200	b_{bp} (mm)	300	d_0 (mm)	18	b_f (mm)	900
	t_{wc} (mm)	6,5	t_{bp} (mm)	20	A_s (mm^2)	157	d_f (mm)	1450
	t_{fc} (mm)	10	e_x (mm)	35	L_b (mm)	350		
	A (mm^2)	5380	e_{x1} (mm)	35	L_{emb} (mm)	300		
	I_y (cm^4)	3692	p (mm)	260	h_{bh} (mm)	10		
	$W_{pl,y}$ (cm^3)	429,5	e (mm)	70	d_w (mm)	50		
	I_z (cm^4)	1336	w (mm)	160				
	$W_{pl,z}$ (cm^3)	203,8						

Table 5.3: Material properties of the observed connection

	Column steel profile		Base plate	Anchor bolts	Concrete	
Material properties	E (GPa)	210	210	210	E_{cm} (GPa)	31
	f_y (MPa)	355	275	300	f_{cm} (MPa)	33
	f_u (MPa)	490	430	500	f_{ck} (MPa)	25

Implementing abovementioned parameters into the software resulted with the following designs presented in Figure 5.3, while test identifications are represented in Table 5.4.

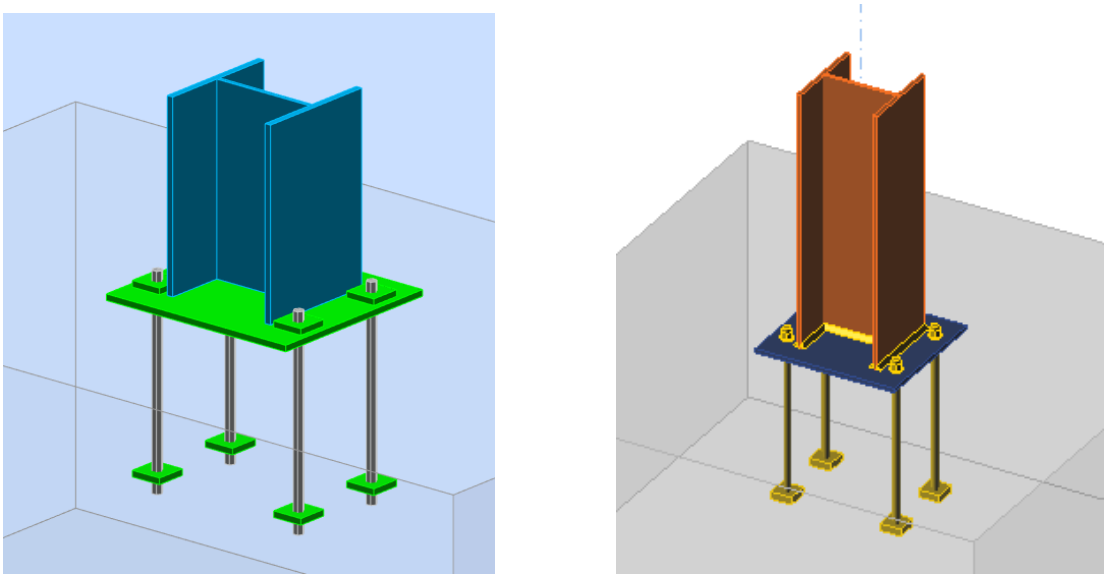

a) b)

Figure 5.3: Software designs of the connection – a) *Robot Structural Analysis*, b) *IDEA StatiCa*

Table 5.4: Identification and characteristics of the test specimens

TEST ID	Loading conditions	Column profile	Column steel grade	Base plate thickness (mm)	Base plate steel grade
SPE1-M0	In-plane bending	HEA 200	S355	10	S275
SPE1-M90	Out-of-plane bending				
SPE1-M45	Biaxial bending				

5.3.2 Code parameters

Not all programs have the same options in terms of input parameters, thus all possible parameters are set to equal values. The parameter defined by the user is column length, which is set-up to 3 m, and the concrete is set to non-cracked. In *Autodesk Robot Structural Analysis*, the frame is set to non-sway and the reduction factor of anchors resistance is equal to 1.0.

Since *IDEA StatiCa* works on the CBFEM method, described in chapter 4, much more input parameters are available. Thus, besides the default values referenced by software or Eurocode, ETAG, and CIDECT (see Table 5.5), the number of analysis iterations is set up to 25, divergent iterations count is equal to 3 and the minimum size of an element is 10 mm, up to a maximum of 50 mm. Code parameters were changed for some specific cases where the software displayed inconsistent results, with the aim of improving them, but the results have not changed significantly.

Table 5.5: Code parameters used for the observed connection

Parameter	Value	Reference
γ_{M0}	1.00	EN 1993-1-1: 6.1
γ_{M1}	1	EN 1993-1-1: 6.1
γ_{M2}	1.25	EN 1993-1-1: 6.1
γ_{M3}	1.25	EN 1993-1-8: 2.2
γ_{C}	1.5	EN 1992-1-1: 2.4.2.4
γ_{Inst}	1.2	ETAG 001-C 3.2.1
Joint coefficient β_j	1	EN 1993-1-6: 6.2.5
Effective area - influence of mesh size	0.1	-
Friction coefficient - concrete	0.5	EN 1993-1-8
Friction coefficient in slip-resistance	0.3	EN 1993-1-8 tab 3.7
Limit plastic strain	0.05	EN 1993-1-5
Cracked concrete	No	
Local deformation limit	0.03	CIDECT DG 1, 3-1.1
Sway	No	

5.3.3 Analysis procedure

In order to achieve equal conditions as those achieved in *Seco (2019)*, the considered connection was examined for loading conditions where axial force was combined with bending moment over the major axis (*M0*), bending moment over the minor axis (*M90*), or biaxial bending moment (*M45*). The biaxial bending moment load is achieved by applying a bending moment of equal values in direction of two orthogonal axis (x and y), thus the resultant of these moments as a result load gives a bending moment at an angle of 45°, whose value can be easily determined by the Pythagorean theorem. The N-M curves were obtained by combining the axial force (which was gradually increased from tensile ones to a maximum value of compressive force) with in-plane, out-of-plane, or biaxial bending moment. The moments were modified until the limit state of the connection was reached, which represented the moment resistance

for a given axial force. In the following sub-chapters, results are compared against the ones obtained by previously mentioned experimental tests and analytical model.

5.3.4 Comparison against the experimental tests

As abovementioned, the bending moment resistances obtained analytically and by the software are compared against the experimental tests performed by *INSA de Rennes*, which are shortly described in sub-chapter 3.1 of this thesis. It should be noted that this analytical model results are obtained for the material properties that are obtained after raw material experimental tests which are done as part of experimental tests as described in *Seco (2019),* so small differences compared to the results obtained for nominal values of the material are expectable.

Table 5.6: Comparison of the analytical and software results against the experimental tests for SPE1 test series

TEST ID	Experimental test		Analytical model			IDEA StatiCa			Robot		
	Maximum bending moment (kNm)	Failure mode	Maximum bending moment (kNm)	Failure mode	Ana/Exp	Maximum bending moment (kNm)	Failure mode	Soft/Exp	Maximum bending moment (kNm)	Failure mode	Soft/Exp
SPE1-M0	43.2	AB	43.4	AB	1.00	28.5	AB	0.66	20.2	BP	0.47
SPE1-M90	33.3	AB	33.0	AB	0.99	21.6	CB	0.65	12.7	BP	0.38
SPE1-M45	39.4	AB	35.6	-	0.90	19.9	CB	0.51	12.9	BP	0.33

From Table 5.6 it can be noticed that software does not only underestimate the connection capacity, but the failure mode is wrong for most of the cases. Connection calculated by *Robot* reaches its limit with the base plate under bending as the weakest component for all loading conditions. The first element that reaches its limit in *IDEA StatiCa* is a concrete block under pressure for *SPE1-M90/M45,* and the only failure mode that matches the experimental one is for an in-plane bending moment – anchor bolts in tension.

The software pays too much attention to concrete as a parameter, but generally, in some actual structures steel is the element that reaches the failure, as it can be noticed from the experimental test results presented above. In the following sub-chapter 5.4, the performed parametric studies are presented, and among the other parameters, the role of the concrete class is examined and will be commented.

The difference between the accuracy of the software and the analytical model can be seen in ratios. The analytical model has the highest deviation of 8%, which is very satisfactory. Component-based finite element method approach by *IDEA StatiCa* shows deviation up to 49%, while *Robot* with the approach, which is highly related to the Eurocode's component method, reaches the highest deviation of 67% for specimen subjected to biaxial bending moment load.

5.3.5 Comparison against the analytical results

In addition to the graphs that show the connection behavior for the interaction of axial force and bending moment, the improvement by adding the moment and axial force cross-section plastic resistances to the secondary axis has been made. For M0 and M90 loading conditions, nominal values of plastic modulus were chosen when calculating the plastic resistance of the cross-section, while for the cases of M45, a value of 1.1 * M_{plz} (cross-section bending moment plastic resistance increased by 10%) was taken, which

is quite on the safe side. This problem was examined in the article published by *Baptista (2012),* where he described the analytical evaluation of the elastic and plastic resistances of double symmetric rectangular hollow sections under axial force and biaxial bending moment. The idea was to apply the procedure described in this paper to the cross-sections used in this work to obtain the true values of plastic resistance for the corresponding column steel profiles. Unfortunately, this procedure requires a lot of time and will not be covered in this thesis, but it will, if the opportunity arises, be addressed in some further work.

Since for this set-up the experimental tests were performed and compared with the analytical model with very satisfactory results (as presented in the previous subchapter), the curves obtained by the analytical model will be considered as those to which software ones should aspire. Unlike the previous sub-chapter, in this chapter analytical results are obtained for nominal values of material properties. Also, the results obtained with experimental tests are implemented into graphs with aim of getting a better picture of the relation between the curves obtained numerically and analytically and experimental results.

It needs to be highlighted that if the analytical model on the following graphs used raw material properties, its curve would match with the result obtained by experimental tests.

5.3.5.1 In-plane bending moment

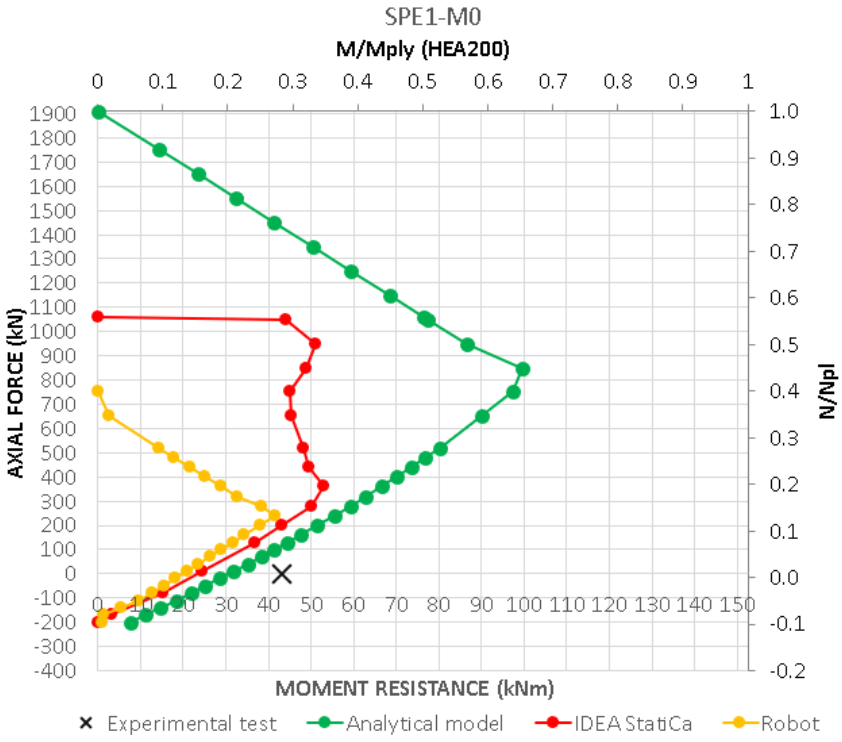

Figure 5.4: Moment resistance curves for connection subjected to axial force and in-plane bending moment

In Figure 5.4 the moment resistance curves are represented for the connection subjected to a bending moment over the strong axis (*M0*) in combination with an axial force.

On the represented curves it can be clearly seen that both software are showing kind of conservative results, each in its own kind of way.

Despite the shape of the curve which looks similar to the analytical one and satisfactory behavior representation for smaller axial force values, the connection analyzed in *Autodesk Robot Structural Analysis Professional* starts losing its resistance too early, and the results are way too much on the safe side. For all tensile axial forces and compressive ones for up to approximately 200 kN, the failure occurs due to connection resistance for bending with the base plate as the weakest component. For higher values of compressive force, the weakest component is the concrete under pressure.

When it comes to *IDEA StatiCa*, slightly better results were obtained in terms of moment resistance capacity, but inappropriate behavior of the connection was observed, which can be seen by the shape of the curve. For a gradual increase of a compressive force, at one point the connection starts showing lower bending moment resistance, but it increases again for higher values of axial force (see the red curve in Figure 5.4). This happens when failure mode changes from the anchor bolts in tension to the concrete block under pressure. In this case, due to its thickness, the base plate bends and due to the poor compressive force distribution, local cracking occurs on the concrete block. Concrete class and base plate thickness will be examined as parameters, but as it was mentioned before, too much attention is paid to concrete. Another inappropriate behavior was observed after the compressive force reached the value of 1050 kN, when for an increase of the compressive force value for just 10 kN (from 1050kN to 1060kN) the connection bending moment resistance decreases from value of 44 kNm to 0 kNm. It is inappropriate for a connection to experience this kind of capacity drop for a small increase of axial force.

The analytical model, as expected, loses its moment resistance capacity when the compressive force reaches the maximum value of cross-section axial force plastic resistance (N/Nply = 1). *IDEA StatiCa* reaches that point when N/Npl is equal to approximately 0.57, and *Robot* reaches it around 0.40, which shows how much the software is on the safe side and that a lot of the column properties remain unused.

When observing the cross-section bending moment plastic resistance (M/Mply), the analytical model goes up to approximately 0.65 of the maximum cross-section capacities, which is satisfactory considering the fact that the connection is subjected to a combination of axial force and bending moment. *IDEA StatiCa* reaches the point of 0.35, while the *Robot* goes up to 0.3.

5.3.5.2 Out-of-plane bending moment

Similar results, as for the in-plane bending moment, were obtained here. *Autodesk Robot's* approach is showing the most conservative results, even more than for in-plane bending moment analysis. Again, despite the good results for low values of axial forces, the connection starts losing its resistance too early and reaches the maximum limit for axial force value of approximately 500 kN in compression. Failure occurs due to bending of the base plate for all axial forces up to 200 kN in compression, after that concrete block under pressure occurs to be the weakest component.

In this case, analyzes performed in *IDEA StatiCa* again showed similar behavior as for the previous case. Thus, the changes in the slope of the curve are too abrupt. The connection reaches its limit mostly due to concrete in pressure, while only for small values of axial force (around zero) it occurs due to anchor bolts. Similarly to the *M0* case, the results cease to follow analytical ones and are moving away from the

experimental result in a moment when the failure mode changes from anchor bolts in tension to a concrete block under compression.

Axial force-moment resistance curves, for connection subjected to the bending moment over the weaker axis, are represented in Figure 5.5.

Figure 5.5: Moment resistance curves for connection subjected to axial force and out-of-plane bending moment

5.3.5.3 Biaxial bending moment

Moment resistance curves, for connection subjected to axial force and biaxial bending moment are represented in Figure 5.6. As mentioned before, an axial force was applied and the moment resistances were obtained by an iterative procedure.

For the biaxial bending moment, *Autodesk Robot's* approach has proven itself as even more conservative. Despite the satisfactory behavior simulation for smaller axial force values, the connection reaches its maximum moment resistance way too early, around the value of 120 kN of the compressive force, and after that the resistance decreases. The capacity of the connection has shown to be underestimated and the results obtained by *Robot Structural Analysis Professional* are way too much on the safe and designing this kind of connection with this approach can cause a big and unnecessary economic loss. Again, for axial forces up to approximately 200 kN in compression, the failure occurs due to connection resistance for bending with the base plate as the weakest component. For higher values of compressive force, the weakest component is the concrete under pressure.

An interesting fact that has been noticed in the *Robot's* approach is that for an axial compressive force of, for example, 360 kN, the connection has the utilization ratio of 0.46 (see Figure 5.7a), while for the same

connection subjected to the same value of axial force with additional bending moments in each direction of only 0.01 kN, as represented in Figure 5.7b (which makes the biaxial bending moment of 0.014 kN), the connection loses its capacity and the utilization ratio of the connection raises up to 1.06.

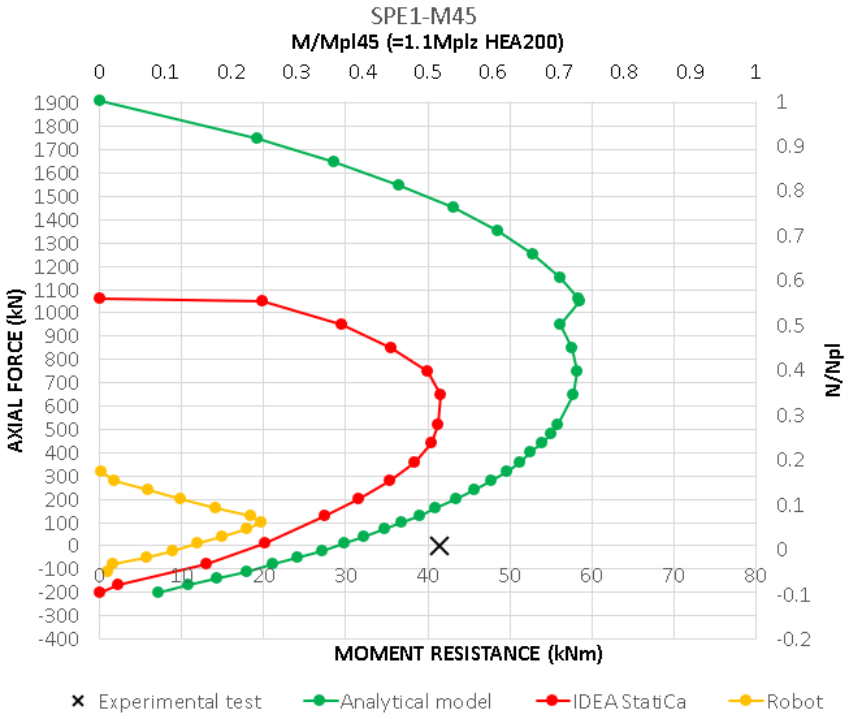

Figure 5.6: Moment resistance curves for connection subjected to axial force and biaxial bending moment

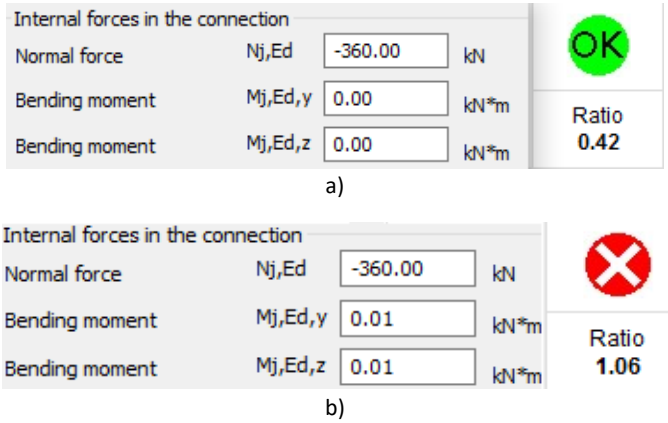

Figure 5.7: *Autodesk Robot's* ratio difference for minimal biaxial bending moment applied

This shows how sensitive this approach is when the connection is subjected to a biaxial bending moment. Initially, for minimal applied loads, the connection capacity is drastically reduced.

Although the changes in the slope of the curve now have a smooth transition, the connection analyzed in *IDEA StatiCa* still experiences an inappropriate drop in terms of moment resistance. For higher axial force values the limit is occurred due to the concrete block under pressure, while for the ones below 200 kN in compression, the base plate under bending is the weakest component.

5.3.6 Concluding remarks

Tests and represented curves allowed to gain further insight into the software analysis of this type of connection. The main conclusions are:

- The approach used by *Autodesk Robot Structural Analysis Professional* has proven to be very conservative, both for in-plane and out-of-plane bending moment, but especially when it comes to a biaxial bending moment for which it shows very low resistance and initially reduces connection capacity when a biaxial bending moment is applied.
- *IDEA StatiCa* shows a little bit more satisfactory results, but still inappropriate behavior was observed for higher compressive force when connection experiences a big drop in terms of moment resistance. Too much attention is paid to the concrete.
- Comparing to the experimental tests analyzes in both software generally result in wrong failure modes, paying too much attention to the concrete or base plate.

5.4 Parametric studies

5.4.1 Introduction

To investigate the effects of certain elements on the connection behavior, a parametric study has been performed. The effects of the base plate thickness t_p, column steel profile type, as well as the foundation concrete class were investigated, and the results will be presented in the following sub-chapters. Beside the mentioned parameters, for test *PC4* (check Table 5.7), the whole configuration is changed with the aim to check the relation between results for more massive connections and set-up in which all parameters are changed.

The concrete foundation is set up to be the same as in experimental work described in *Seco (2019),* for this reason, the connections were tested only for small values of tensile forces since higher tensile forces would lead to the foundation lifting.

Just like for previous studies, all specimens in this chapter were subjected to the axial force combined with the in-plane, out-of-plane or biaxial bending moment. For each specimen and each loading condition, numerical calculations were performed on a way that for each selected axial force, the moment resistance was obtained by an iterative procedure. The applied bending moments were calculated and then modified until the connection reached its capacity. For each calculation notes were recorded, describing connection behavior and failure mode.

As can be seen in the legend of the graphs, the old results (obtained for *SPE1-M0/M90/M45*) are represented as a curve with circles on it, while those whose parameters have changed are marked with triangles.

5.4.2 Geometry, materials and loading conditions

Four different configurations with various material characteristics are observed in this chapter and each of them is subjected to three different loading conditions (see Table 5.7). For the *PC4* test series, where the column cross-section is changed to HEA 500, it was also necessary to change all the other parameters to make the connection suitable for use. The anchoring length is increased from 350 mm to 500 mm, and the weld's throat width is increased from 7 mm to 15 mm.

Table 5.7: Geometry and material specifications of parametric study

TEST ID	Loading conditions	Cross section	CS steel grade	BP thickness tp (mm)	BP steel grade	Base plate dimensions (mm)	e (mm)	e_x (mm)	p (mm)	w (mm)	Anchor bolts diameter	Anchor bolts class	Concrete class (fck)	Concrete dim. (mm)
PC1-M0	In-plane	HEA200	S355	10	S275	330 x 300	70	35	260	160	16	5.6	C35/45	1450 x 910 x 650
PC1-M90	Out-of-plane													
PC1-M45	Biaxial													
PC2-M0	In-plane			30									C25/30	
PC2-M90	Out-of-plane													
PC2-M45	Biaxial													
PC3-M0	In-plane	IPE200		10										
PC3-M90	Out-of-plane													
PC3-M45	Biaxial													
PC4-M0	In-plane	HEA500		30	S355	750 x 530	135	75	600	260	30	8.8	C35/45	2000 x 1500 x 1000
PC4-M90	Out-of-plane													
PC4-M45	Biaxial													

5.4.3 Results and comparison

5.4.3.1 Test PC1

The concrete class of the foundation was increased up to C35/45, and the following graphs were obtained and compared with the old connection with the concrete foundation class of C25/30.

As can be seen in the legend of the graphs, the old results (obtained for f_{ck}=C25/30) are represented as a curve with circles on it, while new ones are marked with a triangle.

Observing software curves, the higher concrete class resulted in increased moment resistance of the connection, especially for higher compressive axial forces, while the analytical model curve remained almost the same. This shows that the model proposed by *Seco (2019),* is focused mainly on the steel elements, which is more accurate since it has been proven that in reality the steel is usually the element that governs the designs of the column base connections and reaches failure before concrete.

Despite showing bigger moment resistance capacities, the connection modeled in *Robot* reaches its limit too soon, with the base plate in bending as the weakest component. Comparing this failure modes to the ones obtained by the same connection with the weaker concrete class (SPE1-M0), there is not a big difference in failure mode types, and they occur for similar values of axial force. Even though the concrete class affects the moment resistance of the connection, the shape of curves obtained by *IDEA StatiCa* software still shows inappropriate connection behavior, which was described in sub-chapter 5.2.3.1 of the numerical study. For this case of bending moment load, the connection limit is reached due to anchor

bolts for all axial forces up to approximately 500 kN in compression, after that the concrete block is the first element that causes failure.

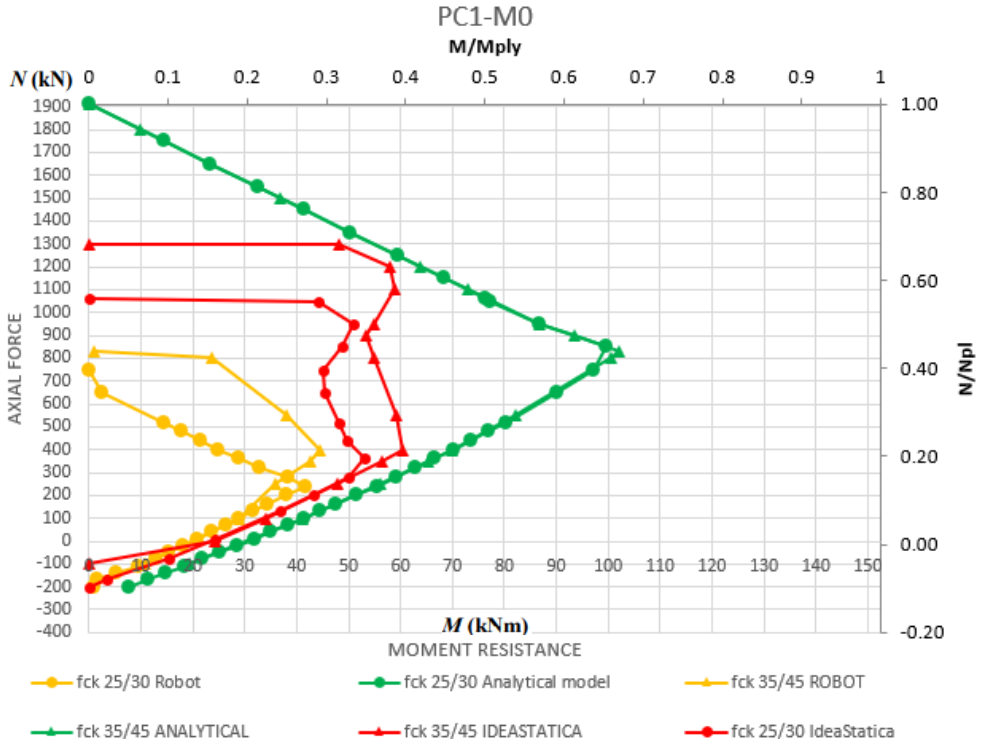

Figure 5.8: PC1-M0 moment resistances

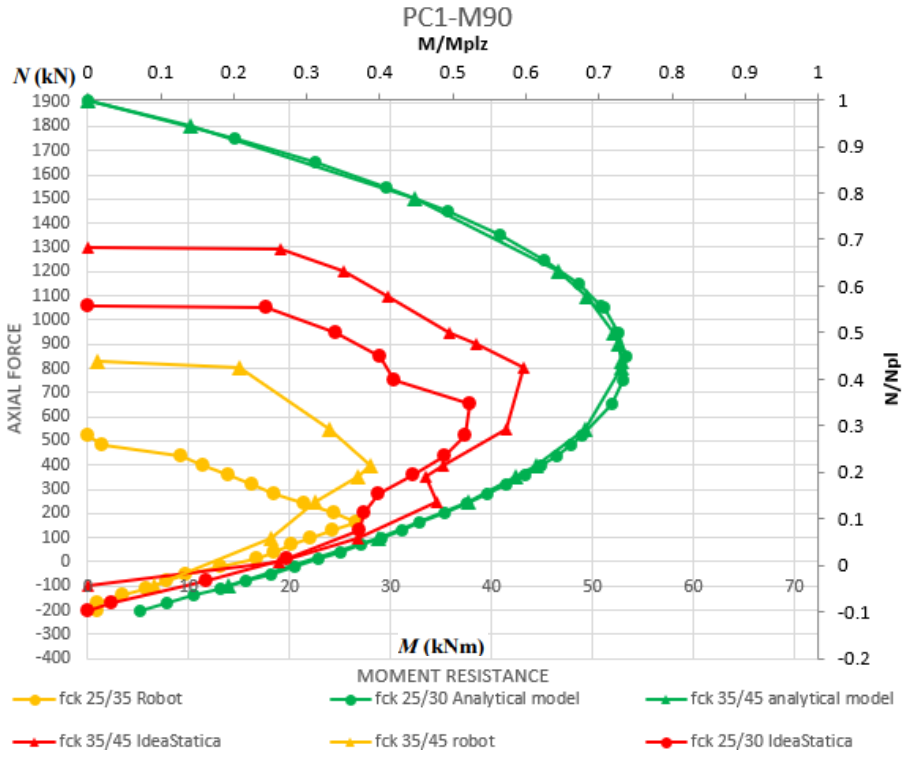

Figure 5.9: PC1-M90 moment resistances

For the bending moment over the minor axis (*PC1-M90*), the situation was very similar to the previous case. The increase of the concrete class just "postponed" the connection failure, increasing its moment resistance capacity for a little, but predicting the same failure modes.

Just like for the in-plane bending moment case, the limit of the connection in Robot software is reached due to the base plate in bending, but this time for the axial force up to around 240 kN in compression, and after that, the weakest component is the concrete under pressure.

Different failure modes occurred in *IDEA StatiCa* software, where the limit is firstly reached due to anchor bolts, and for higher compressive force (above 200 kN) the limit is reached due to exceeded concrete stress utilization.

The curves obtained for load combination of axial force and biaxial bending moment are presented in the following figure:

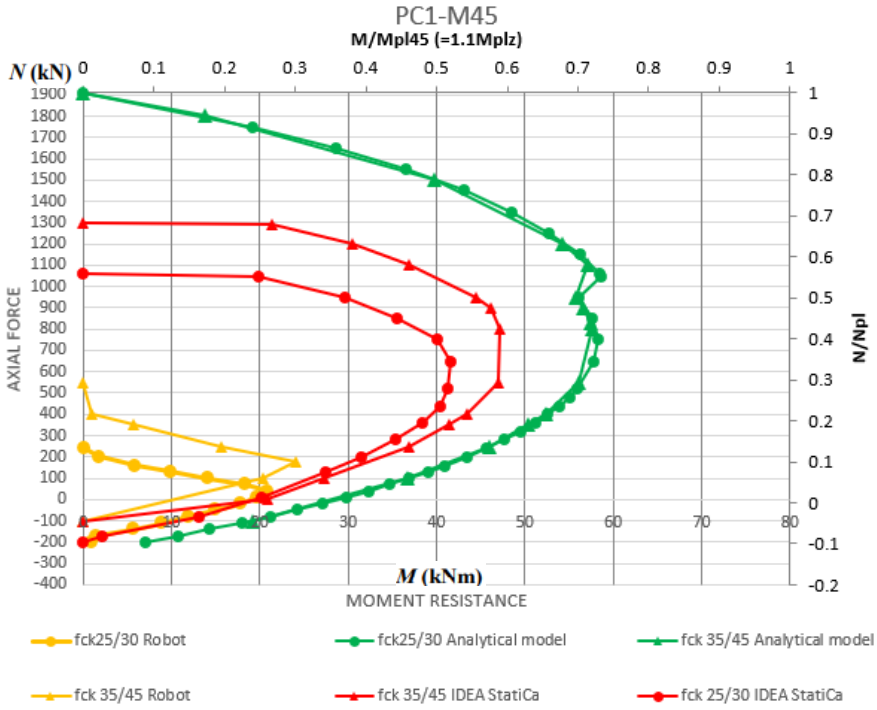

Figure 5.10: PC1-M45 moment resistances

The same conclusions as before can be written for the M45 case. Failure in *Robot* again occurs firstly due to the base plate in bending for lower, and concrete pressure for higher compressive forces (above 200 kN). An interesting fact is that in *IDEA StatiCa* for PC1-M45 reaches its limit due to concrete block under pressure, no matter the value of axial force (see Table 5.8).

To summarize the conclusions of the *PC1* test for M0, M90, and M45 loading conditions, higher connection moment resistance is noticeable for software approaches. As it was mentioned before, too much attention is given to the concrete since the steel is supposed to govern the connection design.

The analytical model does not have drastic results changes for different concrete properties, which makes it more appropriate to use. Therefore, the software does not only provide conservative results, but also predicts wrong failure modes, and even for the higher concrete class, too many failure modes for not so high values of compressive forces occur due to concrete foundation (CB) as represented in Table 5.8.

Table 5.8: Failure modes for PC1 tests

AXIAL FORCE	FAILURE MODE ROBOT			FAILURE MODE IDEA STATICA		
N (kN)	M0	M90	M45	M0	M90	M45
-100	BP	BP	BP	Concrete not calc.		
0	BP	BP	BP	AB	AB	CB
100	BP	BP	BP	AB	AB	CB
250	BP	BP	BP	AB	CB	CB
350	CB	CB	CB	AB	CB	CB
400	CB	CB	CB	AB	CB	CB
550	CB	CB	CB	CB	CB	CB
800	CB	CB	CB	CB	CB	CB
830	CB	CB	CB	CB	CB	CB
900	CB	CB	CB	CB	CB	CB
950	CB	CB	CB	CB	CB	CB
1100	CB	CB	CB	CB	CB	CB
1200	CB	CB	CB	CB	CB	CB
1295	CB	CB	CB	CB	CB	CB
1298	CB	CB	CB	CB	CB	CB

5.4.3.2 Test PC2

Compared to set-up for specimens *SPE1-M0/M90/M45*, the only modified parameter in *PC2* tests is base plate thickness, which is increased from 10 mm to 30 mm. Obtained results for the connection subjected to a combination of axial force and bending moment over the major axis, are represented in Figure 5.11, where can be noticed how base plate thickness affects the behavior of the connection. In this case, the curve of the analytical model changed, but not significantly. Opposite to that, the software results changed drastically.

Since the Robot failure modes occurred mainly due to the base plate in bending, a lot higher moment resistance capacity is noticeable now. The thicker base plate has smaller bending deformations and by that lever arm between the compressive zone and tensile one (anchor bolts in tension) is increased, which leads to higher connection resistance. With a thicker base plate, stress distribution on the concrete is better, so it does not appear anymore as the weakest component in this software. Consequently, the distribution of the forces on the anchor bolts is also different, and therefore they occur as the weakest component for this set-up and loading conditions.

All the abovementioned conclusions can be written for *IDEA StatiCa* too, as the results now are almost equal to the analytical ones. Failure modes are described at the end of this sub-chapter in Table 5.9.

For the same connection subjected to axial force and out-of-plane bending moment, the following curves were obtained (see Figure 5.12):

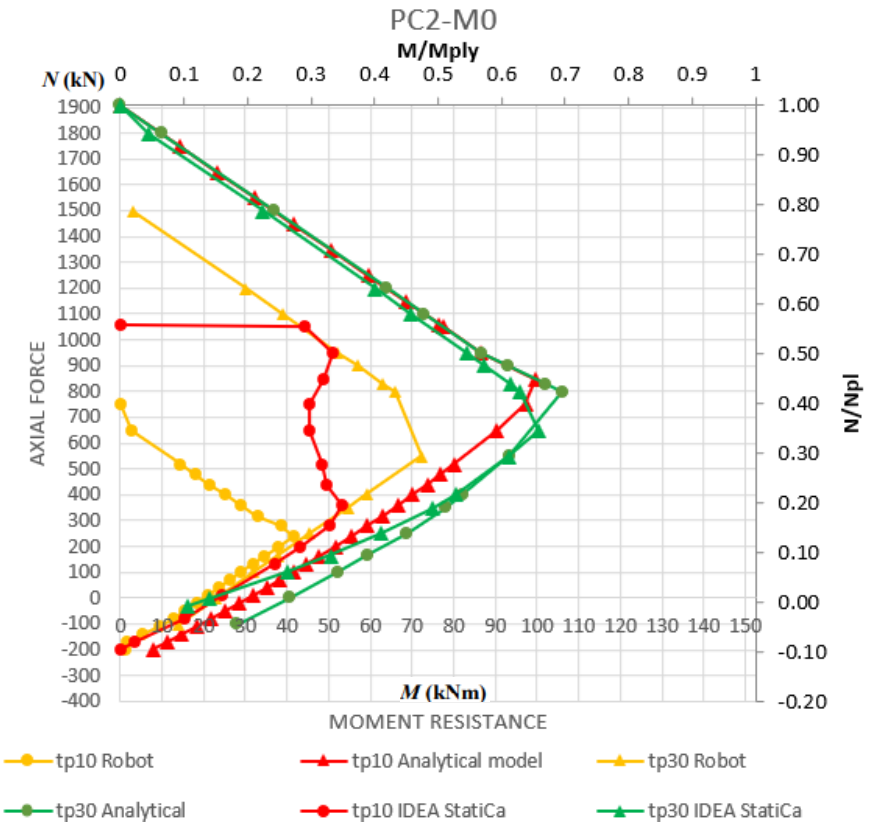

Figure 5.11: PC2-M0 moment resistance curves

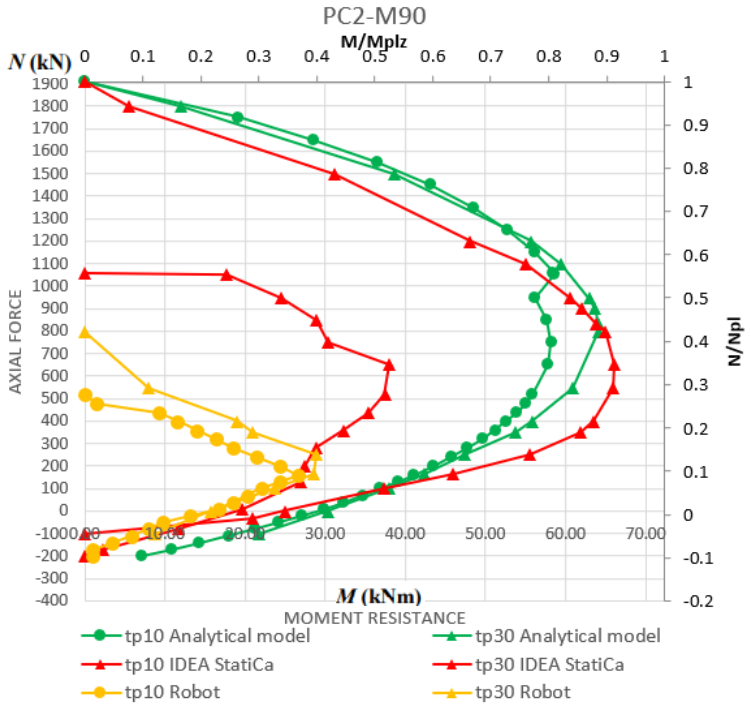

Figure 5.12: PC2-M90 moment resistance curves

For the *M90* loading conditions, the results obtained with an analytical model are improved, and the connection has a higher moment capacity. Results obtained by software *Robot* have not changed a lot

compared to the ones obtained for the connection with a thinner base plate. Approach used by *Robot* by *Autodesk* accesses the connection calculation too carefully for loading conditions of out-of-plane and biaxial bending moment (which will be showed below). The biggest curves difference is noticed for *IDEA StatiCa*, which shows drastically higher results, and, according to the results, the moment resistance of this connection is higher than that shown by the analytical model. The accuracy of IDEA StatiCa results should be further verified and determined to check if it still on the safe side, but the results are very satisfactory.

Similar changes are obtained when the connection was subjected to axial force and biaxial bending moment (see Figure 5.13).

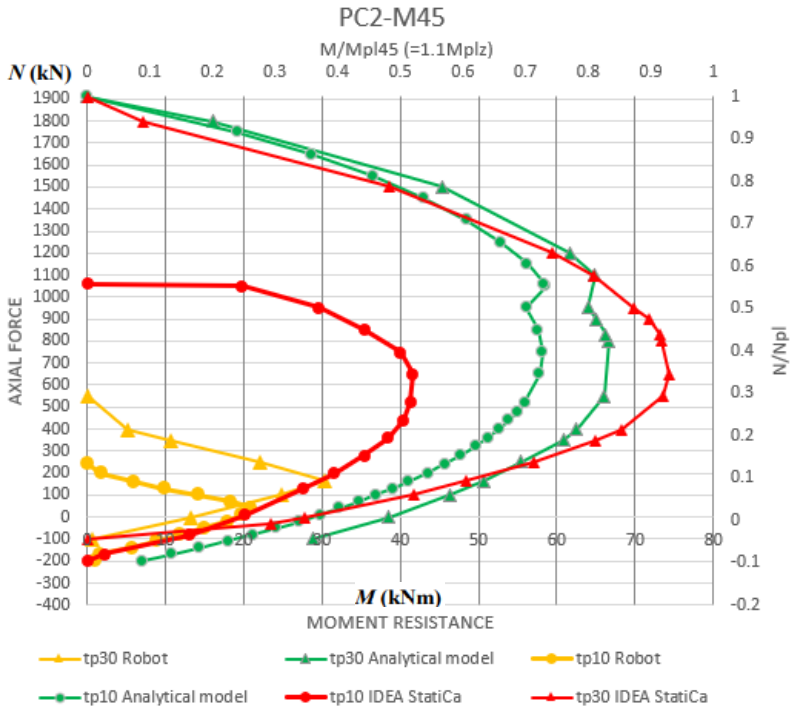

Figure 5.13: PC2-M45 moment resistance curves

As mentioned above, despite the failure mode have changed for this case and the thicker base plate contributed connection capacity, the approach used by *Autodesk Structural Analysis* obtains the results that are way too much on the safe side. The curve obtained by the analytical model has changed and shows higher moment resistance capacity now. When it comes to *IDEA StatiCa*, the curve now shows the maximum moment resistance which is almost double compared to the previous ones. Since for thinner base plate all failure modes, for biaxial bending moment load, occurred due to concrete block under pressure, thicker base plate resulted in better stress distribution on the concrete, so the failure modes had changed. Now, for lower compressive forces and tensile ones, failure occurs due to anchor bolts in tension, while for high compressive forces welds are the weakest component. Base plate thickness plays an important role in *IDEA StatiCa* and it shows that with the right design, this software can have very satisfactory results.

Table 5.9: Failure modes for PC2 tests

AXIAL FORCE	FAILURE MODE ROBOT			FAILURE MODE IDEA STATICA		
N (kN)	M0	M90	M45	M0	M90	M45
100	AB	AB	AB	Concrete not calc.		
30	AB	AB	AB	CB	AB	AB
0	AB	AB	AB	CB	AB	AB
-100	AB	AB	AB	CB	CB	AB
-165	AB	AB	CF	CB	CB	AB
-250	AB	CF	CF	AB	CB	AB
-350	AB	CF	CF	AB	W	AB
-400	AB	CF	CF	AB	W	AB
-550	AB	CF	CF	AB	W	W
-650	AB	CF	CF	AB	W	W
-800	AB	CF	CF	W	W	W
-830	AB	CF	CF	W	W	W
-900	AB	CF	CF	W	W	W
-950	AB	CF	CF	W	W	W
-1100	AB	CF	CF	W	W	W
-1200	AB	CF	CF	W	W	W
-1500	AB	CF	CF	W	W	W
-1800	AB	CF	CF	W	W	W
-1910	AB	CF	CF	W	W	W

5.4.3.3 Test PC3

The cross-section profile plays an important role in column base connections. As represented in Table 5.7, for test *PC3* it is the only modified parameter compared to *SPE* tests. So, HEA 200 is replaced with IPE 200 which is also commonly used as a steel column.

Numerical and analytical results are represented in this sub-chapter and a similar relationship between the curves can be noticed for changed cross-section but in smaller values. Both software and analytical model showed lower connection capacity, which is expectable since IPE profiles have weaker properties than HEA ones. This set-up has a base plate thickness of 10 mm which is the weakest component of this set-up and reaches failure before column under pressure. A thin base plate in *Robot*, just like it happened for the SPE1 test series, causes failure of the concrete block in pressure due to poor stress distribution.

For *IDEA StatiCa* same thing is noticed, but next to cracking of the concrete, for lower axial forces the connection fails due to anchor bolts in tension, where the bending moment is dominant instead of axial force.

Curves obtained for this connection subjected to in-plane bending moment are shown in Figure 5.14.

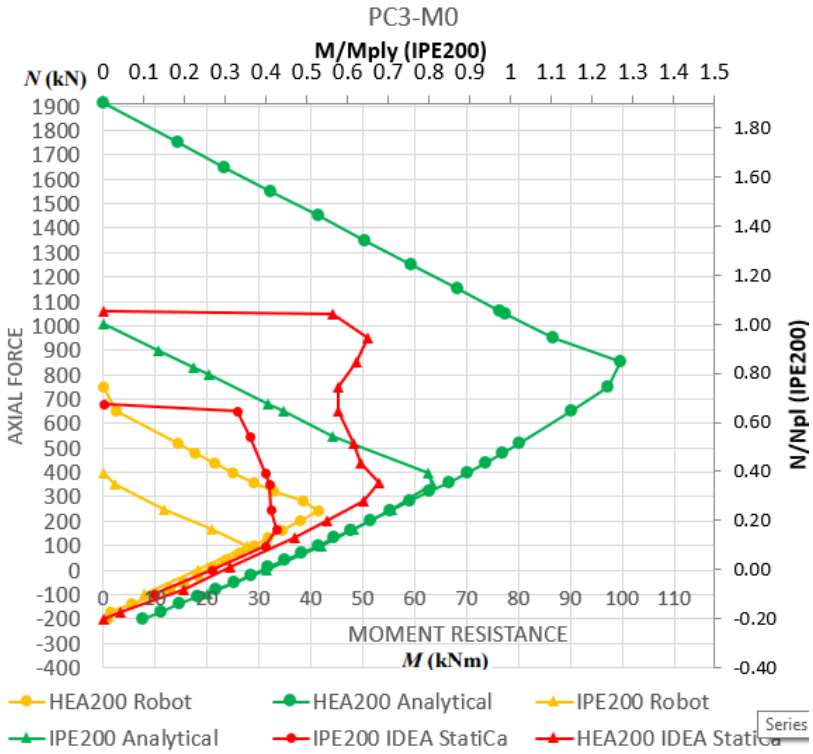

Figure 5.14: PC3-M0 moment resistance curves

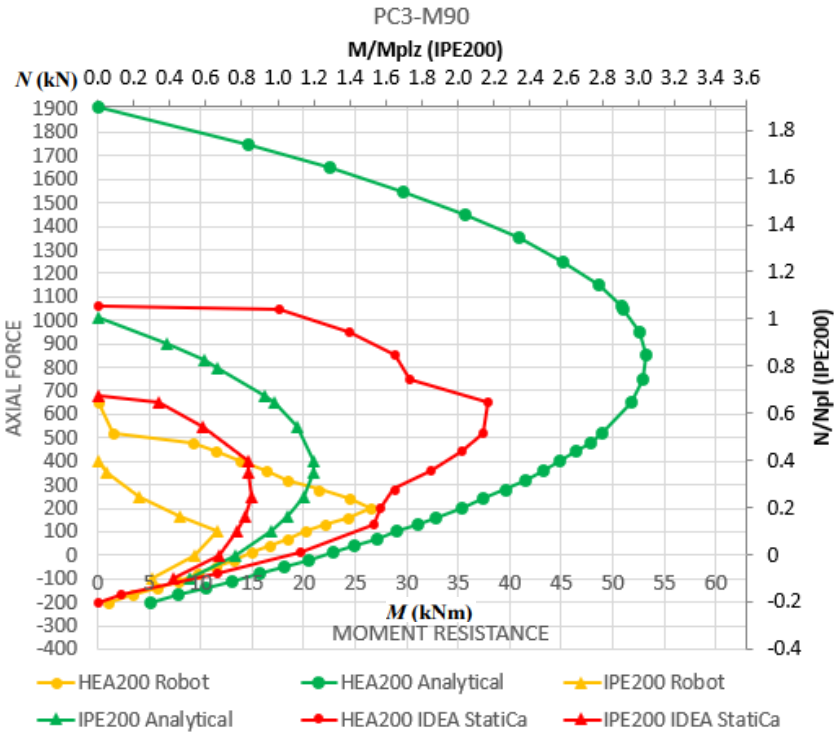

Figure 5.15: PC3-M90 moment resistance curve

For connection subjected to bending moment over the weaker axis, changing the steel profile from HEA200 to IPE200 decreases lever arm, and it is to expect that resistance will be reduced, as can be seen in Figure 5.15.

For both software, when it comes to out-of-plane bending moment, failure occurs generally due to concrete block in pressure.

For final loading conditions, test PC3-M45, moment resistance curves are represented in Figure 5.16, and although in much smaller values, the relationship between curves is similar as it is for the *SPE1-M45* (connection with HEA200 cross-section).

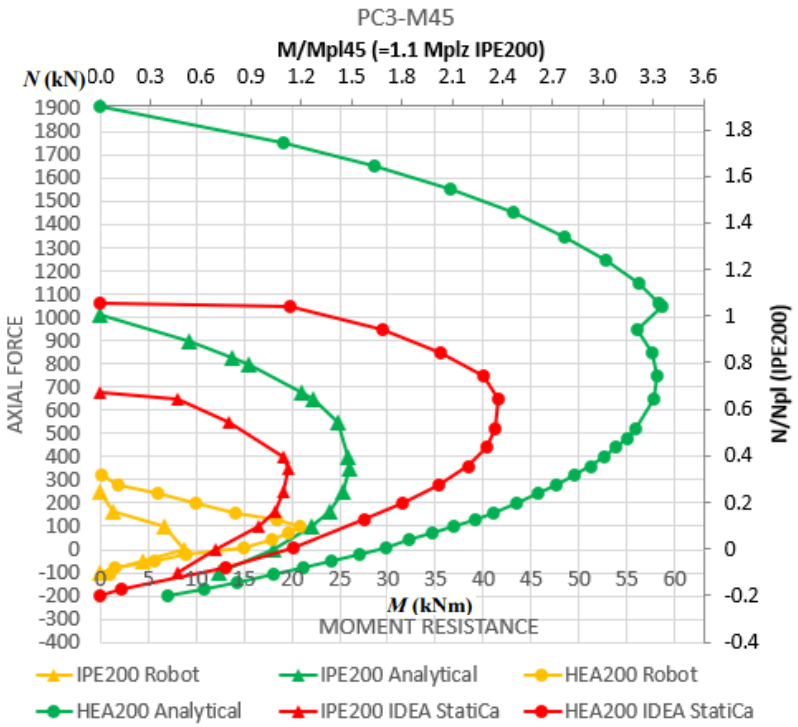

Figure 5.16: *PC3-M45* moment resistance curves

For the same reason as for *M90* loading conditions, connection capacities are lower. Thus, *Robot* underestimates the capacity of the connection even more than for the abovementioned PC3-M0 and PC3-M90 cases. Although too much on the safe side, *IDEA StatiCa* shows better results for this specific case than for previous ones in the PC3 test series.

5.4.3.1 Test PC4

To check the relation between software and analytical model results for more massive connections and all different parameters, the following tests were performed with set-up as presented in Table 5.7. The mentioned parameters resulted in design as in Figure 5.17.

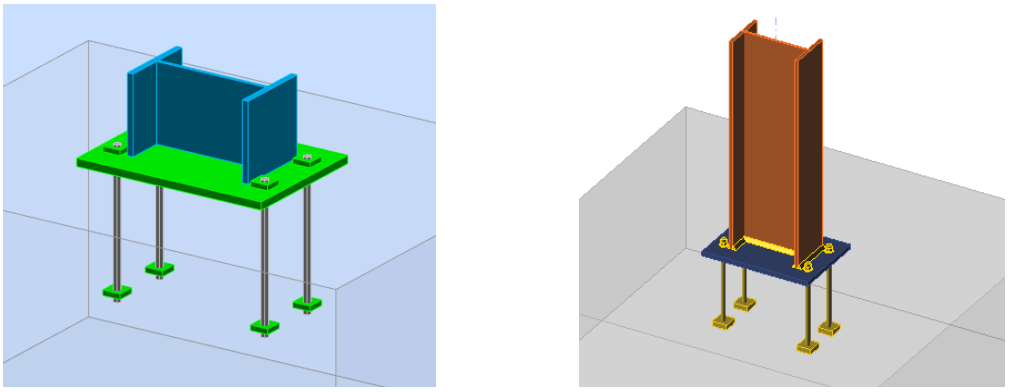

a) b)

Figure 5.17: Software designs for *PC4* test in a) *Robot* and b) *IDEA StatiCa*

Curves obtained for all loading conditions (*M0, M90, M45*), are represented in the figures below.

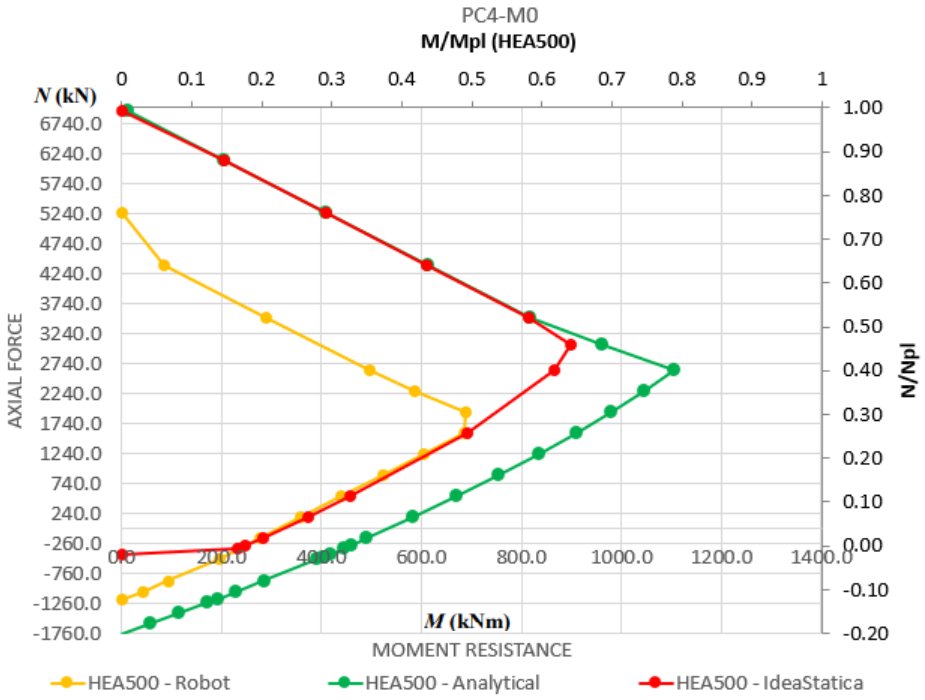

Figure 5.18: *PC4-M0* moment resistance curves

Software results showed way better approximation for these cases then they used to for the previous tests.

For this connection, which is more massive with all increased parameters, both software results with higher moment resistance values. *IDEA StatiCa* due to thicker base plate has a better stress distribution and does not reach its limit capacity due to concrete, but due to local bending of the column flange, welds and anchor bolts for lower axial force.

Robot also showed better results and failure modes, so the bending of the base plate is not the weakest component anymore. Anchor bolts for lower axial forces and concrete for higher forces in compression are the elements that fail first.

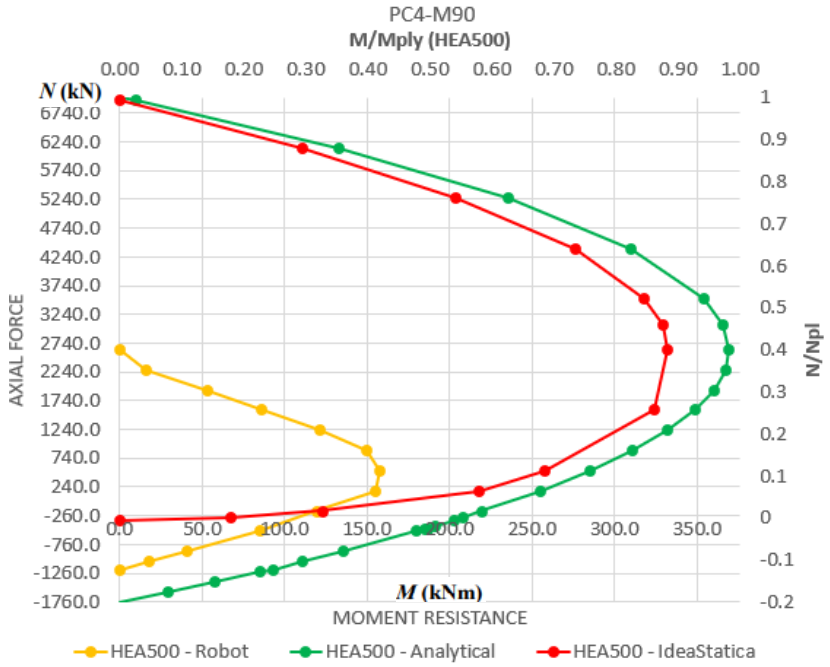

Figure 5.19*: PC4-M90* moment resistance curves

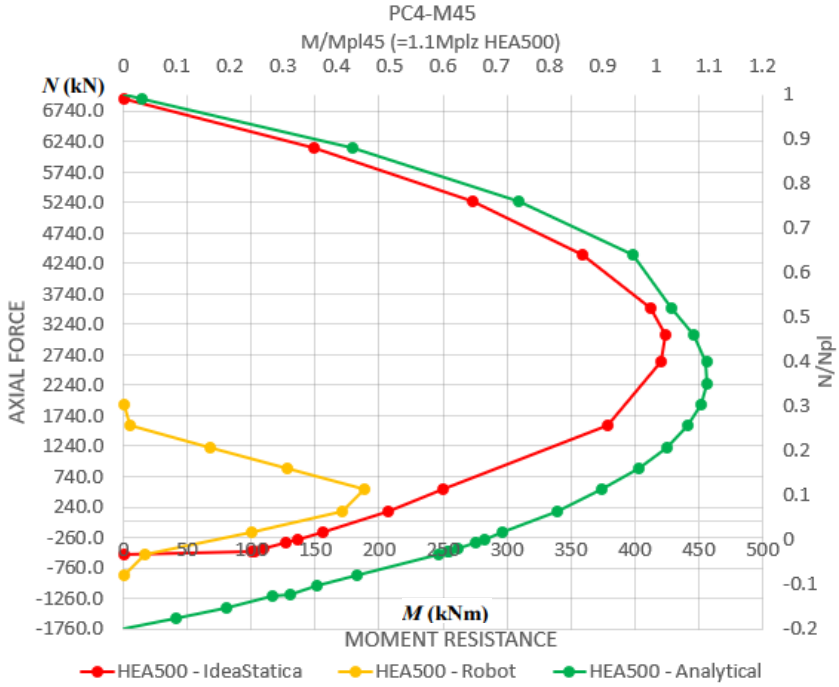

Figure 5.20: *PC4-M45* moment resistance curves

5.4.4 Concluding remarks – parametric study

With the aim of conducting quality parametric study and a better understanding of the role of each parameter of the connection, a large number of numerical calculations and written notes for each of them has been conducted. Some main conclusions are summarized below:

- The increase of the concrete class resulted with greater moment resistance in the software results, which is not appropriate since in reality the steel is usually a component that reaches failure first and it governs connection design. Thus, besides being too much on the safe side, software methods also resulted with wrong failure modes for many cases.
- The column base plate thickness plays an important role when it comes to connection bending moment capacity, since it affects stress distribution and directly affects the length of the lever arm between compressive and tensile zone inside the connection. Thus, software and analytical model shows higher moment resistance results, especially *IDEA StatiCa* whose results are very satisfactory.
- Steel column profile greatly influences moment resistance capacity of the connection, especially when out-of-plane bending moment is dominant. Column width affects the length of the lever arm, which affects connection capacity and stiffness.
- After changing all the parameters for those with stronger properties, the analytical model still shows the highest connection moment resistance capacity, followed by *IDEA StatiCa* with satisfactory results, while *Robot* remains too much on the safe side.
- *IDEA StatiCa* shows quite satisfactory results for specific set-ups, which means that for appropriate design of the connection this software will approximate its behavior very well.

6 CONCLUSIONS

6.1 Objectives and description

The main goal of this dissertation was to analyze the accuracy of software solutions in terms of column base connections in buildings and compare the results with ones obtained by an analytical model developed and verified experimentally and numerically by *Seco*. Firstly, the construction with some realistic spans (4m x 7m) was designed in SCIA Engineer and loaded by a dead and live load according to Eurocode regulations. For obtained results as the most appropriate column cross-section turned out to be HEA200 with the utilization factor of 0.75 obtained in SCIA (ULS Check -EN-EC Steel Check). Since *SCIA Engineer* has a BIM link with *IDEA StatiCa*, the connection was exported to the software to design a proper connection. The same construction with equal loads was designed in *Autodesk Robot Structural Analysis Professional* and the column base connection is automatically withdrawn into the connection design section of the software. In both programs, *IDEA StatiCa* and *Robot* by *Autodesk*, the equal connection was designed in a way it completely matches the configuration which was used in Seco (2019) (as described in subchapter 5.2.1 in this thesis). After redefining the analytical model proposed by *Seco (2019),* preparing it for use, and creating an excel spreadsheet for this type of research, the analysis could have begun.

The axial force on the column was gradually increased from the tension all the way to the maximum amount of the compressive force, that the connection can take before failure. Each of these axial forces were combined with the bending moment in one direction, in-plane, out-of-plane or bending moment at an angle of 45°. For each loading condition, by the iterative procedure, the maximum bending moment that the connection can withstand before failure was obtained.

Looking at the records, for Numerical study 118 bending moment resistances of one specific connection (SPE1) were obtained in software (*Robot* and *IDEA StatiCa*), with over 200 additional runs and over 350 notes recorded for each run, all with the aim of better understanding the behavior of the connection under software analysis.

Further, together for all set-ups of the Parametric study, 265 moment resistance values were obtained, with recorded notes that describe behavior and the failure mode for each of them. Considering the fact that an iterative procedure takes several attempts to reach the correct result, these analyzes require a large number of calculations and a long period of time.

The analytical moment resistance values for each set-up and loading condition were obtained too, so numerical results always had a relevant one to be compared with.

6.2 Conclusions

The results obtained by numerical analyzes and the parametric study shows how software with different approaches simulate the behavior of the column base for different loading conditions.

Firstly, let us focus on *Autodesk Robot Structural Analysis Professional* whose approach is highly related to the guidance given by Eurocode. It was previously highlighted that this program greatly underestimates the connection capacity for all performed tests, but additionally, the wrong failure modes are predicted for most of the cases, which is confirmed in Table 5.6, when results are directly compared to ones obtained by experimental tests. Also, when it comes to biaxial bending moment, in Figure 5.7 is shown how much resistance the connection loses when a minimum amount of bending moments in both directions is applied. This shows that approach used by *Robot* is initially wrong and gives very rough results. Since the base plate was the weakest component for most of the configurations and loading conditions, it was to be expected that set-up with a thicker base plate will result in better connection capacity and different failure modes. But despite better results for in-plane bending moment, the results obtained for loading conditions of the out-of-plane or biaxial bending moment are still too conservative.

Secondly, the software whose approach is a merge of FE analysis and stress distribution combined with component method checks – IDEA StatiCa shows more satisfactory results for all performed tests. Despite better approximation of connection moment resistances, wrong failure modes are occurring, and too much importance is given to concrete, as many of the failures occur due to it. At one point, for almost all *M0* cases*, IDEA StatiCa* for an increase of compressive force starts showing lower moment resistance capacity. After the axial force continues to increase, the connection starts showing higher moment resistances again. This happens at the moment when failure mode changes from anchor bolts in tension to concrete block under compression, on which software is very sensitive. This problem can be solved by increasing the column base plate thickness, so the compressive force has better distribution on the concrete, so it can stand higher compressive forces and local cracking is avoided. Also, considering the curves obtained after performing PC2 tests, the conclusion is that the base plate thickness has a really big influence on the column base connection behavior when analyzed in this software. For PC2-M90 and PC2-M45 results obtained by IDEA StatiCa show higher moment capacity than the analytical model, leading to the question of whether these results remain entirely on the safe side. It must be highlighted that for a specific change of parameters IDEA StatiCa shows very satisfactory results, as it did for the PC4 test series.

The abovementioned facts can be summarized in the following figure where comparison against the experimental tests is presented graphically.

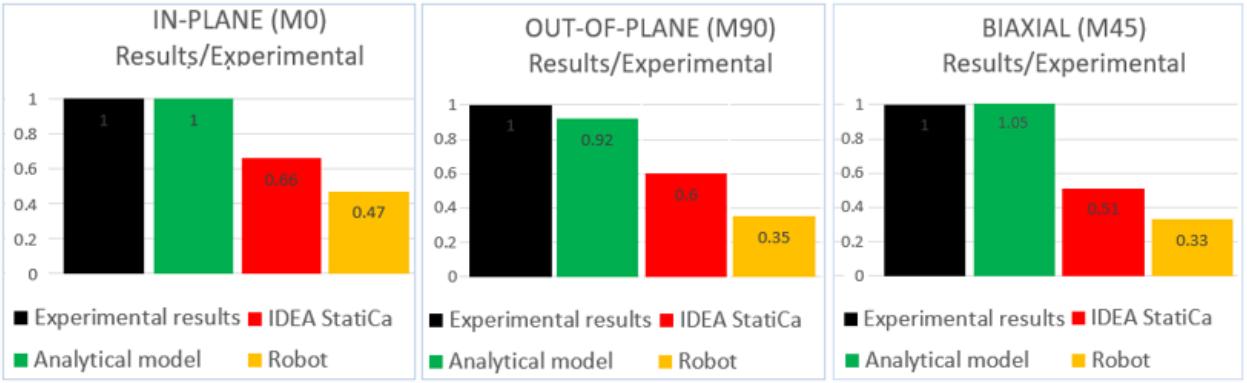

Figure 6.1: Comparison of the software and analytical results against experimental tests

To conclude, the difference between software results is obvious. *Autodesk Robot Structural Analysis has* proven itself as a very conservative for all performed tests. Unlikely to that, for the specific set-up of parameters *IDEA StatiCa* showed satisfactory results. From this thesis can be concluded which parameters affect connection behavior the most, and by respecting the mentioned conclusions when designing a connection can result in a connection whose behavior is well simulated by *IDEA StatiCa*. Calculation of these kinds of connections with *Robot* will lead to an over-dimensioned design of connection, which can lead to big and unnecessary economic losses.

REFERENCES

Abdollahzadeh, G. R. and Ghobadi, F. (2013) 'Mathematical modeling of column-base connections under monotonic loading', *Civil Engineering Infrastructures journal*, 2013.

Abejide, O., *Effectiveness of Base Plate Thickness Design Criteria in Steel Columns*, Medwell Journals, n. º 2, pp. 1207-1217, 2007.

Amaral, P. M. (2014) *Steel column bases under biaxial loading conditions*. Integrated *Masters in Civil Engineering – 2013/2014 – Department of Civil Engineering, Faculty of Engineering of the University of Porto, Porto, Portugal, 2014*.

Autodesk Robot Structural Analysis Professional, *User's Guid*e [Online]. Available: http://help.autodesk.com/view/RSAPRO/2018/ENU/?guid=GUID-4A734308-B2F3-4147-A310-BD47C48E9ED1 (Accessed on 09/07/2020)

Bajer, M. *et. al.,* 'Influence of selected parameters on design optimization of anchor joints', in *12th International Conference on Steel, Space and Composite Structures*. Prague, 2014.

Correia, R., Dimensionamento de Bases de pilares metálicos - Versão para discussão, Faculdade de Engenharia da Universidade do Porto, 2013.

Da Silva Seco, L*., Column base plates under 3D loading (These de doctorat de)*, l'INSA de Rennes, Comue Universite Bretagne Loire, 29/11/2019,

EN 1993-1-8: Eurocode 3: Design of steel structures, Part 1-8: - Design of joints, European Comitee for Standardization, 2003.

Fasaee, M. A. K., Banan, M. R. and Ghazizadeh, S. (2018) 'Capacity of exposed column base connections subjected to uniaxial and biaxial bending moments', *Journal of Constructional Steel Research*, 148, pp. 361–370.

Grauvilardell, J., Lee, D., Hajjar, J., Dexter, R., *Synthesis of Design, Testing, and Analysis Research on Steel Column Base Plate Connections in High-seismic Zones*, Structural Engineering Report No. ST-04-02, Department of Civil Engineering – University of Minnesota, October 2005.

Horová, K. *et. al*., *Base plates of hollow sections,* Conference paper, Czech Technical University in Prague, 2010.

IDEA StatiCa, *Theoretical background* [Online]. Available: https://www.ideastatica.com/support-center/all?category=theoretical_background (Accessed on 09/07/2020)

Jaspart, J. P. and Vandegans, D. 'Application of the component method to column bases', *Journal of Constructional Steel Research*, 48, pp. 89–106., 1998.

Lee, D. Y., Goel, S. and Stojadinovic, B. (2008a) 'Exposed column-base plate connections bending about weak axis: I. Numerical parametric study', *Steel Structures*, 8, pp. 11–27.

Lee, D. Y., Goel, S. and Stojadinovic, B. (2008b) 'Exposed column-base plate connections bending about weak axis: II. Experimental study', *Steel Structures*, 8, pp. 29–41.

Lescouarc'h, Y. (1988) *Les pieds de poteaux encastrés en acier*. France: CTICM.

Márai, P. *et al.* (2014) 'Resistance model for fixed column bases', in *EUROSTEEL*. Naples. Michal, S.

Sokol, Z, Column Bases, 18 10 2005. [Online]. Available: http://people.fsv.cvut.cz/www/wald/CESTRUCO/Texts_of_lessons/07-GB_Column_Bases.pdf. [Accessed on 17 04 2020].

Sokol, Z., Wald, F., *Modelování tuhosti a únosnosti tažené části patek sloupů*, Czech Technical University in Prague, 2000.

Stamatopoulos, G. N. and Ermopolous, J. C. (2011) 'Experimental and analytical investigation of steel column bases', *Journal of Constructional Steel Research*, 67, pp. 1341–1357.,2011.

Wald, F., Hofmann, J., Kuhlmann, U., *Design of steel-to-concrete joints, Design manual I - version for revision*, Czech Technical University in Prague, February 2014.